Emile C.L. Marnette

Sulfur cycling in two Dutch moorland pools

40951

Emile C.L. Marnette

Sulfur cycling in two Dutch moorland pools

1. Veldwerkapparatuur dient zo eenvoudig mogelijk te worden ontworpen.

2. In sedimenten met een ruimtelijk sterk varierend watergehalte, is een juiste keuze van de eenheid waarin sedimentgegevens worden uitgedrukt essentieel voor het interpreteren van deze gegevens.
Dit proefschrift

3. De zwavelinput als gevolg van atmosferische depositie in beide onderzochte vennen wordt voor een belangrijk deel (55 - 90%) geconsumeerd door biochemische processen in het sediment.
Dit proefschrift

4. Voor een accurate budgettering van zwavel in geïsoleerde oppervlaktewateren is een goede schatting van de lokale atmosferische droge depositie op het wateroppervlak van groot belang.

5. De verhouding tussen pyritisch zwavel en zuurvervluchtigbaar zwavel is meer afhankelijk van redoxomstandigheden dan van de concentratie van organisch koolstof en sulfaat.
Davison W. et al. (1985) Geochim. Cosmochim. Acta 49: 1615-1620.
Dit proefschrift

6. De intensiteit en het onderwerp van onderzoek aan wetenschappelijke instellingen in Nederland wordt in steeds grotere mate bepaald door de kracht en de richting van de politieke wind. Hierdoor krijgt dit onderzoek een groter maatschappelijk draagvlak, dat als positief moet worden ervaren. Echter door verschuivingen in politieke prioriteiten wordt het oorspronkelijk beoogde onderzoek vaak niet gerealiseerd.

7. Het realiseren van een goede ontsluiting van Wageningen via treinverkeer zal de groene kleur van de stad duidelijk versterken.

8. Sommige verkeersobstakels vormen een speels element in het verkeer; zij vereisen een zekere rijvaardigheid van de automobilist om ze met een zo hoog mogelijke snelheid te nemen.

9. Gegeven de huidige mogelijkheden tot geboortecontrôle, is de beslissing tot het "nemen van kinderen" een puur egoïstische.

10. De overweldigende verkoop aan het amerikaanse volk van toegangsbewijzen voor de in de VS georganiseerde WK voetbal '94 is eerder een uiting van de eigenschap alles wat nieuw is te moeten beleven, dan van een buitengewone interesse in het spel.

11. Het inhuren van een "head hunter" kan je de kop niet kosten.

voor Thijs
en Monic

SUMMARY

Due to atmospheric acid deposition, the chemistry of many moorland pools has changed, resulting in changes in their fauna and flora. Most moorland pools are sensitive to acid loading because underlying and surrounding soils are low in chemical buffering capacity. Biological processes in the sediment like denitrification and SO_4^{2-} reduction are of major importance to internal alkalinization necessary to neutralize the atmospheric input of potential acidifying N and S components. This study deals with the cycling of sulfur in moorland pools and was aimed at a better understanding of the factors influencing the S cycle in these freshwaters.

Characterization and quantification of sulfur pools in sediment and overlying water column. Determination of spatial variability of chemical characteristics related to S-cycling.

In highly organic moorland pool sediment (mean C content of top 10 cm = 9.8% dwt) about 46% of the total S is in organic S form, whereas in sandy sediment (mean C content = 1.4% dwt) the organic S fraction makes up about 75% of the total S pool. The sediments of the moorland pools Gerritsfles and Kliplo, have been compared statistically with respect to total S and S-related sediment contents (Chapter 6). The pools differ significantly in their horizontal and vertical distribution of S. Statistical analyses indicate that spatial variation of S in Kliplo is due to organically bound S. For Gerritsfles spatial interrelation between C, S or Fe could not be recognized. As evidenced by this study, a choice for a measurement unit like mass fraction (g g^{-1}) or volumetric mass (mg cm^{-3}) is crucial for the interpretation of spatial variability. In spatial studies of sediment constituents, it is essential to express contents of these constituents in volumetric mass fractions, since spatial sediment patterns are often obscured by spatial variations in bulk density. Taking into account spatial variability is concise for a proper quantification of S-budgets of pools or lakes.

Determination of SO_4^{2-} reduction rates and transformation rates of SO_4^{2-} into organic and inorganic S fractions. Estimation of S oxidation rates in sediments and overlying water column.

In Gerritsfles S cycling near the sediment/water boundary was investigated by measuring (1) SO_4^{2-} reduction rates in the sediment, (2) depletion of SO_4^{2-} in the

overlying water column and (3) release of ^{35}S from the sediment into the water column (Chapter 2). Two locations differing in sediment type (highly organic and sandy) were compared with respect to reduction rates and depletion of SO_4^{2-} in the overlying water.

Sulfate reduction rates, estimated by diagenetic modelling and whole core $^{35}SO_4^{2-}$ injection, ranged from 0.27 to 11.2 mmol m^{-2} d^{-1}. Rates of SO_4^{2-} consumption in the overlying water were estimated by changes in SO_4^{2-} concentration over time in *in situ* enclosures and varied from -0.51 to 1.81 mmol m^{-2} d^{-1}. Maximum rates of oxidation to SO_4^{2-} in July 1990 estimated by combination of SO_4^{2-} reduction rates and rates of *in situ* SO_4^{2-} uptake in the enclosed water column were 10.3 and 10.5 mmol m^{-2} d^{-1} at an organic rich site and at a sandy site respectively.

Experiments with $^{35}S^{2-}$ and $^{35}SO_4^{2-}$ tracer suggested (1) a rapid formation of organically bound S from dissimilatory reduced SO_4^{2-} and (2) transport of mainly non-SO_4^{2-}-S, from the sediment into the overlying water.

Sulfate reduction rates in sediments with higher volumetric mass fraction of organic matter did not significantly differ from those in sediments with a lower mass fraction of organic matter.

The role of inorganic S, with emphasis on pyrite, in the S cycle of Gerritsfles and Kliplo.

In Gerritsfles and Kliplo, pyrite is the most important iron sulfide phase (Chapter 3). The redox status appeared to be a main factor in determining whether pyrite or a monosulfide, defined by the content of acid volatile sulfur (AVS), is formed. Sedimentary FeS_2-S/AVS-S molar ratios in sediments of Gerritsfles and Kliplo, which are overlain by a continuously oxygenated water column, were 32 and 55 respectively whereas in other lakes, where stratification caused anaerobic conditions in the hypolimnion, FeS_2/AVS ratios were <1.

Framboidal pyrite, presumably formed slowly through sulfurization of iron sulfide precursors is thought to be an important pathway of pyrite formation in the freshwater sediments of Gerritsfles and Kliplo. The presence of single-crystal pyrite indicates that pyrite in both sediments may also form rapidly. The close association of pyrite framboids and organic matter, and the undersaturation of bulk porewaters with respect to amorphous FeS suggest that the framboidal pyrite is formed at microsites within organic matter. Alternating reduced and more oxic conditions in the sediment will supply Fe^{2+} and zerovalent sulfur respectively for the formation of pyrite. That a large fraction of pyrite is in (dead) plant cells may be explained by preferential oxidation of pyrite at locations where pyrite is not so protected

against O_2 intrusion, in contrast to the pyrite located inside organic matter microsites.

Calculation of a chemical S-budget in both freshwater systems using models and chemical data of pool- and rainwater.

The chemical composition of surface waters of Gerritsfles and Kliplo and of incident precipitation, were monitored from 1982 to 1990. Sulfur and water budgets were calculated using a hydrochemical model developed for well-mixed non-stratifying lakes (Chapter 4). In Gerritsfles and Kliplo respectively 70 and 80% of the incoming S is lost to the sediment primarily through reduction of SO_4^{2-}, indicating that SO_4^{2-} reduction is an important mechanism to buffer the incoming acidic S compounds.

Total atmospheric deposition of S has decreased significantly after 1986 at both locations. A model describing the sulfur budget in terms of input, output and reduction/oxidation processes predicted a fast decrease of poolwater SO_4^{2-} concentrations after a decrease of atmospheric input. However, SO_4^{2-} concentrations in the surface water were lowered only slightly or remained constant so there must be an extra source of SO_4^{2-} to the water column. Two possible mechanisms can explain this extra source of SO_4^{2-}: desorption of SO_4^{2-} from the sediment and the release of SO_4^{2-} through desiccation of a part of the pool bottom after dry summers. Further investigations would be needed to study the relative importance of these mechanisms.

Mineralization of sedimentary organic S

The mineralization rate of organic S compounds in Gerritsfles was estimated to reveal its importance in the overall S cycle (Chapter 5). The mineralization rate of organic S was estimated indirectly from diagenetic modelling of pore water NH_4^+ depth profiles and the ratio of organic N and S contents. Since the mineralization rates of organic N and S do not follow the stoichiometry of the contents of organic N and S, it was only possible to estimate a maximum rate of organic S mineralization. The maximum rate of organic S mineralization was 25 mmol m^{-2} y^{-1}, only 1-2% of the SO_4^{2-} reduction in Gerritsfles sediments so, mineralization of organic S therefore, appears to play a minor role in the overall S-cycle.

VOORWOORD

Dit onderzoek is uitgevoerd aan de vakgroep Bodemkunde en Geologie te Wageningen en aan het Nederlands Instituut voor Oecologisch Onderzoek te Niewersluis. Het project werd gefinancieerd door de Programma Commissie Basiskennis Bodemonderzoek, die ik daarvoor zeer erkentelijk ben.

De laatste regels die ik schrijf in dit boekje wil ik graag gebruiken om de mensen te bedanken die aan de totstandkoming van dit proefschrift een bijdrage hebben geleverd.

Met name wil ik mijn promotor, Prof. Dr. Nico van Breemen hartelijk bedanken voor het geven van de juiste stimulans op de juiste momenten en voor zijn waardevolle kritiek en advies met betrekking tot dit onderzoek. Nico, ik denk dat een succesvolle afsluiting van dit project mede op jou conto mag worden geschreven. Ook mijn copromotor Dr. Thomas Cappenberg ben ik erkentelijk voor zijn medewerking, en voor de vrijheid en faciliteiten die hij mij heeft geboden om op het NIOO een belangrijk deel van dit onderzoek uit te voeren.

De initiator van dit project, Tom Feijtel, wil ik bij deze bedanken voor zijn niet aflatende enthousiasme en zijn verfrissende ideeën. Tom, ik ben je zeer erkentelijk voor je inzet in de beginfase van het onderzoek en ik heb uitstekende herinneringen aan onze samenwerking.

Dit onderzoek is voor een belangrijk deel gestoeld op chemische analyses van een groot aantal monsters. De mensen van het nat lab, mineralogisch lab en het micromorfologisch lab van B&G hebben hierin een prima klus geleverd. Met name Eef Velthorst en Neel Nakken waren enthousiaste metgezellen op de vele veldtrips en ik heb veel waardering voor hun inzet en efficientie. Frans Lettink wil ik bedanken voor zijn uitermate betrouwbare vaste fase analyses.

Mijn mede-auteurs Kees Hordijk, Herman van Dam, Harm Houweling, Jan-Willem Erisman en Alfred Stein bedank ik voor hun bijdragen aan onze gezamelijke manuscripten. Kees Hordijk heeft me niet alleen in analytisch opzicht goede diensten bewezen, ook was hij een goede discussiepartner. Herman van Dam was altijd bereid om zijn uitgebreide kennis en data ter beschikking te stellen.

Tijdens mijn verblijf op het NIOO heb ik alle medewerking gekregen om mijn werk daar goed te kunnen doen en ik wil daarom al diegene bedanken die daaraan hebben bijgedragen.
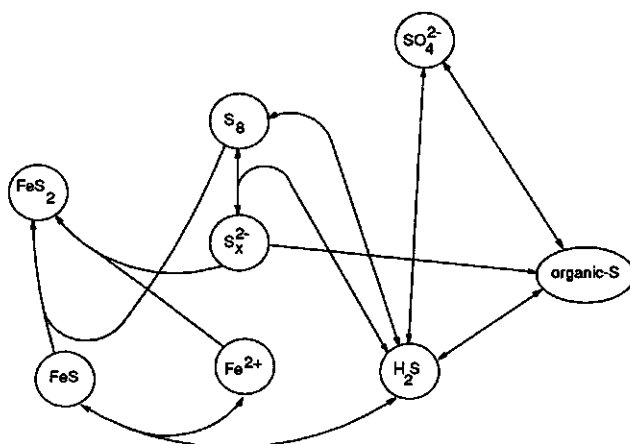
CONTENTS

Chapter 1

Introduction

Atmospheric deposition of sulfur and nitrogen has increased during the last decades over several regions of the world. Up to the seventies not much was known about the impact of atmospheric deposition on poorly buffered freshwater systems. In The Netherlands a large number of these waters are particularly situated in the non-calcareous poorly buffered regions. Most of these freshwaters are moorland pools or dune lakes, originally oligotrophic waters which are predominantly fed by rainwater. The pool waters are therefore highly sensitive to atmospheric deposition. Moorland pools act as important habitats for a diversity of flora and fauna characteristic for these environments (Van Dam 1987). Because these biota are relatively rare in The Netherlands and surrounding countries, they represent a high value for nature conservation. Many of these isolated moorland pools have been biologically impoverished through the impact of atmospherically derived acid (Van Dam and Kooyman-van Blokland 1978). This thesis deals with the sulfur dynamics in two moorland pools with emphasis on the inorganic part of the S cycle.

The sulfur cycle

Sulfur dynamics are complex since numerous biochemical reactions and interactions may occur. Figure 1 gives a simplified view of some important reactions and pathways sulfur can follow in aquatic systems. The importance of the individual pathways in the overall S cycling may be quite different for each ecosystem, depending on its environmental setting. This thesis deals with shallow isolated freshwater systems with surface waters that are continuously oxygenated. The scene of action can therefore schematically be represented by an oxic

Fig.1. Simplified scheme of sulfur transformations in sediments. More oxidized inorganic compounds are shown towards the top. Organic-S may cover a large range of oxidation states.

water column underlain by anoxic sediment that may be partly oxygenated. Biochemical reactions involving sulfur are strongly determined by redox conditions

Table 1. Oxidation states of sulfur in various compound classes in natural aquatic systems.

Oxidation state	General structure	Nomenclature
-2	R-S-H	Thiol, mercaptan Hydrogen sulfide (R=H)
-2	R-S-R'	Sulfide, thioether
-1	R-S-S-R'	Disulfide
0	$\overset{O}{\underset{}{\overset{\|\|}{R\text{-}S\text{-}R'}}}$	Sulfoxide
+2	$R\text{-}S\text{-}R'$ with O above and O below (||)	Sulfone
+2	$^-O\text{-}S\text{-}S^-$ with O above and O below (||)	Thiosulfate
+4	$R\text{-}S\text{-}OH$ with O above and O below (||)	Sulfonic acid
+6	$RO\text{-}S\text{-}O^-$ or $RO\text{-}S\text{-}OR'$ with O above and O below (||)	Ester sulfate
+6	$^-O\text{-}S\text{-}O^-$ with O above and O below (||)	Sulfate

From Anderson & Schiff (1987). R and R' may represent carbon moieties, H or nitrogen functional groups (not shown). In addition the following inorganic forms are relevant in this study: FeS, pyrite (FeS$_2$), elemental S, sulfur dioxide (SO$_2$) with oxidation states of -2, -1, 0 and +4 respectively.

and visa versa. Sulfur can occur in a variety of redox states in natural environments (Table 1). The thickness of the oxidized part of the sediment may vary in time due to mixing effects in the water column (e.g. Jørgensen and Revsbech 1985; Sweerts 1990), seasonal changes in temperature (Jørgensen and Sørensen 1985), photosynthetic activity (Spratt et al. 1987), oxygen transport by plant roots (Feijtel 1986) and sediment mixing through bioturbation (Matisoff et al. 1985). Fluctuating redox potentials in the top sediment are responsible for a more intensive cycling of sulfur.

The production of sulfide

Microbial dissimilatory sulfate reduction is a major pathway for the production of $\Sigma H_2 S$ in sediments. Sulfate reducing bacteria are obligatory anaerobic organisms which gain their metabolic energy from oxidation of organic compounds or molecular hydrogen, using sulfate (or metastabile molecules like sulfite (SO$_3^{2-}$) and thiosulfate (S$_2$O$_3^{2-}$)) as a terminal electron acceptor. The most important organic substrates that are utilized by sulfate reducers are acetate, lactate, formate and pyruvate (Bak 1988). In marine systems with high sulfate concentrations (~28 mM), sulfate reduction plays a major role (Jørgensen 1977a,

maximally 50%) in the anaerobic mineralization of organic matter in sediments. In freshwaters,where the sulfate concentration is a few orders of magnitude lower, the

contribution of sulfate reduction to anaerobic respiration may still be considerable (up to 20%, Cappenberg et al. 1984). Respiration of organic matter proceeds via a successive use of electron acceptors. If present simultaneously, the electron acceptor giving the highest energy yield will be utilized: $O_2 > NO_3^- > Fe^{3+} > SO_4^{2-} > CO_2$. The occurrence of the individual respiratory processes under natural conditions is, however, not strictly based on this socalled thermodynamic sequence. The kinetics of each process and the influence of microorganisms (e.g. the formation of metabolic products like sulfide) also help determine which respiratory processes will prevail. Furthermore these processes do not proceed in separate sedimentary strata but may spatially overlap. Jørgensen (1977b), for example, reported sulfate reduction at anaerobic micro-sites in oxic sediment.

Sulfides also can be produced by the disproportionation of thiosulfate (Bak and Cypionka 1987; Jørgensen 1990), which is the transformation of the outer S atom (oxidation state -2) to ΣH_2S and the inner S atom (oxidation state +6) to sulfate. This process does not result in a net change of redox state and is carried out by bacteria that conserve energy for growth by a type of inorganic fermentation that does not require an electron acceptor or donor. So far, microorganisms that are able to grow on disproportionation of thiosulfate (Bak and Pfennig 1987) have been found only in freshwater sediments. Thiosulfate exists in a relatively small pool in natural freshwater sediments and is expected to turn over rapidly (Jørgensen, 1990). An indirect source of sulfide is assimilatory sulfate reduction, which represents the uptake of sulfate by green plants and microorganisms and subsequent reduction and incorporation in a variety of cell components like amino acids. Through aerobic or anaerobic breakdown of these S-containing organic substances sulfides may be released. Assimilatory sulfate reduction normally plays a minor role in view of dissimilatory processes.

The fate of sulfide

Sulfides are subject to oxidation or to precipitation reactions with metals. Oxidation processes of sulfide are complex and may follow chemical and biological pathways via a large variety of sulfur species. In the oxic sediment layer, sulfide is chemically oxidized by oxygen to elemental sulfur (S_8), sulfite, thiosulfate and eventually to sulfate (Millero 1986). Below the oxic zone, were no oxygen is present, nitrate, ferric iron, manganese and probably organic molecules (Howarth 1984; Aller and Rude 1988) may serve as electron acceptor for the oxidation of sulfide. Jørgensen (1990) reported that the major part of reduced sulfur is oxidized under anoxic conditions in freshwater sediments. Once elemental sulfur is formed

this can react with water to hydrogen sulfide or bisulfide (HS⁻), polysulfides (S_x^{2-}, pH >7), thiosulfate (pH >6) or probably polythionates ($S_nO_6^{2-}$, pH <6) (Schoonen and Barnes 1991). Thiosulfate was found to be an important product of anoxic sulfide oxidation in two Danish freshwater sediments (Jørgensen 1990). Half of the sulfide was ultimately oxidized to sulfate and the other half was reduced back to sulfide via thiosulfate, forming a shunt in the S-cycle. Under neutral or alkaline conditions, elemental sulfur may react with hydrogen sulfide to form polysulfides (Chen and Morris 1972; Millero 1986). Above transformations can proceed chemically but may as well be microbiologically mediated.

Dissolved sulfides easily precipitate with iron to form various iron sulfides. Figure 2 shows a pH-redox stability diagram for minerals that are expected to occur in non-calcareous freshwater sediments. The diagram is calculated for the mean concentrations of sulfate, iron and total dissolved sulfide measured in a freshwater sediment.
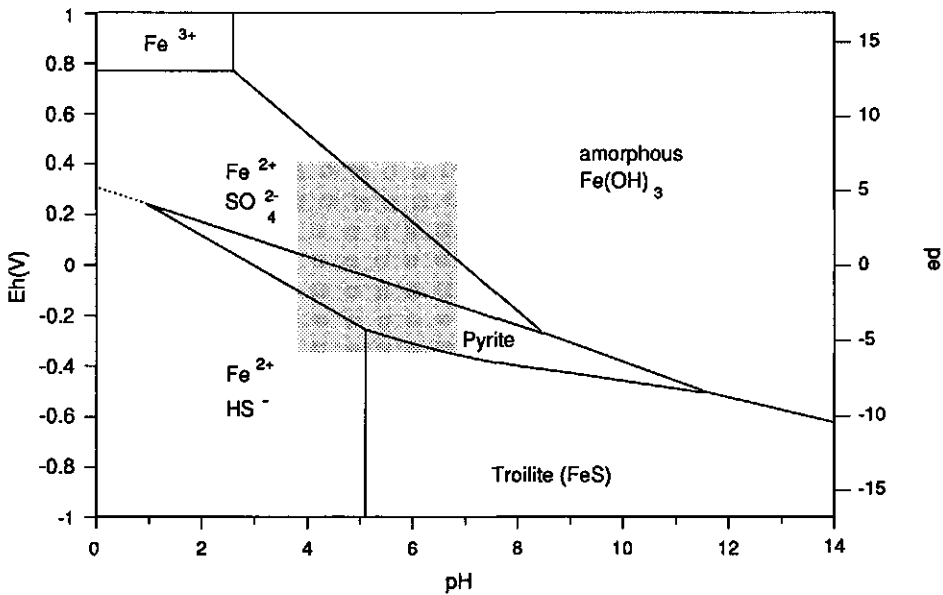
Fig.2. pH-redox stability diagram for several iron sulfide minerals in the freshwater sediment of Gerritsfles at 2 cm depth. Equilibrium constants are derived from free energy data. Free energy data of the iron sulfide minerals are by Berner (1971), amorphous Fe(OH)₃ by Lindsay (1979) and Fe²⁺, HS⁻ and SO₄²⁻ by Robie et al. (1978). Equilibrium constants for H₂S/HS⁻/S²⁻ equilibria are by Millero (1986) and the Fe²⁺/Fe³⁺ equilibrium constant by Lindsay (1979). The following concentrations are used: SO₄²⁻=52, [Fe²⁺]=60, [ΣH₂S]=12 µmol l⁻¹.

Within the pH-redox range of the sediment either pyrite or troilite (a crystalline FeS) can be stable iron sulfides. Depending on kinetics, metastable sulfides may form and persist in anaerobic bottom sediments. Pyrite may form through the sulfurization of intermediate iron sulfides like amorphous FeS, mackinawite ($FeS_{0.94}$), troilite or greigite (Fe_3S_4), which is a slow process (years, e.g. Sweeney and Kaplan 1973; Raiswell 1982) yielding framboid-like crystals. Fast formation of pyrite (hours) results in single crystals (Howarth 1979; Rickard 1975) and was proposed to form via intermediate complexes of Fe^{2+} with bisulfide or polysulfides (Luther 1991). The reoxidation of pyrite is proposed to be mediated by oxygen (Goldhaber 1983), iron (Luther 1987), or by both iron and oxygen where iron acts as a conduit for electrons travelling from pyrite to dissolved oxygen (Moses and Herman 1991). Chemical oxidation of pyrite would yield thiosulfate and sulfate as endproducts (Luther et al. 1986) while during bacterial oxidation of pyrite polysulfides and ultimately organic S products (e.g. thiols) would be formed. Finally sulfide or its oxidation products may react with humic substances to form organic S compounds (Mango 1983; Francois 1987).

Sulfur budgets

Studies on major ion budgets of lakes have demonstrated that within-lake alkalinity generation may represent an important source of buffering of incoming acid precipitation (e.g. Cook and Schindler 1983; Cook et al. 1988; Baker et al. 1988). Especially in (abiotically) poorly buffered freshwater systems as moorland pools, biological processes may play a crucial role in the buffering of the acidic load. Dissimilatory SO_4^{2-}-reduction has been recognized as a significant alkalinity generating process (e.g. Rudd et al. 1986a,b), producing one equivalent alkalinity for every equivalent SO_4^{2-} reduced. Sulfate reduction leads to permanent increases of alkalinity in water and sediment only if the sulfide produced is permanently precipitated. In North America and Norway several studies using mass budgets have been conducted to investigate how freshwater ecosystems respond on (artificial) acidification (e.g. Schindler et al. 1980; Rudd et al. 1986a,b; Baker et al. 1989). Mass budgets require detailed information on the physical, chemical and biological properties of the ecosystems and may be useful as independent information for further experimental studies or model studies (Baker et al. 1986; Kelly et al 1987, Chapter 4 this thesis).

Study sites

This study was conducted in two moorland pools Gerritsfles and Kliplo in The Netherlands (Fig.3). Some characteristics of both pools are given in Table 2. Gerritsfles (52°10'N,5°49'E, 40 m above MSL) is developed on a placic horizon (iron pan). The iron pan was presumably formed by precipitation of illuviated iron compounds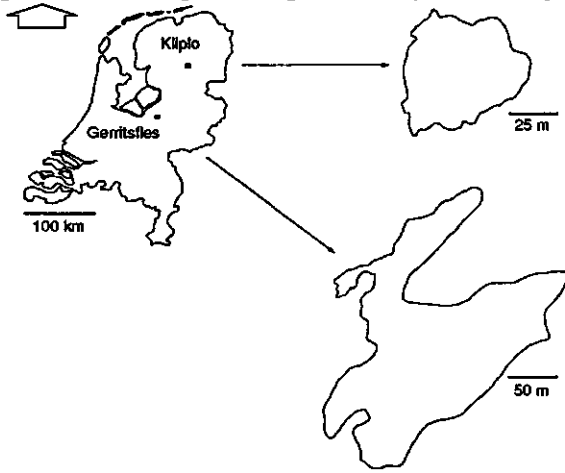 at the boundary of an aerated zone and a water-saturated substratum (Van Dam & Buskens 1993). During the first half of the 19th century, Gerritsfles rapidly developed through the large input of iron by aeolian drift sand. This influx of iron stopped around 1900 when the drift sand area was planted with Scots pines (*Pinus Sylvestris* L.). Gerritsfles is surrounded by a zone of wet podzolic soils. To the East mainly well-drained podzols occur, which developed in fine sands, often with gravelly material at shallow depth. To the West mainly drift sands are present with gravel in the subsoil (Van Dobben et al. 1992).

Fig.3. Location of the study sites in The Netherlands and their shape.

Kliplo (52°50'N,6°26'E, 13 m above MSL) probably belongs to a type of moorland pool that is developed in a hollow of cover sand created by wind action. A perched water table was formed through illuviation and precipitation of dispersed humic compounds (Van Dam & Buskens 1993). Kliplo is situated in an area with a complex of wet and dry soils without distinct soil formation. The parent material consists of non-loamy or weakly loamy fine sands (Van Dobben et al. 1992).

Outline of the thesis

The purpose of this study was to get a better insight in the S-cycling in non-calcareous poorly buffered freshwaters. Two moorland pools that have a well-defined hydrology and have been subjected to other studies (e.g. Van Dam 1987)

Table 2. Physiographical, historical (Van Dam & Buskens 1993) and chemical data for Gerritsfles and Kliplo

	Gerritsfes	Kliplo
Recent history		
Age	< 200 y	probably Subboreal
1800-1850	Origin and extension	Excavation of peat
1850-1900	Eutrophication and alkalinization by washing of sheep	Eutrophication and alkalinization by washing of sheep and rearing of ducks
1900-1950	Acidification by termination of sheep washing	Acidification by termination of sheep washing and rearing ducks
1950-1985	Strong acidification by atmospheric deposition	Slight acidification by atmospheric deposition
1985-1993	Stabilization of acidification	Stabilization of acidification
Land use in surroundings	Drift sand, heath land, shrubs and forest	Drift sand, forest
Morphometric and hydrolic properties		
Surface area (ha)	6.8	0.6
Mean depth (m)	0.7	0.8
Mean water residence time (y)	0.85	0.93
Hydrological type	Perched water table, isolated	Perched water table, isolated
Lake water 1990 (± SD)		
Mean pH	4.5 ± 0.3	(n=12)	5.1 ± 0.4
Mean Fe (μmol l^{-1})	4 ± 3	(n=12)	9 ± 5
Mean SO_4^{2-} (μmol l^{-1})	96 ± 20	(n=12)	83 ± 16
Sediment 0-6 cm (± SD)		
Mean total S (%)	0.89 ± 0.35	(n=6)	0.59 ± 0.59 (n=86)[*]
Mean organic S	0.35 ± 0.08	(n=6)	nd
Mean total C	3.3 ± 3.2	(n=102)	9.4 ± 8.1 (n=132)
Mean total Fe	0.4 ± 0.2	(n=99)	0.6 ± 0.3 (n=132)

nd: not determined, n: number of samples.
Values of sedimentary contents are means of three depths (0-2, 2-4 and 4-6 cm).
[*] Means of depths 0-2 and 4-6 cm

were chosen as locations for this research. To examine the dynamics of the sulfur cycle, the following aspects were investigated:

1) Characterization and quantification of sulfur pools in sediment and overlying water column (*In* Chapters 3 (inorganic S contents and pore water chemistry), 4 (pool and pore water SO_4^{2-} concentrations) and 5 (organic-S fractionation)). Spatial variability of chemical characteristics related to S-cycling (Chapter 6).

2) SO_4^{2-} reduction rates and transformation rates of SO_4^{2-} into organic and inorganic S fractions and S oxidation rates in sediment and overlying water column (Chapter 2).

3) The role of inorganic S, with emphasis on pyrite, in the S cycle of Gerritsfles and Kliplo (Chapter 3).

4) Chemical S-budgets in both freshwater systems using models and chemical data of pool- and rainwater and the response of pool water SO_4^{2-} concentrations on decreasing atmospheric S input (Chapter 4).

5) The mineralization rate of organic-S and its role in the overall S-cycle (Chapter 5).

Finally the main conclusions and some afterthoughts are given concerning the present study and suggestions are made for future research.

Chapter 2

Sulfate reduction and S-oxidation in a moorland pool sediment

Emile C.L. Marnette, Kees A. Hordijk, Nico Van Breemen & Thomas E.
Cappenberg

ABSTRACT.   In an oligotrophic moorland pool in The Netherlands, S cycling near the sediment/water boundary was investigated by measuring (1) SO_4^{2-} reduction rates in the sediment, (2) depletion of SO_4^{2-} in the overlying water column and (3) release of ^{35}S from the sediment into the water column. Two locations differing in sediment type (highly organic and sandy) were compared, with respect to reduction rates and depletion of SO_4^{2-} in the overlying water.

Sulfate reduction rates in sediments of an oligotrophic moorland pool were estimated by diagenetic modelling and whole core $^{35}SO_4^{2-}$ injection. Rates of SO_4^{2-} consumption in the overlying water were estimated by changes in SO_4^{2-} concentration over time in *in situ* enclosures. Reduction rates ranged from 0.27-11.2 mmol m^{-2} d^{-1}. Rates of SO_4^{2-} uptake from the enclosed water column varied from -0.5, -0.3 mmol m^{-2} d^{-1} (November) to 0.43 - 1.81 mmol m^{-2} d^{-1} (July, August and April). Maximum rates of oxidation to SO_4^{2-} in July 1990 estimated by combination of SO_4^{2-} reduction rates and rates of *in situ* SO_4^{2-} uptake in the enclosed water column were 10.3 and 10.5 mmol m^{-2} d^{-1} at an organic rich and at a sandy site respectively.

Experiments with $^{35}S^{2-}$ and $^{35}SO_4^{2-}$ tracer suggested (1) a rapid formation of organically bound S from dissimilatory reduced SO_4^{2-} and (2) the presence of mainly non SO_4^{2-}-S derived from reduced S transported from the sediment into the overlying water. A $^{35}S^{2-}$ tracer experiment showed that about 7% of $^{35}S^{2-}$ injected at 1 cm depth in a sediment core was recovered in the overlying water column.

Sulfate reduction rates in sediments with higher volumetric mass fraction of organic matter did not significantly differ from those in sediments with a lower mass fraction of organic matter.

INTRODUCTION

Sulfur cycling in aquatic and terrestrial ecosystems has received increasing attention due to concern about the potential impact of atmospheric S-deposition. Many oligotrophic moorland pools, which are widely spread over The Netherlands, are acidified due to atmospheric inputs of anthropogenically derived sulfur and nitrogen (Van Dam 1987). Oligotrophic and mesotrophic moorland pools possess a variety of characteristic fauna and flora. Due to anthropogenic activity many of these moorland pools have lost their original character. Most moorland are sensitive to acid loading because their underlying and surrounding soils are low in chemical buffering capacity. Therefore biological processes in the sediment like denitrification and SO_4^{2-} reduction are of major importance to internal alkalinization necessary to neutralize the atmospheric input of potential acidifying N and S

components.

In two of the three moorland pools studied by Van Dam (1987), where littoral sediment was exposed to the atmosphere during the dry summer of 1976, water SO_4^{2-} concentrations increased and pH decreased due to oxidation of reduced sulfur. In subsequent years, however, SO_4^{2-} reduction resulted in an increased pH and alkalinity of the pool water (Van Dam 1987). The role of SO_4^{2-} reduction in alkalinity generation of acidified lakes is well documented (e.g., Rudd et al. 1986a; Giblin et al. 1990). Cook et al. (1986) reported that nearly 60% of alkalinity generation in littoral sediments in Lake 223 (northwestern Ontario) was accounted for by net loss of SO_4^{2-} through SO_4^{2-} reduction. For every equivalent of SO_4^{2-} reduced an equivalent alkalinity is generated:

$$2\ CH_2O + SO_4^{2-}\ \rightarrow\ 2\ HCO_3^- + H_2S \tag{1}$$

Subsequently, the alkalinity is removed again when reduced S is reoxidized. For long-term or permanent alkalinity production by SO_4^{2-} reduction therefore, reduced sulfur must be immobilized by reaction with Fe or organic matter and be buried in the sediment (Giblin et al. 1990; Rudd et al. 1986a) or removed by leaching or volatilization. The net gain of alkalinity is equivalent to the removal or permanent burial of S.

In Gerritsfles, an acidified moorland pool in the Netherlands, fluxes over the sediment water interface were calculated from dissolved porewater ΣH_2S and SO_4^{2-} concentration profiles (Feijtel et al. 1989). The ΣH_2S flux over the sediment water interface may have been overestimated, however, because part of the ΣH_2S may be oxidized to S species of intermediate oxidation state, and leave the sediment unnoticed. So the S flux from the sediment to the overlying water involves partly oxidized S-species in addition to dissolved ΣH_2S. The primary aim of this study was to assess the S flux from the sediment into the water column and to estimate reoxidation rates of S to SO_4^{2-} in the overlying water.

In Gerritsfles the thickness of the detrital layer overlying quarzitic sands varies considerably. There is a large spatial variability of organic matter mass fraction and the size of the pools of reduced S in the upper 10 cm of the sediment (Marnette & Stein, 1993a) where SO_4^{2-} reduction takes place. The second aim of this study was to test the hypothesis that in organic sediments with a high mass fraction of reduced S, reduction rates were higher than in sandy sediments with a low mass fraction of reduced S.

METHODS AND MATERIALS

Study site and sample collection

Experiments were carried out in Gerritsfles (5°49'E, 52°10'N, 40 m above mean sea level), a shallow freshwater lake in the centre of The Netherlands. The pool has a simple hydrology, characterized by a small catchment area and a perched water table due to an impermeable iron pan (Schimmel & Ter Hoeve 1952). The surface area of the pool is about 5 ha and the mean depth 0.65 m. The mean pH and SO_4^{2-} concentration of the lake water are 4.4 and 102 μM respectively. Gerritsfles is located in a heath-dominated ecosystem. The sediments are unconsolidated quartz sand covered with a detrital layer. The detrital layer varies in thickness (0 - 50 cm) over the sediment area and mainly originates from peat moss (*Sphagnum*).
Sulfate reduction rates were estimated by 1) diagenetic modelling of SO_4^{2-} porewater profiles, and 2) whole core injection with radiolabelled SO_4^{2-} in the laboratory. Sulfate uptake of the sediment from the overlying water was measured from SO_4^{2-} depletion in *in situ* enclosures. Release of sulfur from the sediment into the pool water was assessed by whole core injection with radio-labelled S^{2-} in the lab. Sediment was collected by means of a coring device using Acrylic liners (5 or 7 cm diameter, 30 cm long). For diagenetic calculations, triplicate cores (5 cm diameter) were collected on November 14, 1990. Water temperature at the sediment-water interface was 8°C. The cores contained securely taped (Scotch tape no.471) 3-mm holes at 0.5-1 cm intervals. Sediment samples were obtained in the field from every core by inserting hollow stainless steel tubes through the holes. The sediment was transferred into mini-vials (maximum volume 1.5 ml) which were completely filled to minimize possible oxidation. Samples were stored at -5°C and immediately centrifuged (6000 rpm) upon return to the laboratory.

For experiments involving radiolabelled sulfate, 2 cores (7 cm diameter) were collected on July 9, 1990 at sites with either a thin surface layer (1-2 cm) of detrital material or a thick (>8 cm) detrital layer.

To assess release of sulfur to the water column, we used sediment sampled in August 1989 from an organic-rich part of the sediment. Water temperature at the sediment-water interface at time of sampling in July and August was 20°C. All cores collected at the specific sites were taken within less than 1.5 m distance from each other.

Estimating rates of sulfate reduction and sulfate uptake

1. Diagenetic modelling

Berner's (1964, 1980) diagenetic model describes the change of sulfate concentration with time as a function of diffusion, sediment accumulation and bacterial sulfate reduction:

$$\frac{\partial C}{\partial t} = D_s * \frac{\partial^2 C}{\partial x^2} - \omega * \frac{\partial C}{\partial x} - f(x) \tag{2}$$

where C represents the SO_4^{2-} concentration (µM), D_s the whole sediment molecular diffusion coefficient ($m^2\ s^{-1}$), ω the sedimentation rate ($m\ s^{-1}$) and f(x) the depth dependent sulfate reduction rate ($µmol\ s^{-1}$).

Measured sulfate concentrations were fit to the form

$$C(x) = (C_o - C_\infty) * \exp(-b * x) + C_\infty \tag{3}$$

where C_o is the sulfate concentration at the sediment-water interface (x=0) and C_∞ is the sulfate concentration at a depth below which no further concentration change occurs.

Assuming a steady state situation at the time of sampling ($\partial C/\partial t_x = 0$) with time-independent D_s, ω and f(x), the sulfate reduction rate can be expressed as

$$f(x) = (C_o - C_\infty) * (D_s * b^2 + \omega * b) * \exp(-b * x) \tag{4}$$

D_s was determined independently using the ^3H_2O technique described by Rudd et al.(1986b) and modified by Sweerts et al. (1991). The mean ^3H_2O diffusion coefficient of the upper 4-cm sediment was obtained graphically using an error function (Duursma & Bosch 1970). Experiments were executed with non-asphyxiated (with bioturbation) cores. The measured value refers to the effective or apparent diffusion coefficient in water, D_e which is the sum of D_s and the increased diffusion due to faunal activity. The diffusion coefficients of SO_4^{2-} and ^3H_2O in water (D_o) are related through

$$D_o(SO_4^{2-}) = D_o(^3H_2O) * 0.5 \tag{5}$$

(Li & Gregory 1974). D_o was corrected for temperature (Li & Gregory 1974). The change of porosity in the sediment with depth is considerable (0.95 at the sediment water interface, 0.75 at 3-4cm depth) so using a single D_s as a mean value for the

top 4 cm is not justified. D_s was estimated at 0.5 cm depth-intervals by the following procedure:

$$\theta^2 = \frac{D_o}{D_s} \qquad\qquad\qquad \text{Berner, 1980} \qquad (6)$$

$$\theta^2 = \phi * F \qquad\qquad\qquad \text{Andrews \& Bennet, 1981} \qquad (7)$$

$$F = \frac{1}{\phi^m} \qquad\qquad\qquad \text{Archie, 1942} \qquad (8)$$

where θ denotes the tortuosity [dimensionless], F the formation factor [dimensionless] (i.e., the ratio of the electrical resistivity in pore water and in whole sediment) and ϕ the sediment porosity [dimensionless].

Equations (6), (7) and (8) yield

$$D_s = D_o * \phi^{m-1} \qquad\qquad\qquad\qquad\qquad (9)$$

The mean measured diffusion coefficient was fitted by averaging D_s of each individual sediment layer calculated by eq.(9) over 4 cm depth with a single value of m for the whole column, yielding m=1.788.

Porosity used in eq.(9) was estimated from the mass fraction of water (1 g water equals 1 ml) and the dry bulk density of the sediment. Dry bulk density of the sediment was estimated from the organic dry mass, the inorganic dry mass (1.2 g/ml and 2.6 g/ml respectively: Rudd et al. 1986b) and the water content. The organic dry mass was estimated by loss of mass upon ashing at 430°C.

For the sedimentation rate 1 mm yr^{-1} was used (Van Dam, 1988b). The model is not sensitive to variations in sedimentation rates in the range of 0-5 mm yr^{-1}. A five-fold increase in the sedimentation rate would result in an increase in the calculated SO_4^{2-} reduction rate of < 6%.

2. $^{35}SO_4^{2-}$ core injection

Sulfate reduction was estimated by $^{35}SO_4^{2-}$ core injection in two ways: 1) from the activity of the formed chromium reducible (inorganic) sulfur pool (Fossing & Jørgensen 1989), 2) by depletion of radioactive sulfate in the sediment (Hordijk et al. 1985).

In each of four sediment cores (two cores with a thick organic top layer and two with a thin detrital layer), 10 μl of $^{35}SO_4^{2-}$ solution (Amersham, 17.1*10^4 Bq ml^{-1}) were injected from four directions at 1, 3, 5, 7 and 9 cm sediment depths. After a 19 to 22 hrs incubation at *in situ* temperature (20°C) the cores were sliced into 2-

cm segments. The segments were transferred immediately to 40 ml 20% (w/v) zinc acetate (ZnAc) and frozen to terminate bacterial activity and to fix sulfides. The segments were weighed before and after addition of zinc acetate and subsamples were taken for the determination of the water content. The homogenized sediment was centrifuged and 1 ml of the supernatant and 3 ml Milli-Q water were transferred into a scintillation vial for determining radioactivity. The sediment pellet was washed twice with demineralized water to remove $^{35}SO_4^{2-}$. A subsample (2-3 g) was transferred to a reaction flask and reduced sulfur was then distilled as H_2S from the sediment into two ZnAc traps (cf., Canfield et al. 1986). The traps were pooled and a 5 ml subsample was transferred into a scintillation vial for measurement of the radioactivity.

Sulfate concentrations were determined by HPLC. Because SO_4^{2-} analyses by HPLC is interfered by zinc acetate, two parallel cores at each site were collected to assess SO_4^{2-} concentration in porewater. They were sliced in 2-cm segments, centrifuged (6000 rpm) and porewater SO_4^{2-} was measured. Sulfate reduction rates (SRR) based on the activity of reduced inorganic sulfur were calculated according to the equation:

$$SRR = \frac{(SO_4^{2-}) * a * 24 * 1.06}{A * h} \ nmol \ SO_4^{2-} \ m^{-2} \ d^{-1} \qquad (10)$$

where a is the total radioactivity of ZnS, A is the total injected radioactivity, h is the incubation time in hours, (SO_4^{2-}) is the initial sulfate concentration in the sediment in nmol per cm^3 sediment, and 1.06 is a correction factor for the expected isotope fractionation (Jørgensen & Fenchel 1974).
SRR based on depletion of $^{35}SO_4^{2-}$ was calculated from (Hordijk et al. 1985):

$$SRR = \frac{(SO_4^{2-}) * \ln(\frac{A}{A_{rest}}) * 24 * 1.06}{h} \ nmol \ SO_4^{2-} \ cm^{-3} \ d^{-1} \qquad (11)$$

where A_{rest} is the rest activity of SO_4^{2-} after incubation.

To estimate abiotic removal of SO_4^{2-} in Gerritsfles sediment like SO_4^{2-} adsorption to the solid phase, Feijtel et al. (1989) measured $^{35}SO_4^{2-}$ depletion in slurries after inhibition of SO_4^{2-} reduction with Na_2MoO_4. A 96±4% recovery of $^{35}SO_4^{2-}$ was found, suggesting no SO_4^{2-} adsorption to the solid phase.

3. In situ enclosure experiment.

Although methods to assess sulfate uptake rates in underwater sediments exist (e.g. Jørgensen 1978; Berner 1964; Fossing & Jørgensen 1989), SO_4^{2-} uptake

measurements *in situ* are scarce (Kelly & Rudd 1984). Enclosures have been used to manipulate lake water conditions (e.g. Kelly & Rudd 1984; Schiff & Anderson 1987). To our knowledge, *in situ* enclosure experiments for measuring SO_4^{2-} depletion in the water column under ambient field conditions have never been done before.

A change of the SO_4^{2-} concentration in the water column can result from several processes. Dissimilatory SO_4^{2-} reduction in the sediment and assimilatory SO_4^{2-} uptake by algae, microorganisms and living *Sphagnum* can remove SO_4^{2-} from the overlying water. Abiotic processes that may remove SO_4^{2-} play a minor role in Gerritsfles sediment. On the other hand, SO_4^{2-} may be released by mineralization (conversion of carbon bonded S to SO_4^{2-} or release of SO_4^{2-} by cleavage of ester sulfates) or by bacterial or chemical oxidation of reduced inorganic S to SO_4^{2-}.

Pool water SO_4^{2-} concentrations in *in situ* enclosures were monitored to estimate net sulfate consumption rates. The enclosures were constructed from two acrylic columns with different dimensions (Fig.1). The enclosures were placed in the sediment and reached above the pool water. The wide bottom part of the column protruded 5 to 10 cm into the overlying water. The upper part of the column was narrower to reduce the water volume - sediment area ratio in the enclosure so that changes in sulfate concentration due to SO_4^{2-} reduction could be measured more accurately. Water in the enclosure was open to the atmosphere. To obtain homogeneous water samples and to avoid development of anaerobic conditions above the sediment, water in the enclosure was mixed by pumping it down from the top of the column to just above the sediment. In lab installations a methylene blue dye was used to determine minimum pumping rates giving complete mixing (within 20 minutes) without disturbing the sediment. Redox potentials measured by a Pt electrode just above the sediment-water interface indicated that permanent aerobic conditions were maintained (E_h = 724±3 mV at pH = 4.6). Without pumping the Eh dropped to -59 mV within 24 hours. Resuspension of the sediment was avoided through the use of cut-off syringes and plungers (Fig.1) that directed the water flow away from the sediment.

Enclosures were placed at highly organic, intermediate and low organic (sandy) sediment sites (23, 10 and 4% mass fraction organic matter, respectively). The water circulation in the enclosures was interrupted for one hour after each one hour of pumping to minimize battery use. Every two or three days 10-ml samples were withdrawn from the enclosures with a syringe (10 ml) and filtered through a 0.45µm millipore filter for SO_4^{2-} analysis. Three columns were installed on July 5, 1990 and were monitored for a 26 days period. A second and third series of two columns each started on July 31 and November 5, 1990, respectively and were
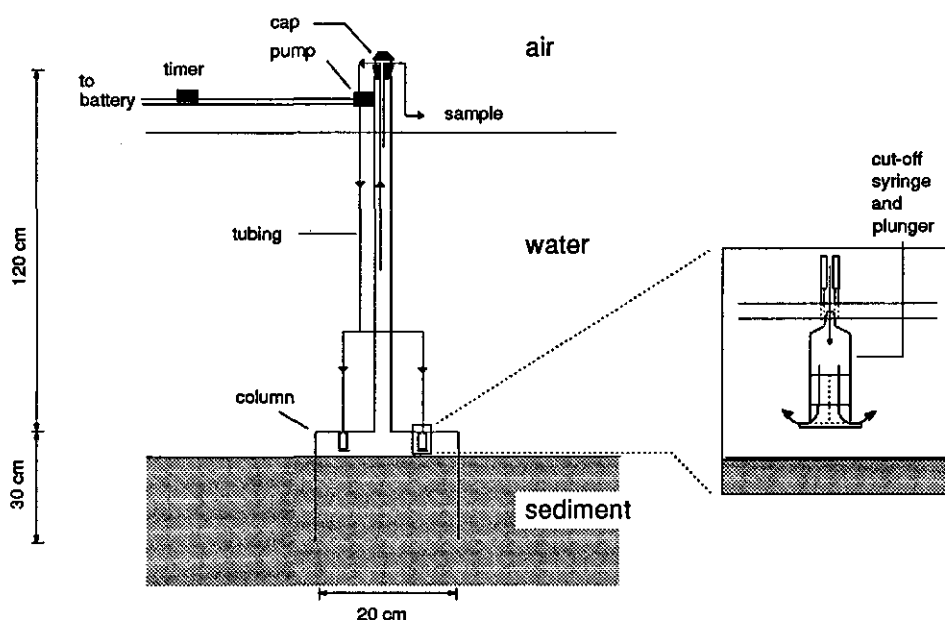
Fig.1. *In situ* enclosure for monitoring SO_4^{2-} concentrations in the overlying water column.

monitored for 9 days. At April 15, 1991, one more column was monitored for 9 days.

Release of sulfur from the sediment into the overlying water column

The release of sulfur from the sediment into the overlying water column was assessed by whole core injection of $^{35}S^{2-}$ (added as a Na_2S solution) followed by monitoring the activity of ^{35}S in the (oxygenated) overlying water. After incubation, several sulfur species were analyzed in the water column to characterize sulfur transported from the sediment. In the radioactive cores $^{35}SO_4^{2-}$ and acid volatile ^{35}sulfur (^{35}AVS) was measured.

In total three cores, which were collected on August 14, 1989 were used. To assure that $^{35}S^{2-}$ would not be injected in the oxic layer, the oxygen penetration depth in the top sediment layer of one core was assessed by means of an oxygen microelectrode as described by Sweerts et al. (1989). Oxygen did not penetrate deeper than 2.5-3.5 mm into the sediment. In the two other cores 20 µl $4.42*10^6$ Bq/ml $Na_2^{35}S$ solution (Amersham) was injected from four directions at 1 cm sediment below the sediment-water interface (total injected activity: $3.53*10^5$ Bq). The cores were incubated for about 72 h at *in situ* temperature (20°C). The

overlying water was gently stirred (4 rpm) with a motor driven impeller to maintain an aerobic, well mixed water column and a fixed diffusive boundary layer (Sweerts et al. 1989). At 2-8 hours time intervals, two 5-ml portions of the overlying water from the ^{35}S-injected cores were transferred into scintillation vials and radio activity was counted.

Analyses

Sulfate concentrations were determined by ion chromatography (Hordijk et al. 1984).

Inorganic S in sediments was assessed using the single step chromium reduction method (Fossing & Jørgensen 1989). Chromium reducible sulfur comprises ΣH_2S, S°, FeS and FeS_2.

Radio activity was counted after addition of 10 ml Instagel II (Packard) in a Packard Tri Carb 4530 liquid scintillation spectrometer for 10 minutes at a window width of 4-167 KeV. Quench corrections were made by means of the external-standard channel-ratio method using chloroform as quencher.

Radiolabelled SO_4^{2-} was measured after separation from other dissolved S species by HPLC and ^{35}AVS was determined after separation through microdistillation (Hordijk et al. 1985).

RESULTS

Sulfate reduction and sulfate uptake

1. Diagenetic modelling

The ^3H_2O sediment diffusion coefficient, D_e (in non-asphyxiated cores) of the 4-cm sediment top layer was measured as $1.26\cdot10^{-5}$ cm^2 s^{-1} at 7°C. Sweerts et al. (1991) reported in an asphyxiated core a D_s of $0.93\cdot10^{-5}$ cm^2 s^{-1} at 7°C (corrected for temperature). The difference of $0.3\cdot10^{-5}$ cm^{2}s^{-1} is relatively large compared to studies in other lakes (Sweerts, 1991), but may not be significant. Sulfate reduction rates calculated with D_s (Sweerts et al. 1991) and D_e however differed by less than 12%. Diagenetic modelling of three SO_4^{2-} profiles in Gerritsfles (eq.4), yielded sulfate reduction rates of 0.27, 0.66, and 0.38 mmol m^{-2} d^{-1}, linearly integrated over the upper 10 cm sediment (Fig.2a,b,c).
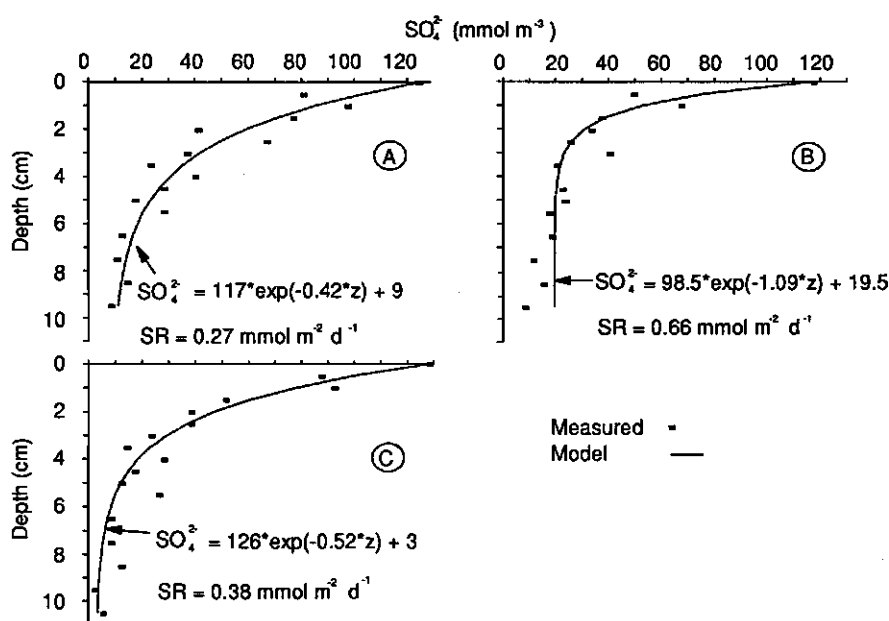
Fig.2. Porewater SO_4^{2-} concentration profiles of three organic rich sediment cores, (measured and exponentially fitted, where z is the depth below the sediment-water interface) and integrated modelled SO_4^{2-} reduction rates (SR).

2. $^{35}SO_4^{2-}$ core injection

Sulfate profiles from the duplicate cores at the organic location were not significantly different (p=0.124) while the difference between both SO_4^{2-} profiles at the sandy location (p=0.07) was greater. An inventory study on spatial variability indicated that SO_4^{2-} concentrations in sandy top sediment (0-2 cm) of Gerritsfles did not vary more than 14% (SD in % of mean, N=15, unpubl.). Since porewater SO_4^{2-} concentrations ((SO_4^{2-}), eq.10,11) and radioactivities of labelled S (a, A, A_{rest}, eq.10,11) were measured in separate cores, we calculated SO_4^{2-} reduction rates using combinations of labelled S profiles and SO_4^{2-} profiles.

Sulfate reduction rates invariably decreased with depth (Fig.3). Depth-integrated SO_4^{2-} reduction rates calculated from production of inorganic reduced ^{35}S (eq.10) were significantly (p<0.0001) lower than those based on depletion of $^{35}SO_4^{2-}$ (eq.11, Table 1). Mean depth-integrated SO_4^{2-} reduction rates in organic cores were lower than in sandy cores but the differences were not significant.

SO$_4^{2-}$ reduction rates [nmol cm^3 d^{-1}]
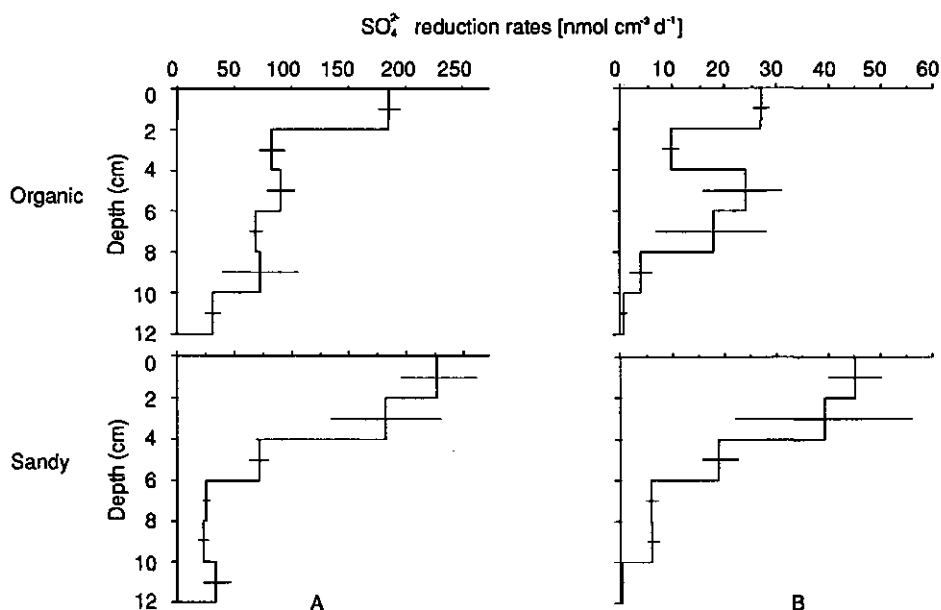
Fig.3. Variation in SO$_4^{2-}$ reduction rates with depth in organic rich and sandy cores calculated from A) rest activity of ^{35}SO$_4^{2-}$ and B) formation of inorganic ^{35}S. Note the differences between the scales. Bars indicate ±SD.

3. In situ enclosure experiment.

Rates of uptake of SO$_4^{2-}$ could be estimated by the slopes of the linear regression of changes in SO$_4^{2-}$ concentration over time ($R^2 > 0.91$, Fig.4).

An apparent decrease of SO$_4^{2-}$ (expressed in mmol m^{-2}) was observed in the overlying water in July 1990 and April 1991 (Fig.4a,b,d) while SO$_4^{2-}$ increased in November 1990 (Fig.4c). Rates of SO$_4^{2-}$ uptake are given in Table 1.

Release of sulfur from the sediment into the overlying water column

Transport of reduced ^{35}S from the sediment into the water column is illustrated in Fig.5. The duplicate results were very similar. Spatial variability between both cores did not lead to exceptional differences in ^{35}sulfur release. About 7% of the ^{35}S^{2-}-label injected at 1 cm depth in the sediment was recovered in the overlying water after 60 hours incubation. The curve shows a sigmoid shape with a short lag at the start of the incubation. There is a linear ($R^2 = 0.996$) increase of the fraction recovered activity in the water column and total injected activity during the first ca. 24 hours of 3.7% d^{-1}. Only a small fraction of the ^{35}S in the water column

Starting date July 5 1990

Sulfate (mmol m⁻²)

■ Sandy
● Intermediate
▲ Organic

A

Starting date July 31 1990

B

Starting date November 5 1990

Sulfate (mmol m⁻²)

C

Starting date April 15 1991

D

Time (days) Time (days)
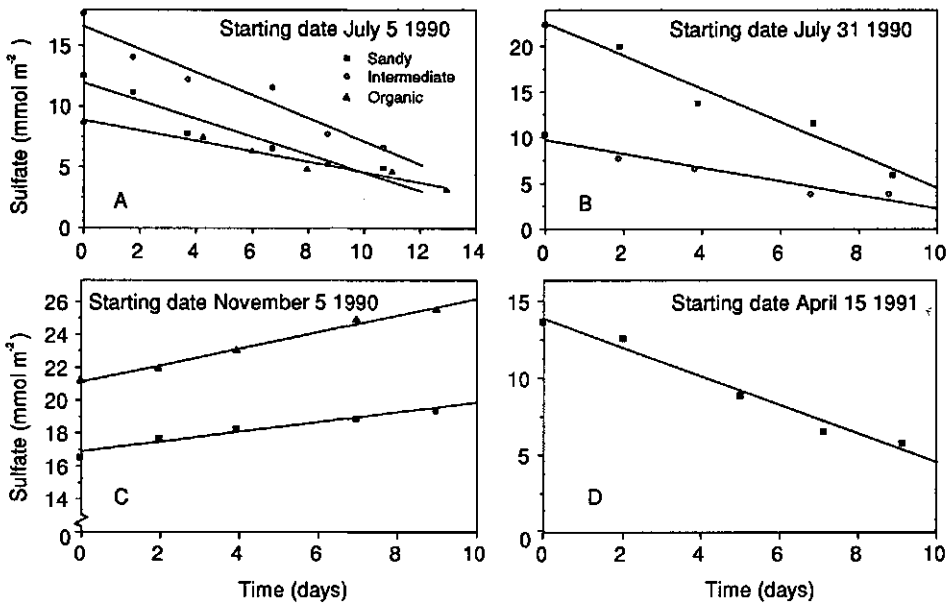
Fig.4. Change of amount of SO_4^{2-} per m^{-2} in *in situ* enclosures on sediments with high, intermediate and low (sandy) organic matter mass fractions during different periods in 1990 and 1991.

Table 1. (Net) sulfate reduction rates calculated by diagenetic modelling, determined with labelled experiments and measured *in situ*.

	diagenetic modelling	labelled experiments				*in situ* SO_4^{2-} uptake	
sediment type	org	org[1]	org[2]	san[1]	san[2]	org*	san*
Jul '90		10.7±0.7	1.7±0.4	11.2±1.9	2.3±0.5	0.43	0.73
Aug '90							1.81
Nov '90	0.27					-0.51	-0.30
	0.66						
	0.38						
Apr '90						0.94	

org = organic rich sediment, san = sandy sediment
[1] calculations based on rest activity of $^{35}SO_4^{2-}$ (±SD, N=4)
[2] calculations based on formation of reduced inorganic ^{35}S (±SD, N=4)
* %C: see Table 3
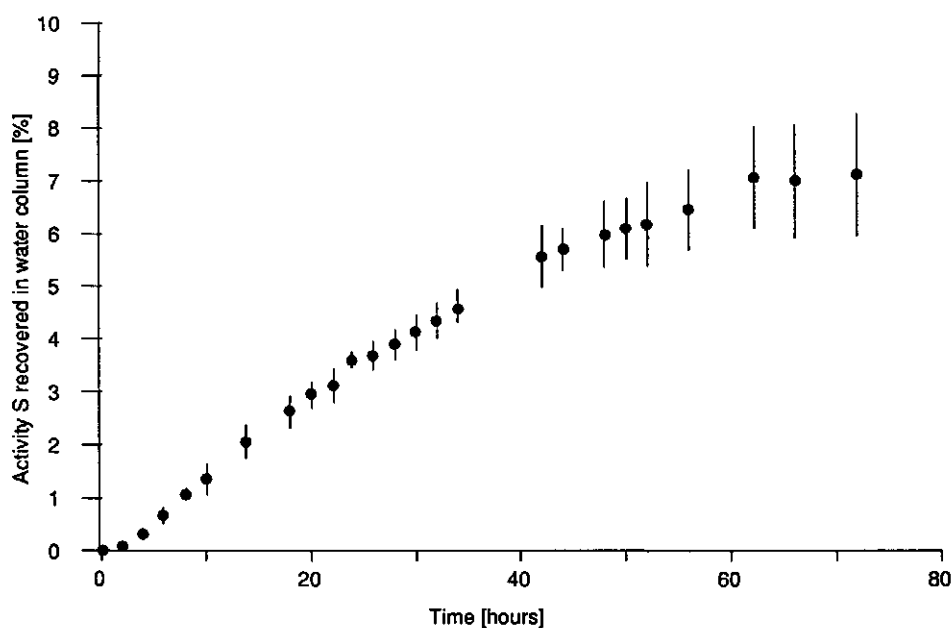
Fig.5. Mean amount of activity recovered in the overlying water column of two sediment cores injected with $^{35}S^{2-}$ at 1 cm depth versus time. The bars indicate the range of the two replicate cores.

(about 3%) consisted of SO_4^{2-} and a negligible fraction (about 0.3%) consisted of ^{35}AVS.

DISCUSSION

The value of 10.3 mmol m^{-2} d^{-1} determined by Feijtel et al. (1989) from $^{35}SO_4^{2-}$ depletion in sediment slurries from Gerritsfles agrees well with the results from the present study (10.7, 11.2 mmol m^{-2} d^{-1}). We reported a wide range of sulfate reduction rates (0.27 - 11.2 mmol m^{-2} d^{-1}) in Gerritsfles sediment. These rates are in the same order of magnitude as those reported for other sediments (Table 2). Sulfate reduction rates determined by $^{35}SO_4^{2-}$ depletion are somewhat higher than those estimated by Kuivila et al. (1989) and Ingvorsen et al. (1981) who calculated SO_4^{2-} reduction rates from formation of ^{35}AVS. However if also organic bound S and pyrite are formed, SO_4^{2-} reduction rates based on formed ^{35}AVS are underestimated. Bak et al. (1991) reported extremely high SO_4^{2-} uptake rates (20.4 mmol m^{-2} d^{-1}) when measuring SO_4^{2-} depletion from the water column of Lake Constance sediment under anaerobic conditions, but 3.5 times slower rates under

Table 2. Sulfate reduction rates in several freshwater systems

lake water SO_4^{2-} concn. (μM)	sulf. red. rate (mmol m^{-2} d^{-1})	method of determin- ation	reference
105	0.12	a[1]	Kuivila et al.(1989)
135	0.17 - 1.2	c	Sinke et al.(1990)
300	20.4	d*	Bak et al.(1991)
1200-2000	4.2	d	Herlihy & Mills (1989)
220	0.4 - 2.8	a[1]	Ingvorsen et al.(1981)
105	0.27 - 0.36	d	Kelly & Rudd (1984)
200	3.6	a[3]	Hordijk et al.(1985)
100	10.3	b	Feijtel et al.(1989)
100	1.7, 2.3	a[2]	This study
100	10.7, 11.2	a[3]	This study
100	-0.51 - 1.81	d	This study
100	0.27 - 0.66	e	This study

a: $^{35}SO_4^{2-}$ injection
  [1] based on formed acid volatile ^{35}S
  [2] based on chromium-reducible S
  [3] based on rest activity of $^{35}SO_4^{2-}$
b: slurry incubation based on rest activity of $^{35}SO_4^{2-}$
c: based on SO_4^{2-} flux over the sediment-water interface
d: loss SO_4^{2-} from water overlying cores
e: from diagenetic calculations
*: over 10 cm sediment depth

aerobic conditions.

Sulfate reduction rates estimated from $^{35}SO_4^{2-}$ depletion were 4-8 times higher than rates estimated from the accumulation of chromium-reducible (i.e., reduced inorganic) ^{35}S (Table 1). So only 12-25% of reduced $^{35}SO_4^{2-}$ is recovered as inorganic S. The remaining 75-88% is most likely transformed to organic S. Organic S was reported as a dominant initial product of dissimilatory sulfate reduction by Baker et al. (1989), Nriagu & Soon (1985) and Rudd et al. (1986a). S addition to humic substances during early diagenesis by chemical reactions between organic matter and H_2S or its oxidation products were found to be important mechanisms in marsh and marine sediments (Ferdelman et al. 1991; Francois 1987). Sediments high in sedimentary iron (>20 mg g^{-1}) typically have a large fraction of sulfur bound in iron monosulfides, but even then organically bound S may be the main initial product of sulfate reduction (Baker et al. 1989). In Gerritsfles low sedimentary iron content (about 3.5 mg g^{-1}) and undersaturation of porewater with respect to iron sulfides (Marnette et al. 1993b) may explain the

initial high formation rate of organically bound S.

Diagenetic calculation of SO_4^{2-} reduction rates obtained from porewater SO_4^{2-} concentrations ignore the possible effects of a diffusive flux of ΣH_2S over the sediment water interface followed by back oxidation of sulfide to SO_4^{2-} in the overlying water (Carignan 1988). Also possible oxidation of reduced S to SO_4^{2-} in the top sediment layer is not incorporated in the calculations and therefore diagenetic modelling may underestimate SO_4^{2-} reduction rates.

The change of SO_4^{2-} concentration in the *in situ* enclosures is a balance between several processes that consume and produce SO_4^{2-} in the sediment and water column. Some processes however are of minor importance in Gerritsfles. Sulfate consumption in sediment and overlying water is a combination of assimilatory and dissimilatory SO_4^{2-} reduction. Gerritsfles is a clear water pool without abundant growth of algae and assimilatory SO_4^{2-} uptake in the water column is negligible with respect to the observed changes of SO_4^{2-} in the enclosures. Also uptake of SO_4^{2-} by living *Sphagnum*, estimated from the annual detrital S burial flux of organic matter (15 μmol m^{-2} d^{-1}, Feijtel et al. 1989), is minor ($< 5\%$) compared to the change of SO_4^{2-} in the enclosures. Assimilatory SO_4^{2-} uptake in the sediment is relatively low compared to dissimilatory SO_4^{2-} reduction (Brown, 1986) so dissimilatory SO_4^{2-} reduction must be considered as the main SO_4^{2-} consuming process in Gerritsfles sediment. Sulfate release in the enclosures is the result of oxidation of inorganic S and mineralization of organic S compounds to SO_4^{2-}. The inorganic (dissimilatory) reduced S pool is much more susceptible to oxidation than is the organic S pool (Wieder and Lang 1988) and therefore oxidation of inorganic S compounds is likely the main source of SO_4^{2-} release in the enclosed water column. Mineralization of organic S compounds may proceed under oxic and anoxic conditions, but the conversion to SO_4^{2-} requires a final oxidative reaction, except in case of mineralization of ester sulfates. The change of SO_4^{2-} in the enclosed water column therefore may be considered as the net result of dissimilatory SO_4^{2-} reduction, oxidation of reduced S compounds and mineralization of ester sulfates.

Differences in SO_4^{2-} removal rates between July and November sediments indicate that there might be a seasonal factor controlling SO_4^{2-} removal. Although we do not have seasonal replicated observations of removal rates of SO_4^{2-} at the specific sites, the difference between the negative SO_4^{2-} uptake rates (November) and the positive SO_4^{2-} uptake rates (July, August and April) are likely to be real, because during an incubation period trends of SO_4^{2-} removal at the specific sites were similar.

In July, SO_4^{2-} removal from *in situ* enclosures was significantly lower than $^{35}SO_4^{2-}$ reduction (based on rest activity of $^{35}SO_4^{2-}$, Table 1) in the sediment. This indicates an apparent release of S into the water column. The SO_4^{2-} increase in the enclosure

in November can be explained only by a net release of S due to oxidation and mineralization of S compounds. The rather steep SO_4^{2-} gradients at the sediment-water interface (Fig.2) suggested that oxidation to SO_4^{2-} did not occur in the sediment. There was no clear subsurface peak of SO_4^{2-} that pointed to SO_4^{2-} formation from S oxidation or mineralization of ester sulfates in the sediment which could result in an upward SO_4^{2-} flux. Consequently there must have been a diffusive flux of reduced sulfur species from the sediment coupled with oxidation to SO_4^{2-} in the overlying water.

Temperature may be an important factor by controlling processes that affect sulfate removal. Low temperature in November may have caused low microbial activity allowing oxygen to penetrate deeper into the sediment. Provided microbial reduction processes would have been hampered by low temperatures more strongly than oxidation processes, this should have resulted in a net flux of oxidized S into the water column. Since no subsurface SO_4^{2-} peak was observed, the mobilized S must have involved intermediate S species that were oxidized to SO_4^{2-} only after diffusion into the water column. In July, when sediment temperatures are high (20°C), an extra S flux into the water column due to oxidation of the top sediment layer is probably not present.

A flux of reduced S into the overlying water column is supported by results of the $^{35}S^{2-}$ core injection experiment. The ^{35}S-time curve (Fig.5) shows a sigmoid shape with a short lag at the start of the incubation (the time needed for the label to move from 1 cm depth to the water column). The asymptote beyond which no further net increase of label would occur can be attributed to the lack of a constant source of label in the sediment. About 7% of the activity injected as $^{35}S^{2-}$ in the reduced sediment at 1 cm depth, was recovered in the overlying water column after 60 hours (Fig.5). It was not possible to quantify the absolute release of "cold" sulfur to the water column because $^{35}S^{2-}$ was present in heterogenous pools directly after tracer injection and therefore specific activities are not known. Only 3% of the 7% activity recovered in the overlying water column of Gerritsfles consisted of $^{35}SO_4^{2-}$ and 0.3% of ^{35}AVS. Although we do not have absolute data on reduced S release into the water, it is likely that the S flux must be much greater than the oxidation rate to SO_4^{2-} in the water column and that a large part of sulfur in the water column is present in non-SO_4^{2-} form. We do not know in which forms the remaining 97% of ^{35}S, that is not converted to $^{35}SO_4^{2-}$, ends up in the overlying water.

The thickness of the detrital layer on the quarzitic bottom of Gerritsfles did not seem to be correlated with SO_4^{2-} reduction rates in these sediments. Rudd et al. (1986b) reported that in oligotrophic lakes highly flocculent-organic sediments are

not as active microbially per unit volume as compact inorganic sediments because carbon content per unit volume is higher in the more compact sediments. In two lakes with about equal epilimnetic SO_4^{2-} concentrations, Rudd et al. (1986b) measured a much faster sulfate flux into highly inorganic Lake 320S sediments than into the organic sediments of lake 114. In Gerritsfles the carbon content per unit volume in the more compact, sandy sediments was also higher (Table 3). However, SO_4^{2-} reduction rates in the sandy sediments were not significantly different from reduction rates in organic rich sediments (Table 1). Changes in SO_4^{2-} in *in situ* enclosures were consequently smaller at the sandy sites than at sites with a thin organic layer, but the differences may not be significant.

Table 3. Organic C content per unit weight and volume and dry bulk density in Gerritsfles sediment at 0-2 cm and 4-6 cm depth.

	Depth (cm)	C (g g^{-1})	C (g cm^{-3})	Dry bulk density (g cm^{-3})
Organic rich sediment	0-2	0.137	0.025	0.18
Transition zone	0-2	0.058	0.019	0.33
Sandy sediment	0-2	0.027	0.021	0.76
Organic rich sediment	4-6	0.121	0.022	0.18
Transition zone	4-6	0.009	0.127	1.41
Sandy sediment	4-6	0.008	0.116	1.45

From real SO_4^{2-}reduction rates (based on depletion of $^{35}SO_4^{2-}$) and *in situ* SO_4^{2-} uptake (which is considered to be the result of SO_4^{2-} reduction, oxidation of organic and inorganic S to SO_4^{2-} and mineralization of ester sulfates) measured during a same period in July 1990 (Table 1), oxidation rates can be calculated at the two locations in Gerritsfles. The oxidation rate of reduced S to SO_4^{2-} at the organic site amounts 10.7-0.43 = 10.3 mmol m^{-2} d^{-1} and at the sandy site 11.2-0.73=10.5 mmol m^{-2}d^{-1}. These oxidation rates indicate that a large fraction (>90%) of reduced SO_4^{2-} is reoxidized again. We must notice however that these rates are overestimated because an unknown fraction of SO_4^{2-} is released by mineralization of ester sulfates, which is not an oxidative process. Also the unknown variation in determination of *in situ* SO_4^{2-} uptake is a factor of uncertainty, but even with a high variation of 200 or 300%, a large fraction of reduced SO_4^{2-} is reoxidized, since the net *in situ* SO_4^{2-} uptake is low compared to SO_4^{2-} reduction rates (Table 1). For a quantification of whole-lake fluxes associated with these oxidation and reduction processes on annual basis, more replicated samples at several times throughout the year would be necessary.

CONCLUSIONS

The tracer $^{35}S^{2-}$ study indicated that a part of reduced S introduced into the sediment was moved from the sediment into the overlying water. Only a small fraction of labelled S in the water column could be recovered as either SO_4^{2-} (3%) or S^{2-} (0.3%), indicating rapid transport of this mobile reduced S to organic S or S of intermediate oxidation state.

Results of whole core injections of $^{35}SO_4^{2-}$ and measurements on removal of SO_4^{2-} in overlying water in July 1990 demonstrated that there must be a (maximum) flux of reduced S from the sediment into the water column of which 10.3 (organic rich site) and 10.5 mmol S m^{-2} d^{-1} (sandy site) is oxidized to SO_4^{2-}. From SO_4^{2-} reduction rates and oxidation rates it could be calculated that >90% (this value may be overestimated) of reduced SO_4^{2-} was reoxidized to SO_4^{2-}.

With low temperature in November an additional flux of mobilized, non SO_4^{2-}-S from the sediment into the water column was observed. This result in increased SO_4^{2-} concentration in the pool water after complete oxidation.

Sulfate reduction rates in sediments with higher volumetric mass fraction of organic matter did not differ significantly from those in sediments with a lower mass fraction of organic matter.

$^{35}SO_4^{2-}$ core injections indicated that organically bound S is a major (75-88%) initial product of sulfate reduction in Gerritsfles.

An important conclusion of this study is that a model based on the SO_4^{2-} - S^{2-} redox couple and the appropriate transport equations gives a very simplified picture of S cycling in a moorland pool. In future research much more attention must be paid to inorganic S intermediates and organic S forms.

Chapter 3

Pyrite formation in two freshwater systems in The Netherlands

Emile C.L. Marnette, Nico Van Breemen, Kees A. Hordijk and Thomas E. Cappenberg

ABSTRACT. Cycling of Fe and S was investigated in sediments of Gerritsfles and Kliplo, two acidic shallow moorland pools in the Netherlands in order to reveal the importance of pyrite as a pool of inorganic S. The porewater chemistry in both pool sediments is extremely dynamic as e.g. Fe^{2+} concentrations may increase 20 fold within a time span of a month. Periodic oxidized conditions occur in the top several centimetres of the sediment. The redox status appeared to be a main factor in determining whether pyrite or a monosulfide, defined by the content of acid volatile sulfur (AVS), is formed. In Gerritsfles and Kliplo, pyrite was the most important iron sulfide phase; sedimentary FeS_2-S/AVS-S molar ratios were 32 and 55 respectively. In other lakes, where stratification caused anaerobic conditions in the hypolimnion, FeS_2/AVS ratios were <1. Morphological investigation by light and scanning electron microscopy indicated that pyrite was present as single crystals and as framboids. The framboids, mainly associated with organic matter, were thought to form in microsites where they may form slowly. The presence of a single crystal morphology point to a rapid formation of pyrite.

INTRODUCTION

Over the past decade, renewed attention has been paid to the biogeochemistry of sulfur in freshwater systems. This interest stems mainly from concern over the effects of elevated inputs of sulfur derived from industrial activity (Kelly et al. 1982; Likens et al. 1977). In freshwater systems that are located in acid sensitive areas, sulfate reduction and denitrification may consume all or most of the H^+ from acid deposition (Rudd et al. 1986b).

In sediments, decomposition of organic matter and reduction of SO_4^{2-} leads to the production of hydrogen sulfide (e.g. Berner 1970,1984; Jørgensen 1982). Part of the sulfide may react with iron and organic matter to form respectively iron sulfides (Berner 1970,1984) and organo-sulfur compounds (Kohnen et al. 1989). Another part of the sulfide may be oxidized through oxidation from solution or by oxidation of solid-phase sulfur (e.g. Millero 1986; Fossing & Jørgensen 1990; Aller & Rude 1988). The alkalinity generated by sulfate reduction is permanent when the produced hydrogen sulfide is not fully oxidized but remains buried in organic or inorganic form in the sediment.

Studies on distribution of sulfur in freshwater sediments revealed that formation of inorganic solid phase S plays an important role in sediments (Cook & Schindler 1983; Carignan & Tessier 1988) but that in other sediments organic S forms are dominant (Nriagu & Soon 1985; Rudd et al. 1986a). Of the different iron sulfides

that make up the major part of inorganic S in sediments, pyrite is most stable (Berner 1967).

Pyrite formation requires the presence of metabolizable organic matter, SO_4^{2-}, oxidizing compounds such as O_2 or Fe^{3+}, and available reactive iron. Metabolizable organic matter and SO_4^{2-} are necessary for the production of H_2S. H_2S can react with Fe^{2+} to form FeS. Oxygen or other oxidants are required to transform H_2S to a more oxidized phase which can react either directly with Fe^{2+} or via FeS to form pyrite. Most insights on pyrite formation were derived from laboratory studies or studies in marine or brackish environments (e.g., Berner 1984; Raiswell & Berner 1985; Howarth & Merkel 1984). The formation mechanism of pyrite in freshwater systems is thought to be similar to that in marine sediments (Schoonen & Barnes 1991b). Pyrite may form via an iron sulfide precursor and elemental S (e.g., Berner 1970):

$$FeS + S^o \rightarrow FeS_2 \tag{1}$$

where S^0 should be considered as a general S^0 source, consisting of reactants of solid elemental S with water (Schoonen & Barnes 1991b).

Formation of pyrite without intermediate iron sulfide precursors, was reported in salt marshes (Howarth 1979; Giblin & Howarth 1984) where porewaters were undersaturated with respect to amorphous FeS. Oxidizing activity favoured the formation of elemental sulfur and polysulfides which were thought to react directly with Fe^{2+}. The direct reaction pathway may proceed within hours, resulting in the formation of small single pyrite crystals (Rickard 1975; Luther et al. 1982). Framboidal pyrite is formed slowly (in years) via intermediate iron sulfides (Sweeney & Kaplan 1973; Raiswell 1982).

In normal marine sediments (those deposited in O_2-containing environments), pyrite formation is limited by the amount and reactivity of organic matter buried in the sediment (Berner 1984). In most marine pyritic sediments, black FeS is not found at greater depth indicating essentially complete transformation to pyrite (Berner 1970). In freshwater systems, the potential pyrite formation is generally limited by the availability of SO_4^{2-}.

In contrast to marine sediments, there have been only few direct determinations of pyrite in freshwater sediments (Nriagu & Soon 1985; Davison 1988; Giblin et al. 1990). Mean molar ratios of pyritic S to AVS-S (AVS for acid volatile sulfur, i.e the operational definition for the collective monosulfides) reported for lake sediments range widely, from 0.1 - 13 (White et al. 1990; Giblin et al. 1990; Nriagu and Soon 1985; Davison 1985) indicating that, in some systems, formation

of pyrite as an end product prevails over that of AVS.

The objectives of this study were to (1) characterize and quantify pyrite in sediments of two seepage lakes with different morphometry, trophic status and chemical characteristics (2) to evaluate environmental aspects that control the formation of FeS_2 and AVS in these lakes.

METHODS

Study sites

Gerritsfles and Kliplo are two isolated seepage lakes in the Netherlands. The lakes have a simple hydrology, characterized by small catchment areas and a perched water table due to an imperveous layer. Gerritsfles (52°10'N, 5°49'E, 40 m above MSL) is an oligotrophic lake, located in a heath-dominated ecosystem. The bottom sediments are unconsolidated quartz sands and are mainly covered with peat-moss (Sphagnum). The surface area of the pool is approximately 7 ha and during the study period the mean depth was 0.64 m. Kliplo (52°50'N, 6°26'E, 13 m above MSL), an oligo-mesotrophic lake, is also located in a quartz sand area. Kliplo has a surface area of approximately 0.5 ha and a mean water depth of 0.58 m. The western side has a strip of bog (5-10 m wide) that separates the pool from a heathland. At the southeastern side the pool has a sandy beach. Otherwise the pool is enclosed by forest.

Solid phase analyses

In Gerritsfles and Kliplo, duplicate sediment cores (7cm diameter) were collected on 23 October 1991 with a sediment corer as described by Ali (1984). In an anaerobic glove box the cores were sectioned in 2-cm slices. Subsamples were taken for acid volatile sulfur (AVS) and pyrite analyses. Samples for FeS analysis were stored at 4°C under N_2, samples for analyses of pyrite and reactive Fe were freeze-dried, finely ground and stored under N_2. The bulk samples were dried at 70°C and water contents were measured. Subsequently the samples were finely ground and used for determination of organic matter content.

Organic matter content was estimated by the mass loss upon ignition to 450°C. Organic C was calculated by dividing the organic matter content by 1.68, a factor based on earlier work on the relation between weight loss on ignition and organic C content of a large number of samples from Gerritsfles and Kliplo (R^2=0.93, N=95, unpubl.). Porosities and bulk densities of the samples were estimated from

the contents of water and organic matter using specific densities of H_2O (1.0 g cm^{-3}), mineral sediment (2.6 g cm^{-3}) and organic matter (1.2 g cm^{-3}) (Håkanson & Janson 1983; Hillel 1980; Sweerts et al. 1991).

AVS from Gerritsfles and Kliplo samples was determined by sparging 1-3 g of wet sediment with high purity grade N_2 after addition of 8 ml of 12 M (concd) HCl (Wieder et al. 1985). The sample was heated to boiling and the liberated sulfide was trapped in 50 ml of 5% (w/v) zinc acetate. Sulfide was measured with a spectrophotometer as a methylene-blue complex (modified after Johnson & Nishita 1952).

Pyrite was assessed through an assay of pyritic Fe after extraction of non-pyritic Fe with HF and oxidation of pyrite with HNO_3 (Begheijn et al. 1978). Iron was determined colorimetrically with orthophenanthroline (Begheijn et al. 1978). Three pyrite standards (ca. 25 mg) were run. The standards were made of ground pyrite which was previously treated with HCl and HF. The recovery of the standards was >95% (N=3).

Reactive Fe was analyzed on a separate subsample of freeze-dried sediment. Reactive Fe was defined as Fe that is removed by shaking 0.1 g of sediment overnight with 15 ml of cold 5.5M HCl (Giblin et al. 1990). The supernatant was analyzed on Fe by atomic absorption spectrometry. Cold 5.5 M HCl may extract Fe from the exchange complex, Fe from AVS, most iron oxides, $FeCO_3$, Fe between clay lattices and also Fe from organic complexes (Giblin et al. 1990).

Water analyses

Sampler

Porewater in Gerritsfles and Kliplo was sampled by *in situ* dialysis using a sampling device ("peeper", lxhxw=60x30x4 cm) that contained 10 membrane cells with slits parallel to the sediment-water interface (modified after Oenema 1990), covered with a 0.2 μm biologically inert acrylic copolymer membrane filter (Versapor-200: Gelman Sciences). The upper 6 cells (width of slit 5 mm) of the peeper contained about 40 ml, the lower 4 cells (width of slit 1 mm) about 80 ml.

At both ends, the cells were connected with tygon tubes to sampling ports at the water surface. The samplers were installed by a SCUBA diver at the end of November 1989. Because porosity and tortuosity effects retarded equilibration in the sediment, porewater was sampled only once a month. Poolwaters were collected in an acid-washed 100ml polypropylene bottle. Poolwater and porewater were sampled starting from January throughout December 1990.

Sampling and analyses

Porewater samples of Gerritsfles and Kliplo were withdrawn with a syringe at one sampling port while N_2-gas was pumped into the other port. The first 5 ml sample were discarded. A second 5 ml portion was used for analyses of dissolved sulfides (ΣH_2S^{2-} ie $H_2S+HS^-+S^{2-}$). The sample was injected into a 30 ml serum bottle that was preflushed with N_2 and that contained 5 ml of a 2% Zn-acetate/acetic acid buffer (20 g Zn-acetate + 0.2 ml 100% acetic acid per litre, Pachmayr 1960) to fix the sulfides. Dissolved sulfides were measured with a spectrophotometer as a methylene-blue complex (modified after Johnson & Nishita 1952). A third portion of 5ml was used for pH measurement. The pH was measured with a combination electrode immediately after sampling. A final 10-50 ml portion, withdrawn with a 50ml-syringe, was used for analysis of sulfate, total dissolved Fe and dissolved inorganic carbon (DIC). Fe that had crossed the peeper membrane was thought to be Fe(II) (Kelly et al. 1984). Sulfate was measured by High Performance Liquid Chromatography (KH-phtalate, pH 4 as eluent). Dissolved Fe was measured with an atomic absorption spectophotometer after acidification with HCl to pH 2. DIC was determined using a TOC analyzer (Thermo Instruments). In pool waters field-pH, sulfate, total dissolved Fe and DIC were measured. Samples were stored at 4°C prior to analysis.

Porewater equilibrium calculations

Solubility calculation offers a method to evaluate the possible regulation of metastable iron sulfides on pore water composition. Saturation indices (SI) with respect to amorphous FeS (FeS(am)), mackinawite ($FeS_{0.94}$) and greigite (Fe_3S_4) were calculated using ion activity products (IAP) of measured pore water Fe^{2+}, ΣH_2S concentrations and pH assuming equilibrium with orthorhombic sulfur (Schoonen & Barnes 1991a):

$$Fe_xS_xS_y(s) + xH^+(aq) \rightleftharpoons xFe^{2+}(aq) + xHS^-(aq) + yS(s) \qquad (2)$$

$$\log(IAP) = \log\left(\frac{[Fe^{2+}]^x \cdot [HS^-]^x}{(H^+)^x}\right) - C \qquad (3)$$

where [ ] is the solute concentration and (H^+) the activity of hydrogen ions as defined by the measured pH. Concentrations were corrected for non-zero ionic strength (<0.1 mol l^{-1}) by using the Guntelberg correction (C in Eqn.(3), Stumm & Morgan 1970):

$$C = 0.5 \cdot (xz^2_{Fe^{2+}} + xz^2_{HS^-}) \cdot \sqrt{I}/(1 + \sqrt{I}) \tag{4}$$

where z denotes the ionic charge and I the ionic strength in mol l^{-1}.
The saturation index was then calculated as follows:

$$SI = \log(IAP) - \log(K_{Fe_xS_xS_y}) \tag{5}$$

SI>0 indicate supersaturation with respect to $Fe_xS_xS_y$ and SI<0 indicate undersaturation. In Eqn.(4), the average ionic strength of the porewater was used, calculated for a subset of samples based on analyses of all major cations and anions. The average ionic strength for Gerritsfles was $8\cdot10^{-4} \pm 3\cdot10^{-4}$ (mean ± s.d., N=329) mol l^{-1} and for Kliplo $9\cdot10^{-4} \pm 3\cdot10^{-4}$ (mean ± s.d., N=227) mol l^{-1}. Concentrations of HS^- were calculated using the first and second dissociation constant of H_2S. pK1 was corrected for temperature using appropriate equations from Millero (1986). The solubility product of FeS was temperature corrected using van 't Hoffs equation:

$$K_T = K_{298} \cdot EXP(\frac{\Delta H^o_r}{R} \cdot (\frac{1}{298} - \frac{1}{T})) \tag{6}$$

where ΔH^o_r is the enthalpy of reaction at 298°K, K the solubility product, T the absolute temperature and R the gas constant. Since ΔH^o_r values of FeS(am) could not be found from literature, ΔH^o_r was taken from a crystalline FeS phase (troilite; -5193 J mol^{-1}, Robie et al. 1978). The SI values of FeS(am) are upper limits, because organic and inorganic complexation of Fe was not considered. Furthermore, we used the ΔH_r of troilite to correct the solubility product of an amorphous FeS phase for temperature. For thermodynamic reasons, these calculations then overestimate the SI's (G^o_f and S^o_f of an amorphous phase are higher than for a crystalline phase, so, because $G^o_f=H^o_f-TS^o_f$, H^o_f is also higher. Since $\Delta H^o_{r,amorph.FeS}=H^o_{f,Fe}+H^o_{f,HS}-H^o_{f,amorph.FeS}$, the reaction enthalpy ΔH^o_r for amorphous FeS is lower than for a more crystalline phase. Using Eqn.(5) and (6) at temperature < 298°K, we calculate algebraically lower SI values for an amorphous phase than for a crystalline phase). For mackinawite, greigite and pyrite, the reaction enthalpies could not be calculated so SI's were not corrected for temperature.

Micromorphology

Duplicate cores (7 cm diameter) were collected and subcores were taken with a cut-off, sharpened 50-ml syringe. While slowly inserting the syringe, the plunger

was kept at the same place, so there was little or no compaction. The syringes were deep-frozen and sawed into 0.5-cm slices. Subsequently the slices were freeze-dried. Because the top sediment of Gerritsfles and Kliplo consists of colloidal material (porosities > 0.9), some disturbance of the sediment structure through freezing and freeze-drying could not be avoided. The dried slices were impregnated with a polyester resin under vacuum. After the resin was hardened, an uncovered polished 30 μm thick thin section of each slice was prepared (Fitzpatrick 1970). Micromorphology of the sections was studied with a Leitz microscope using plain polarized light and a combination of plain polarized and incident light. With the used optical technique, single angular crystals of pyrite smaller than about 5 μm can not be observed.

For further identification of pyrite, isolation of micro-quantities of *in situ* spherical opaque framboids in the uncovered thin sections was performed with a microscope-mounted drill (Verschuren 1978). An X-ray diffraction pattern was obtained with a Philips PW1000-PW1710 diffractometer by using a scan speed of $0.01°$ (2θ) sec^{-1}.

The framboids and also small single pyrite crystals which could not be observed by light microscopy were investigated by using a Cambridge Instruments Stereoscan 240 scanning electron microscope (SEM) and electron dispersive X-ray (EDX) microanalyses.

RESULTS

Solid phase

Water content, organic matter content, porosities and bulk densities of Gerritsfles and Kliplo sediments are shown in Table 1. Decreasing water content and organic matter content with depth are reflected by increasing bulk densities with sediment depth. Solid phase contents have been expressed as volumetric mass fractions to minimize effects of spatial variation of sediment bulk densities on vertical trends in concentrations.

Carbon contents in Gerritsfles sediment are about constant with depth ranging between 14-23 mg C cm^{-3} (Fig.1). In Kliplo, C contents slowly increase with depth from about 13 near the surface to 33 mg C cm^{-3} at 20 cm with occasional erratic peaks at 9 cm and at 20 cm depth.

AVS contents in the sediments of both pools are low relatively to pyrite (Fig.1). In Gerritsfles contents range from about 0.5-1.7 μmol cm^{-3}, and slowly decrease with depth. In Kliplo AVS contents are somewhat lower; 0.3-0.7 μmol cm^{-3} and are

Table 1. Water content, organic matter content dry bulk density and porosity for Gerritsfles and Kliplo sediments in replicate cores (C1 and C2).

	depth (cm)	water (g g^{-1} dry sed.)		org C (g g^{-1} dry sed.)		porosity (cm^{-3} H$_2$O cm^{-3} dry sed.)		bulk dens. (g dry sed. cm^{-3} wet sed.)	
		C1	C2	C1	C2	C1	C2	C1	C2
Gerritsfles	0-2	5.94	4.57	0.17	0.13	0.93	0.91	0.16	0.20
	2-4	3.25	3.81	0.10	0.17	0.88	0.89	0.27	0.23
	4-6	2.44	3.12	0.11	0.12	0.85	0.88	0.35	0.28
	6-8	2.00	3.01	0.07	0.10	0.83	0.87	0.41	0.29
	8-10	1.80	2.36	0.06	0.10	0.81	0.85	0.45	0.36
	10-12	1.63	1.86	0.07	0.07	0.80	0.82	0.49	0.44
	12-14	1.46	1.82	0.06	0.09	0.78	0.81	0.53	0.45
	14-16	1.30	1.53	0.06	0.07	0.76	0.79	0.58	0.51
	16-18	1.02	1.18	0.05	0.06	0.71	0.74	0.70	0.63
	18-20	0.76	0.94	0.03	0.05	0.65	0.70	0.86	0.74
Kliplo	0-2	6.76	6.44	0.17	0.16	0.94	0.93	0.14	0.14
	2-4	2.45	1.82	0.10	0.08	0.85	0.81	0.35	0.45
	4-6	1.74	1.52	0.09	0.08	0.80	0.78	0.46	0.52
	6-8	1.52	1.32	0.08	0.08	0.78	0.76	0.52	0.57
	8-10	1.32	1.21	0.07	0.13	0.76	0.73	0.58	0.61
	10-12	1.19	1.02	0.09	0.07	0.74	0.71	0.62	0.70
	12-14	1.09	0.96	0.07	0.08	0.72	0.70	0.66	0.73
	14-16	1.05	0.93	0.09	0.08	0.71	0.69	0.68	0.74
	16-18	0.95	0.99	0.08	0.08	0.69	0.70	0.73	0.71
	18-20	1.18	1.87	0.14	0.30	0.73	0.78	0.61	0.42

rather constant with depth.

In Gerritsfles contents of pyrite range from 11-96 μmol cm^{-3} with a clear peak at 2-8 cm below the sediment surface (Fig.1). In Kliplo pyrites show a small subsurface peak and slowly decreases with depth ranging from 8-46 μmol cm^{-3}.

In both pool sediments reactive Fe (5.5 N HCl extractable Fe) increases with depth. In Gerritsfles reactive Fe range from 2-11 μmol cm^{-3} (Fig.1) and in Kliplo reactive Fe is slightly higher (3-17 μmol cm^{-3}). Gerritsfles and Kliplo sediments lack clay. Porewaters of Gerritsfles and Kliplo were invariably highly undersaturated with respect to FeCO$_3$ (siderite) as could be calculated from DIC, H and Fe concentrations, so FeCO$_3$ is assumed to be absent. AVS in Gerritsfles sediment makes up 5-69% (mean 24%) and in Kliplo 2-20% (mean 7%) of total reactive Fe, so in Kliplo more Fe is available to react with sulfides than is in Gerritsfles. The fraction of total reactive Fe not present as AVS is probably Fe(III) oxides and/or organically complexed Fe.

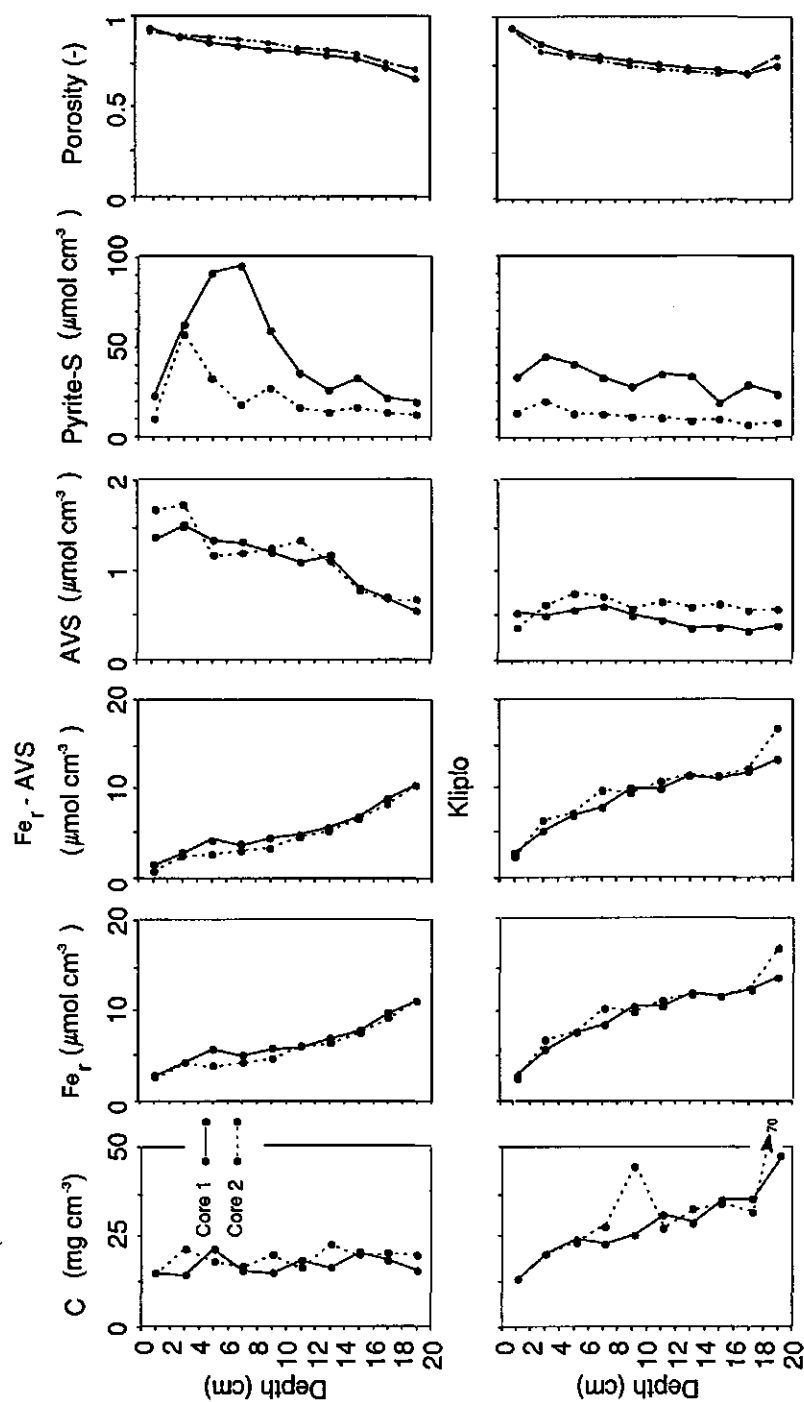**Fig.1.** Contents of C (mg cm^{-3}), reactive Fe, reactive Fe minus AVS-Fe, AVS and pyritic S (μmol cm^{-3}) and porosity (cm^3 cm^{-3}) with depth in Gerritsfles and Kliplo sediments, sampled at 23 Oct. 1991. The AVS-S:AVS-Fe ratio has been taken as 1.
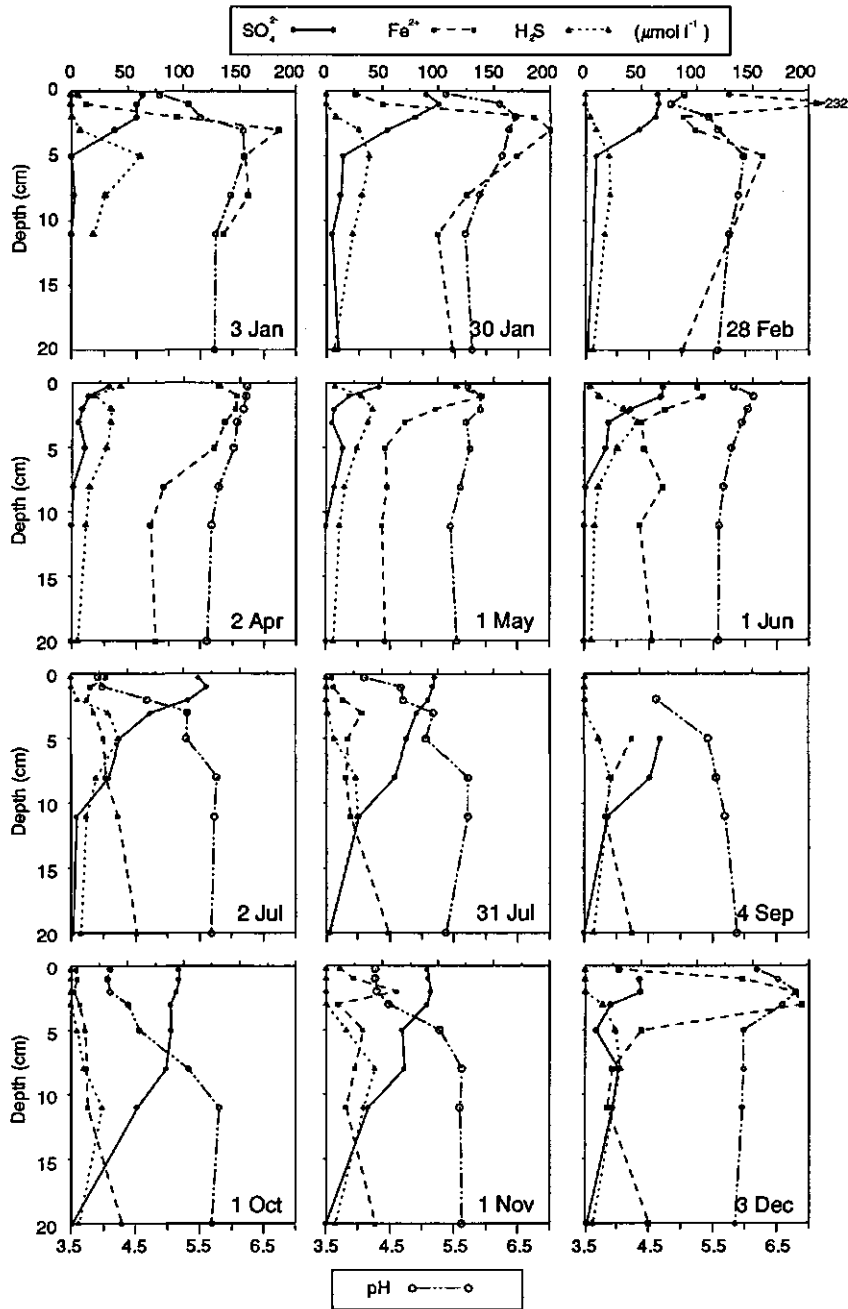
Porewater

Mean porewater pH and concentrations of SO_4^{2-}, dissolved Fe and sulfides during 1990 are given in Table 2. Concentrations of porewater SO_4^{2-}, Fe and sulfides in Gerritsfles sediment are significantly higher ($p<0.0001$) than in Kliplo sediment whereas the mean porewater pH in Gerritsfles is slightly, but significantly ($p<0.05$), lower than in Kliplo.

Porewater chemistry in Gerritsfles and Kliplo is dynamic (Figs.2,3, note the difference in scales between Gerritsfles and Kliplo). Porewater SO_4^{2-} and $\Sigma H_2 S$ concentrations show a classical antagonistic pattern in sediments of both pools as a result of SO_4^{2-} reduction. Porewater $\Sigma H_2 S$ concentrations at the surface sediment of Kliplo are elevated between April (sampling date 1 May) and September (Fig.3). Concomitantly, concentrations of Fe^{2+} and the pH increase and SO_4^{2-} concentrations decrease at the surface sediment. The same phenomena can be observed in Gerritsfles sediment, between February and June (Fig.2).

Micromorphology

Thin sections were examined to establish the morphology of pyrite. Both in Gerritsfles and Kliplo pyrite appeared to occur in framboids varying from 15 to about 25 µm (Plates 1, 2 and 3). The opaque spheres in Plates 1a and 2a are typical framboids which is evidenced by the reflectance of the incident light (Plates 1b,2b) by the individual crystals that make up the framboids. The XRD pattern of the framboids isolated from the microsite shown in Plate 2, revealed low but distinct peaks at 2.21, 2.42, 2.71 and 3.14 Å, typical of pyrite (JCPDS card file # 6-710). SEM-EDX analysis of a framboid (Plate 3) yielded a stoichiometry of 1:2.1 (Fe:S). Semi-quantitative observations revealed a decrease of the number of framboids with depth. Nearly all visible pyrite framboids were associated with organic matter and located within cell structures of partly decomposed organic matter (Plates 1 and 2). Scanning electron microscopy revealed that single pyrite crystals (Plate 4) were present, which were not necessarily associated with organic material. The stoichiometry (Fe:S) of several single crystals was ranged from 1:1.66 to 1:2.10.

Fig.2. Concentrations of SO_4^{2-}, dissolved Fe, ΣH_2S (µmol l^{-1}) and pH with depth in porewaters of Gerritsfles during 1990.
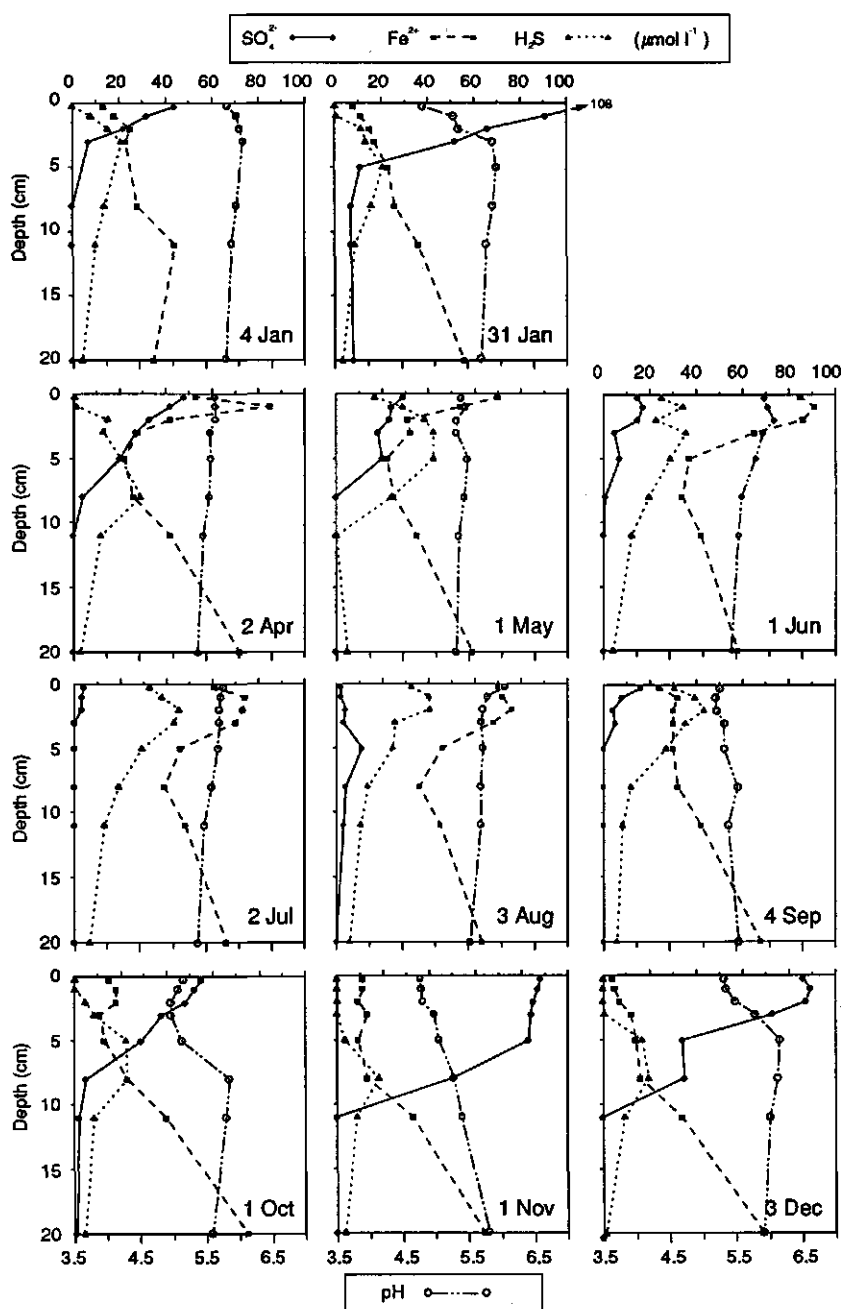
Fig.3. Concentrations of SO_4^{2-}, dissolved Fe, ΣH_2S (µmol l^{-1}) and pH with depth in porewaters of Kliplo during 1990.

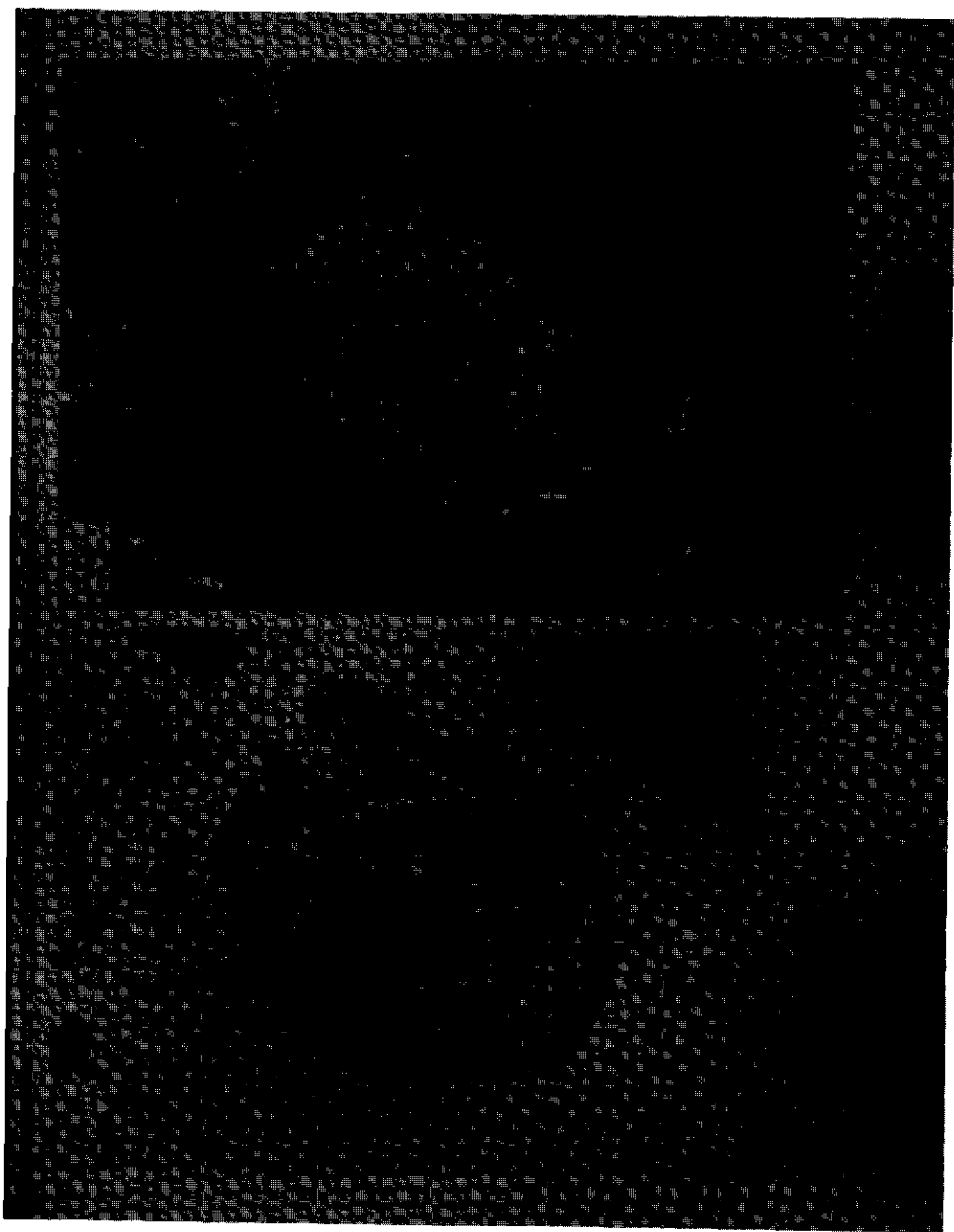**Plate 1a,b.** Pyrite framboids (1) in plant tissue (2) in Kliplo sediment, photographed with a) plain polarized light and b) incident light.
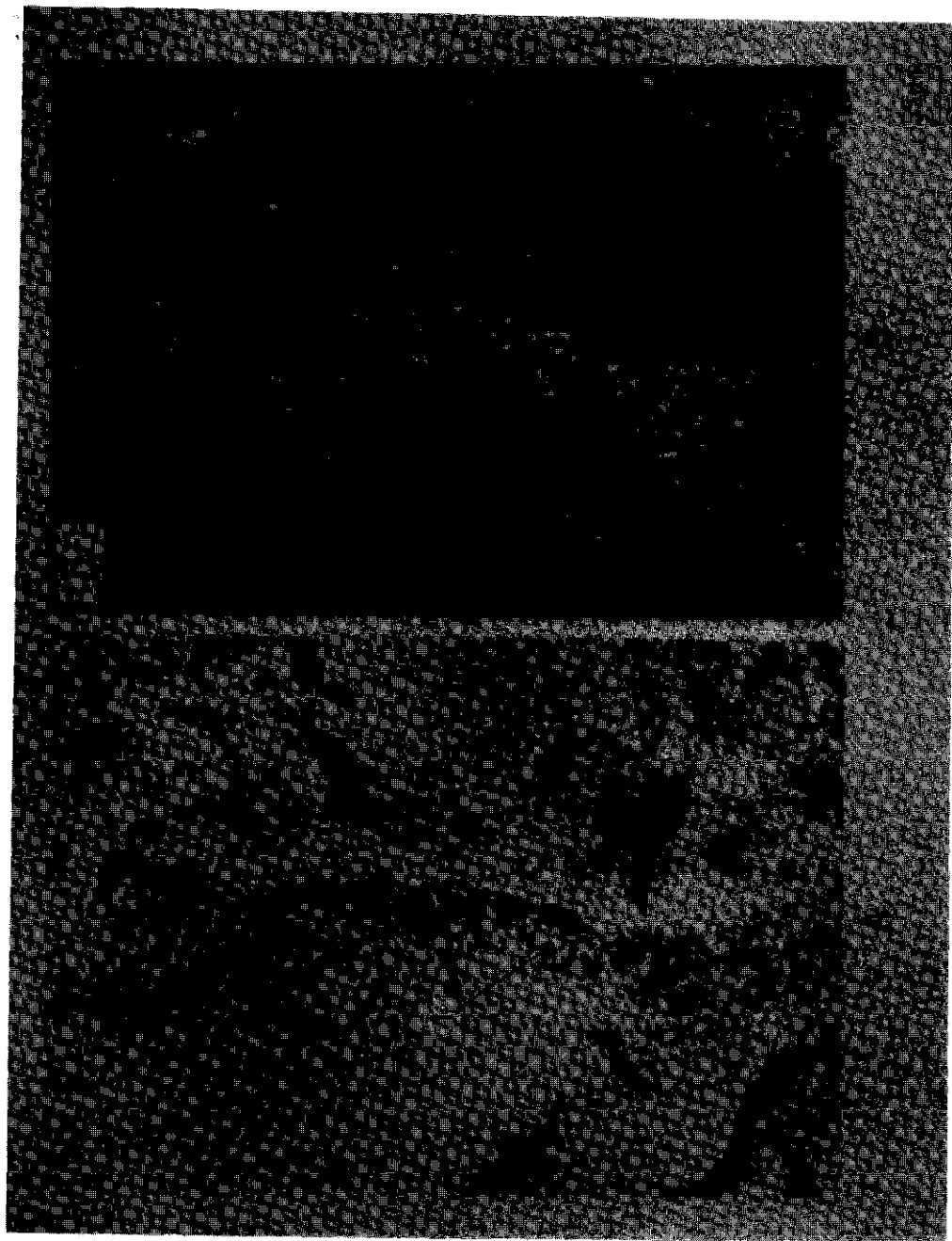
Plate 2a,b. Pyrite framboids (1) in plant tissue (2) in Gerritsfles sediment, photographed with a) plain polarized light and b) incident light.
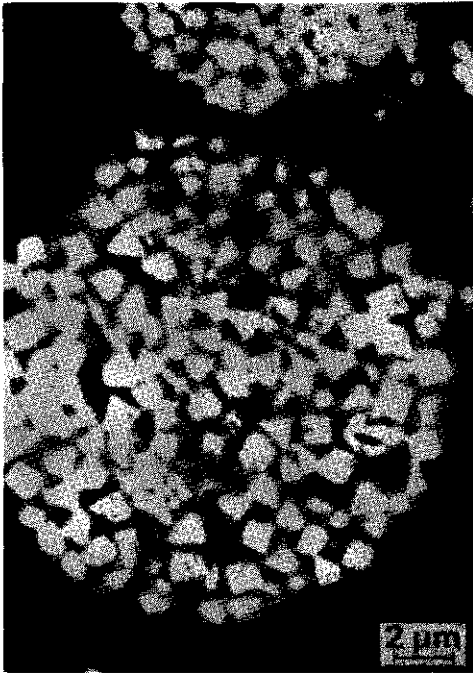
Plate 3. SEM micrograph of a pyrite framboid.

Plate 4. SEM micrograph of single crystals of pyrite. Fe:S ratios determined by SEM-EDX analyses were 1) 1:2.01, 2) 1:1.94, 3) 1:1.66 and 4) 1:1.90.

DISCUSSION

Factors that may influence the formation (rate) of pyrite in freshwater sediments are: 1) availability of easily metabolizable organic substrates 2) supply of sulfur 3) availability of reactive Fe 4) pH of porewaters 5) redox state of the sediment and 6) sedimentation rate.

Organic substrates and supply of sulfur. Supply of SO_4^{2-} and organic substrates to sediments is required for sulfate reducing bacteria to produce sulfides which are (indirectly) needed to form pyrite. Organic substrates become available after mineralization of accumulated sedimentary organic matter. In Gerritsfles the bottom sediments are mainly covered by peat-moss (*Sphagnum*). Bottom vegetation in Kliplo is scarce, but abundant growth of algae provides organic input for microbial

processes in the sediment (Van Dam 1987). The supply of SO_4^{2-} in Gerritsfles and Kliplo is limited to wet and dry atmospheric deposition (Van Dam et al. 1987). We assume sulfate reduction in these sediments to follow first order kinetics (Feijtel et al. 1989) and hence to be SO_4^{2-} limited. Zerovalent sulfur, S(0), either in the form of solid, dissolved elemental sulfur or polysulfides is necessary to the formation of pyrite. Dissolved elemental sulfur is unlikely a reactant in the formation of pyrite because it is highly insoluble in water (Boulegue 1978). Solid elemental sulfur however may function as reagent with water to produce hydrogen sulfide (or bisulfide) and, dependent on pH, polysulfides (pH>7), thiosulfate (pH>6) (Schoonen & Barnes 1991) and probably polythionates (pH<6, Arnston et al. 1960). The source of S(0) in Gerritsfles and Kliplo sediments is most likely the oxidation of ΣH_2S. In the very top sediment layer, O_2 may function as electron acceptor, while in reduced sediment Fe(III) oxi-hydroxides, organic carbon compounds or probably even bicarbonate have to be considered as possible electron acceptors (Fossing & Jørgensen 1990).

Iron. The supply and availability of sufficient reactive Fe is essential to the formation of pyrite. Poolwaters of Gerritsfles and Kliplo are low in dissolved Fe (Table 2) because they are only fed by rain and oxygenated throughout the year. Concentrations of Fe in the porewater are generally higher than in the overlying water (Table 2, Figs.2,3) so supply of Fe through diffusion from the water into the

Table 2. Mean, standard deviation (SD), range and number of samples (N) of pH and concentrations of dissolved Fe, SO_4^{2-} and ΣH_2S (μmol l^{-1}) in poolwater and porewater of Gerritsfles and Kliplo over 1990.

	poolwater					porewater			
	mean	SD	range	N		mean	SD	range	N
Gerritsfles									
pH	4.5	0.3	4.1-5.3	12		5.4	0.7	3.8-6.8	117
Fe	4	3	1-13	12		60	57	2-236	113
SO_4^{2-}	96	20	58-138	12		52	37	0-121	112
ΣH_2S	nd					12	14	0-61	111
Kliplo									
pH	5.1	0.4	4.4-5.9	12		5.5	0.4	4.7-6.5	109
Fe	9	5	1-18	12		34	24	2-91	109
SO_4^{2-}	83	16	50-118	12		30	32	0-108	109
ΣH_2S	nd					14	13	0-46	108

nd : not determined

sediment is negligible. In these types of sediments Fe may be supplied indirectly through burial of Fe(III) after oxidation of Fe(II) which has diffused from the sediment into the lake water. Fe(III) enrichments are commonly observed at or near the sediment-water interface (Carignan and Tessier 1988; Carignan & Nriagu 1985). The continuous burial and reduction of Fe(III) by sulfides or bacteria below the oxic zone serves as a source of Fe^{2+} porewater which may react to iron sulfides or diffuse upward to form new oxy-hydroxides (Carignan & Tessier 1988; White et al. 1989). Temporal increase of dissolved Fe^{2+} in porewaters may result from different processes like pyrite oxidation, reduction of Fe(III) oxides by sulfides or redissolution of FeS. Elevated Fe^{2+} concentrations in porewaters of Gerritsfles and Kliplo are observed exclusively at more reduced conditions (Fig.4), suggesting that not oxidation of iron sulfides but reduction of Fe(III) oxides is responsible for the high Fe^{2+} concentrations in the top sediment. Concentrations of Fe^{2+} rival those found in salt marshes by several workers (Giblin & Howarth 1984; Luther et al. 1991). When substracting AVS (assuming a molar ratio of S:Fe=1) from reactive Fe and considering the remaining Fe content to be Fe(III) oxides, we found no surficial enrichments of Fe(III) oxides in Gerritsfles and Kliplo (Fig.1). The sediment of Gerritsfles is enriched in Fe through formation of Fe sulfides. This can be illustrated by substituting the mineral part of the sediment by material of which it originally was composed. This material consists of aeolian sand with a mean Fe content of about 0.14 % (dw) which is almost entirely present as Fe oxy-hydroxides (Mulder 1988). Iron in aeolian sands will be referred as parent-Fe. Sedimentary reactive Fe (5.5M HCl extractable Fe) in both moorland pools is very low (12-40 μmol (g dw)$^{-1}$) compared to other lake sediments (up to 400 μmol (g dw)$^{-1}$, Giblin et al. 1990), where Fe also originates from watershed input. In Fig.5 parent-Fe is compared with the present Fe fractions in Gerritsfles. About 50% of the parent Fe was still present as Fe oxides (defined as reactive Fe minus AVS-Fe). In both cores the Fe at 20 cm depth is equal to the original parent Fe content, but part of it is transformed into sulfide Fe. Higher up in the profile, the sediment was evidently enriched with Fe, particularly in the form of pyrite, containing about 1.8-2.7 times (integrated over 20 cm depth) as much Fe as expected based on the parent Fe content. Porewater profiles of dissolved Fe^{2+} (Figs.2,3) indicate that over the year there is a net flux of Fe^{2+} from down the sediment to the water column. We expect higher Fe^{2+} concentrations deeper down in the sediment as a result of more Fe-rich layers underlying the poor aeolian sands which suggests that Fe^{2+} in the top sediment is supplied by diffusion of Fe^{2+} from greater depths. The combination of the Fe flux into the water column, the lack of enrichment of Fe(III) oxides and of Fe sulfide at the surficial sediment, points to the formation of pyrite
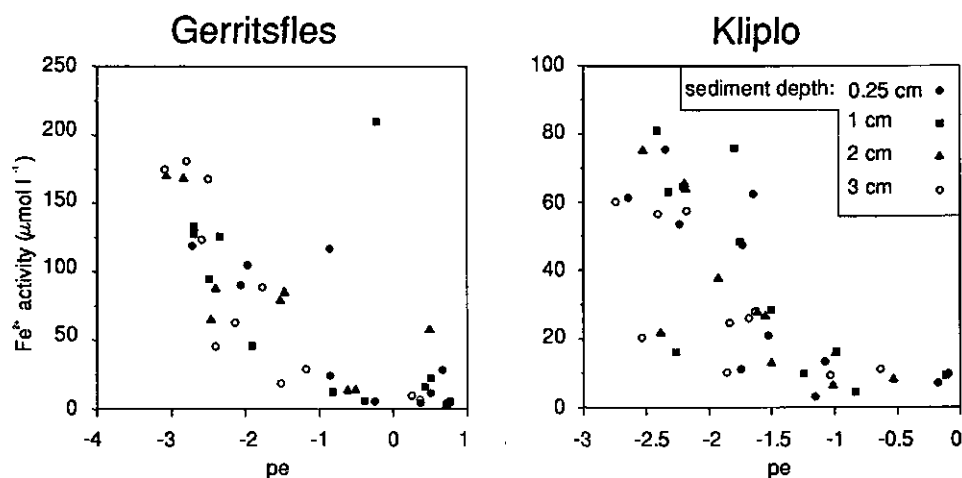
Fig.4. Activity of Fe^{2+} as function of the pe in Gerritsfles and Kliplo porewaters. The pe is calculated from the redox couple HS^-/SO_4^{2-} (Eqn.7).
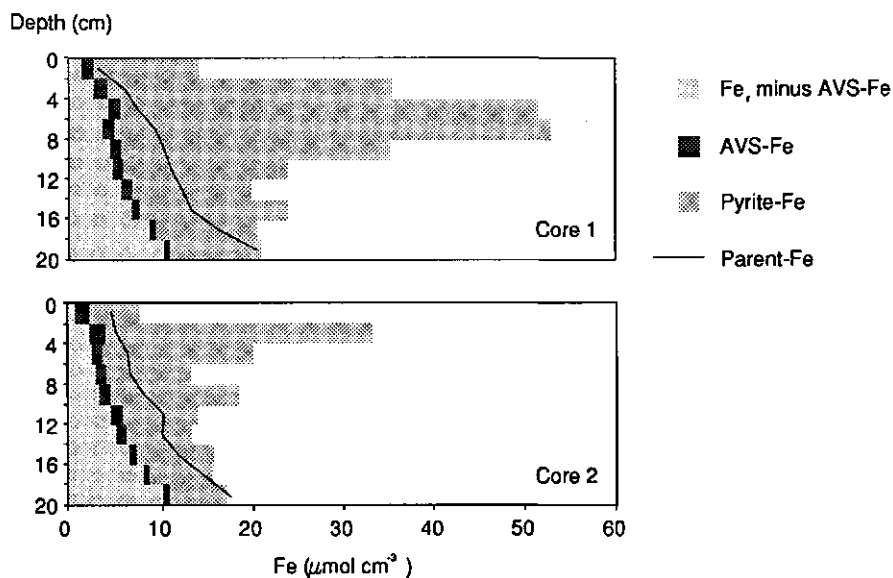
Fig.5. Depth distribution of different Fe fractions ($\mu mol\ cm^{-3}$) in Gerritsfles sediment (for explanation see text).

from Fe oxides reduced in the upper part of the sediment and from dissolved Fe conveyed from deeper sediments.

pH and redox state. Pyrite is thought to form at the interface of the oxic/anoxic zone (Davison et al. 1985) where ferrous and sulfide ions are supplied by the reduced sediment and oxidizing components like O_2 from the oxidized environment. Profiles of calculated pe values in porewaters of Gerritsfles and Kliplo (Fig.6) indicate periodically more oxidized conditions in the sediment, creating a suitable environment for pyrite formation. The pe was calculated following Eqn.(7) using pH and the SO_4^{2-}/HS^- redox couple:

$$SO_4^{2-} + 8e^- + 9H^+ \rightleftharpoons HS^- + 4H_2O \tag{7}$$

The temporal and spatial changes of redox conditions are in agreement with field results by Marnette et al. (1992), based on *in situ* enclosures to investigate SO_4^{2-} uptake and release by the sediment. In July and August 1990 the sediment acted as a sink of SO_4^{2-}. In November 1990, however, the poolwater SO_4^{2-} concentration in the enclosure increased, suggesting temporal oxidation of sedimentary S. Decreased microbial activity because of the low temperatures apparently allowed O_2 to penetrate deeper into the sediment, causing oxidation of reduced S
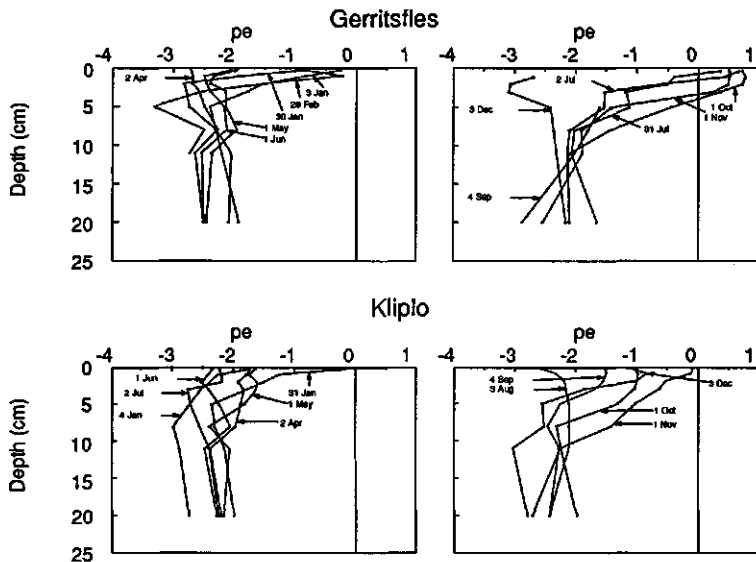

Fig.6. Calculated pe values following Eqn.(7) as function of depth in porewaters of Gerritsfles and Kliplo during 1990.

compounds by O_2 and subsequent transport of SO_4^{2-} into the overlying water column.

Sedimentation rate. Sedimentation rates determine the time span in which pyrite at a certain depth can be formed. Due to low sedimentation rates in Gerritsfles and Kliplo (about 1mm yr^{-1}, Van Dam et al. 1988b) sediments will be located within the zone where sulfide production (sulfate reduction) takes place for a relatively long period. The low sedimentation rates in Gerritsfles and Kliplo may thus contribute to the high pyrite contents relative to AVS.

Solubility considerations.

SI's with respect to Fe(am), mackinawite, greigite and pyrite of pore waters during 1990 are plotted against time in Fig.7. Since no corrections were made for temperature (except for FeS(am)) and for possible organic and inorganic Fe^{2+} complexes, the SI values must be treated as maximum values. Porewaters of Gerritsfles and Kliplo only in a few cases reached equilibrium (SI$\approx$0) with FeS(am), mackinawite and greigite (Fig.7). Cores for solid phase analyses were recovered at the end of October 1991, representing a period when oxidized conditions occur (Fig.6) and when porewaters are undersaturated for the Fe sulfide phases (except pyrite, Fig.7). Yet, pool sediments contain AVS, so in case of undersaturation it is not possible to draw unequivocal conclusions based on porewater SI values. Schoonen & Barnes 1991a showed that undersaturation with respect to FeS(am) may occur in the presence of FeS(am) if the growth rate of pyrite, mackinawite, greigite or the oxidation rate of either Fe^{2+} or $\Sigma H_2 S$ exceeds the dissolution rate of FeS(am). Furthermore the porewaters in this study are bulk samples, which may fail to reflect microsites which are at saturation with FeS (Jørgensen 1977b).

Ratios of FeS₂/AVS

A continuously oxic water layer is probably a main factor favouring pyritization of FeS. In Table 3, a compilation is given of a number of lakes where AVS and FeS_2 contents were determined. Trophic status, epilimnetic, pH, SO_4^{2-} concentration, oxic/anoxic conditions and the FeS_2-AVS ratio are given. It appears that stratified lakes with periodically anoxic conditions at the sediment-water interface, have markedly lower the FeS_2-AVS ratios than lakes with a continuously oxic water layer. In lakes where the hypolimnion did not turn anoxic periodically, 4 to 55 times more FeS_2 was formed than AVS. In the three lakes Windermere, Blelham Tarn and Vechten, where anoxic conditions exist during the stratification period, FeS_2 formation was about equal to 10 times less than AVS. Nextly, the concentration of SO_4^{2-} in the overlying water nor the trophic status of the lakes showed a relationship with AVS and pyrite concentrations, or FeS_2-AVS ratios.
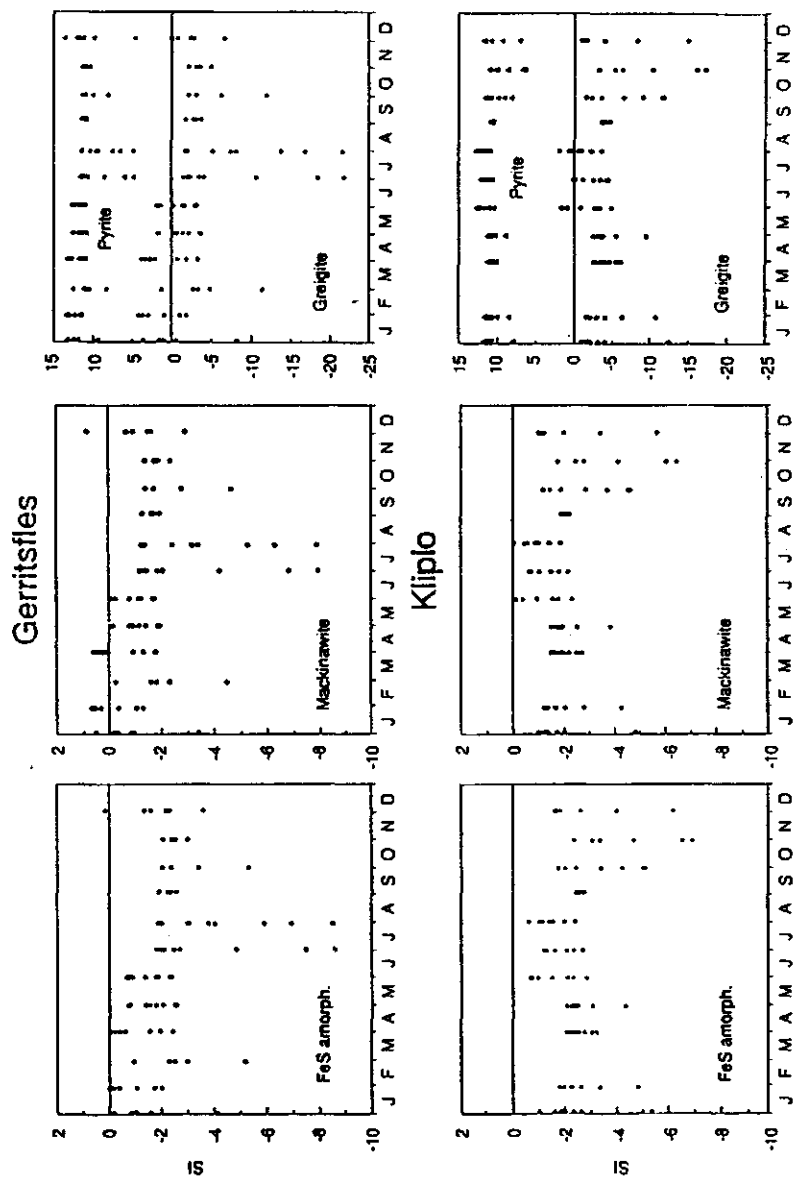
53

Fig.7. Saturation indices (SI) of porewaters of Gerritsfles and Kliplo as function of time with respect to FeS(am), mackinawite, greigite and pyrite.

Table 3. Mean AVS and pyrite-S contents (range between brackets) in sediments collected from different freshwater systems.

	Period. anoxic water column	sed. depth (cm)	AVS (μmol g⁻¹)		FeS₂ (μmol g⁻¹)		FeS₂/AVS	epilimnetic pH	epilimnetic SO₄²⁻ (μM)	reference
Kliplo[#][$]	-	0-20	1	(1-4)	55	(11-242)	55	5.1	67	this study
South Lake[*]	-	0-20	0.6		25		42	4.9-5.4	73	3
Gerritsfles[*]	-	0-20	3	(1-9)	97	(17-264)	32	4.5	100	this study
Ennerdale Water[*]	(-)	0-13		(0-6)		(3-31)	26	6.5	200	4,5
Oneida[‡]		0-20	1.6		28		18	6.9-8.5	470	3
Big Moose Lake[#],12m	-	0-20	114	(10-264)[1]			>10	5.2	63	1
Big Moose Lake[#],17m	-	0-20	85	(<5-237)[1]			>10	5.2	63	1
Big Moose Lake[#],24m	-	0-20	69	(<5-265)[1]			>10	5.2	63	1
Mirror Lake[#]		0-18	3	(<1-15)	39	(12-89)	13	6.4	60	2
Deer Lake[$]	-	0-20	0.9		9		10	5.8-6.5	62	3
Lake Constance[2]		0-10	2	(1-4)	12	(6-20)	6		300	6
Windermere[$]	+	0-6		(0-94)	3		0.9		340	4,5
Vechten[$][‡]	+	0-10	26	(23-31)	3	(2-4)	0.1	7.6-9.0	220	7
Blelham Tarn[‡]	+	0-31		(3-188)	9		0.07		480	4,5

[#] oligotrophic, [$] mesotrophic, [‡] eutrophic
1:White et al.,1989; 2:Giblin et al.,1990; 3:Mitchell et al.,1984;
4:Davison et al.,1985; 5:Davison 1988; 6:Bak,1988; 7:Hordijk et al.,1989.
[1] Cr(II) reducible sulfur including <10% AVS.
[2] Samples from littoral sediment

Contents of C, reactive Fe, AVS (Fig.1) and porewater SO_4^{2-} (Figs.2,3) are not directly correlated to pyrite contents. Such lack of correlation was also observed by others (Davison et al. 1985; Nriagu & Soon 1985) in lacustrine systems. One must realize that FeS_2/AVS ratios in sediments overlain by a continuously oxic water column may seasonally change. During the time of coring in Gerritsfles and Kliplo, the sediment experienced oxidation. During this period, ratios are probably higher because AVS are more rapidly oxidized than pyrite. Higher pyrite contents in Gerritsfles compared to Kliplo are probably due to the fact that Gerritsfles sediment is more subject to oxidizing influences (Fig.6).

Pathway of pyrite formation

Pyrite formation is generally portrayed as a reaction between an FeS precursor (e.g. Davison 1987; Lord & Church 1983) and polysulfides derived from S^0 (Boulegue 1978). When the solution is undersaturated with respect to a precursor phase, pyrite is also thought to form via direct nucleation and growth (Howarth 1979; Giblin & Howarth 1984) by a following reaction (e.g. Rickard 1975):

$$Fe^{2+} + S_5S^{2-} + HS^- \rightarrow FeS_2 + S_4S^{2-} + H^+ \tag{8}$$
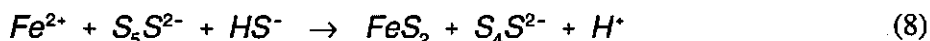
Recent experimental studies (Schoonen & Barnes 1991a; Luther 1991) however, revealed no direct and instantaneous formation of pyrite at room temperature. The rapid nucleation of iron monosulfides prevents the build up of a degree of supersaturation of the solution with respect to iron disulfides (like pyrite) sufficiently high to generate significant FeS_2 nucleation (Schoonen & Barnes 1991a). A refinement of Eqn.(8) was proposed by Luther (1991), suggesting formation of pyrite without the dissolution of a solid FeS phase to Fe^{2+} and HS^-. Equimolar or 1:2 reactions (n=1 or 2 respectively, Eqn.(9)) of Fe^{2+} and polysulfides gave a precursor "FeS" according:

$$Fe^{2+} + nS_x^{2-} \rightarrow "FeS" + \frac{(x-1)}{8}S_8 + (n-1)S_x^{2-} \tag{9}$$
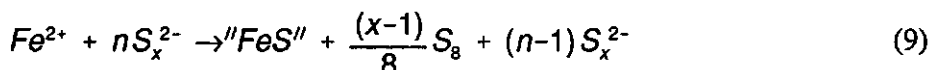
Polarographic results demonstrated that "FeS" consisted of solid phase FeS and an ion pair which is a complex of the form $Fe(SH)^+$ or $Fe[(SH)(S_x)]^-$. FeS_2 is formed from a direct reaction of either solid phase FeS or an ion pair with polysulfide via a cyclic intermediate. The concentrations of Fe^{2+} and HS^- solutions used in Luther's experiments at 25°C (606-3530 and 788-3530 µmol l^{-1} respectively) were close to those in salt marshes and tidal flats. Although porewater Fe^{2+} and ΣH_2S concentrations in our study were much lower (2-236 and 0-61 µmol l^{-1} respectively), the reaction mechanism proposed by Luther (1991) may apply since

Fe^{2+} and sulfide coexist (Figs.2,3) which strongly indicates the presence of soluble complexes. In all experimental studies on pyrite formation at room temperature, pyrite was formed as single crystals, sometimes with a weak clustering. Pyrite framboids were never observed, probably because they form extremely slow at low temperatures (Sweeney & Kaplan 1973). The presence of single crystals of pyrite (Plate 4) in sediments of Gerritsfles and Kliplo is a strong indication for rapid pyrite formation. The abundant presence of pyrite framboids in Gerritsfles and Kliplo (as in Plates 1 and 2), suggests that sulfurization of an iron sulfide precursor (Berner 1970; Sweeney & Kaplan 1973; Rickard 1975) is an important pathway of pyrite formation in these pools. Psenner (1983) and Oenema (1990) explained the close association of pyrite with organic matter by its formation at microsites with high sulfide concentrations. We believe that this is also the case in Kliplo and Gerritsfles. During periods when reduction prevail in the top sediment (e.g. in Gerritsfles, March until July 1990, Fig.3), high sulfide concentrations within organic enclosures establish saturation with respect to FeS(am), while bulk porewaters remain undersaturated (Fig.7). Subsequent intrusions of O_2 will lower dissolved Fe^{2+} concentrations through oxidation and the organic enclosures serve as an oxic/anoxic boundary. Sulfides, produced within the enclosures, may be oxidized to S^0 and because of low Fe^{2+} concentrations S^0 will be available for sulfurization of precursor FeS to pyrite within the enclosures. Simultaneously, the organic enclosures protect the solid phase iron sulfides and pyrite against oxidation. This must be the reason why we find the pyrite framboids predominantly in association with organic matter. The low sedimentation rates in Gerritsfles and Kliplo (Van Dam et al. 1988b) allows the slow formation process of framboidal pyrite to proceed until permanent reduced conditions occur and no more zerovalent sulfur is available for sulfurization of iron monosulfides to pyrite.

CONCLUSIONS

- Porewater chemistry in both pool sediments is extremely dynamic. Dissolved Fe concentrations may increase to 20 fold within a month. Porewater data indicate rapid formation and reduction of Fe-oxides. In Gerritsfles and Kliplo, pyrite was the most important iron sulfide phase; sedimentary FeS_2-S/AVS molar ratios were 32 and 55 respectively. In other lakes, where stratification caused anaerobic conditions in the hypolimnion, FeS_2-S/AVS ratios were <1. Redox status may thus be a main factor in determining whether pyrite or AVS is formed.
- The slow formation of framboidal pyrite through sulfurization of iron sulfide precursors is thought to be an important pathway of pyrite formation in the

freshwater sediments of Gerritsfles and Kliplo. The presence of single-crystal morphology of pyrite indicates that pyrite in both sediments may also form rapidly. The close association of pyrite framboids and organic matter, and the undersaturation of bulk porewaters with respect to amorphous FeS suggest that the framboidal pyrite is formed at microsites within organic matter. Alternating reduced and more oxic conditions in the sediment will supply Fe^{2+} and zerovalent sulfur respectively for the formation of pyrite. The close association of pyrite with organic matter may be explained by preferential oxidation of pyrite at locations where pyrite is not protected against O_2 intrusion while it is protected when located in microsites in organic matter.

Chapter 4

Effects of decreased atmospheric deposition on the sulfur budgets of two Dutch moorland pools

Emile CL Marnette, Harm Houweling, Herman van Dam & Jan Willem Erisman

ABSTRACT   The chemical composition of surface waters of two Dutch moorland pools and of incident precipitation, were monitored from 1982 to 1990. For this period, sulfur and water budgets were calculated using a hydrochemical model developed for well-mixed non-stratifying lakes. Total atmospheric deposition of S decreased significantly after 1986 at both locations. A model describing the sulfur budget in terms of input, output and reduction/oxidation processes predicted a fast decrease of pool water SO_4^{2-} concentrations after a decrease of atmospheric input. However, SO_4^{2-} concentrations in the surface water was lowered only slightly or remained constant. The model suggested that 75-90 mmol m^{-2} y^{-1} had to be supplied from the sediment to account for constant SO_4^{2-} concentration. The possible supply of SO_4^{2-} from the sediment through regulation by (K-)Al-SO_4 containing minerals or desorption of SO_4^{2-} from positively charged surfaces in the sediment was evaluated. Solubility calculations of pore water with respect to alunite, basaluminite and jurbanite indicated that SO_4^{2-} concentration was not regulated by these minerals. Also desorption from positively charged Fe(hydr)oxides could not be responsible for the estimated SO_4^{2-} supply by the sediment. It is suggested here 1) that desorption of SO_4^{2-} from peaty sediments may account for the estimated SO_4^{2-} supply provided that the adsorption complex is periodically recharged by partial oxidation of the upper bottom sediments and 2) that because of exposure of a part of the pool bottom to the atmosphere during dry summers and subsequent oxidation of reduced S, the amount of SO_4^{2-} may be provided which complements the decreasing depositional SO_4^{2-} input. In future research these two mechanisms need to be investigated.

INTRODUCTION

Over the past decade, concern over the impact of elevated loading of anthropogenically derived potential acid on freshwaters has initiated much research. The main attention has been focused on the influence of acid precipitation on the biogeochemistry of freshwater systems in acid-sensitive areas (e.g. Kelly 1982, Rudd 1986b). In extremely acid-vulnerable lakes, within-lake biogeochemical processes appeared to be important sources of alkalinity (Schindler et al. 1980; Cook et al. 1986). During an acidification experiment of a Canadian Shield Lake, about 70% of the H_2SO_4 added over a 7-year period, was lost by SO_4^{2-} reduction in epilimnetic sediments. Sulfate reduction and subsequent retention accounted for 85% of the internal alkalinity generation (Cook et al. 1986). In an experimentally acidified Wisconsin seepage lake, seston deposition appeared to be the most important SO_4^{2-} sink (Baker et al. 1989).

In the Netherlands a large number of oligotrophic to mesotrophic moorland pools occur in poorly buffered, non-calcareous sandy areas. Since the pools are largely fed by atmospheric deposition, they are vulnerable to environmental changes (Van Dam & Buskens 1993). Moorland pools act as important habitats for a variety of plants and animals, characteristic for these environments. Because these biota are comparatively rare in The Netherlands and surrounding countries, they have a high value for nature conservation. Acidification by acid atmospheric deposition is a main threat to isolated moorland pool ecosystems and results in biological impoverishment of the pools (Van Dam & Buskens 1993). Restoration of these pools may possibly be accomplished by the reduction of the acid load.

Although the total potential acid deposition (480 mmol $m^{-2} y^{-1}$ in 1989, Erisman (1989)) still exceeds the critical potential acid load (25 mmol $m^{-2} y^{-1}$, i.e. the quantity of acid above which these types of waters may acidify within a short period, Schuurkes et al. 1987; Van Dam & Buskens 1993), the total potential acid deposition has decreased by about 30% over the years 1980-1989, mainly due to decreased wet and dry SO_x deposition (Erisman 1992). To assess how these types of ecosystems react on the decrease atmospheric S-deposition, two moorland pools that differ in trophic status and morphometry were studied in detail. In this paper we present S budgets of the moorland pools over the period 1982-1990. Trends in SO_4^{2-} concentrations of pool water and deposition were evaluated based on calculations by hydrochemical models and short-term variations in S chemistry. The reaction of the pool water S chemistry on the decrease of atmospheric S deposition was evaluated by means of a simple model.

STUDY AREA

Investigations were conducted in two moorland pools, Gerritsfles and Kliplo, in the Netherlands (Fig.1). Both pools are seepage pools with small catchment areas and they have a perched water table. Gerritsfles (52°10'N, 5°49'E, 40 m above MSL) is an oligotrophic pool, located in a heath-dominated ecosystem. The bottom sediments are unconsolidated quartz sands which are covered by a detrital layer. This organic layer varies in thickness and is absent at some places. The detrital material is mainly derived from peat-moss (*Sphagnum*) which is abundantly present in Gerritsfles. The surface area of the pool is approximately 7 ha and the mean depth about 0.65 m. Kliplo (52°50'N, 6°26'E, 13 m above MSL), an oligo-mesotrophic pool, is located in an area that is characterized by the occurrence of aeolian sands. The bottom sediments consist of organic material which is mainly derived from decomposing algae. Kliplo has a surface area of approximately 0.5
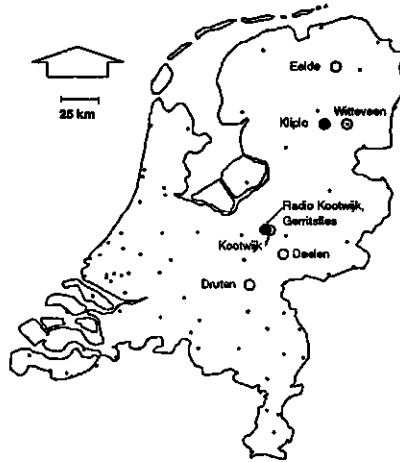
Fig.1. Meteorological stations (open circles, except for Kootwijk) and the study locations Gerritsfles and Kliplo (solid circles). At Kootwijk another research location of the Agricultural University Wageningen is located. The small dots indicate the locations of the National Air Quality Monitoring Network where SO_2 concentrations were measured.

ha and a mean water depth of about 1 m. At the western side a strip of bog (5-10 m in length) separates the pool from a heathland. At the southeastern side the pool has a sandy beach. Otherwise the pool is enclosed by forest. More detailed descriptions are provided by Van Dobben et al. (1992) and Van Dam & Buskens (1993)

METHODS

Modelling

Budgets of SO_4^{2-} and water in two moorland pools were calculated using two models. The model VENSIM (Van Dobben et al. 1992) simulates the water volume of the moorland pools. The model BUDGET (Van Dobben et al. 1992) calculates budgets for SO_4^{2-} in both pools. The *Sulfate* model was specifically developed to investigate how pool water SO_4^{2-} concentrations react on a change of S-deposition. The function of the different models and their relationship is schematically depicted in Fig.2.
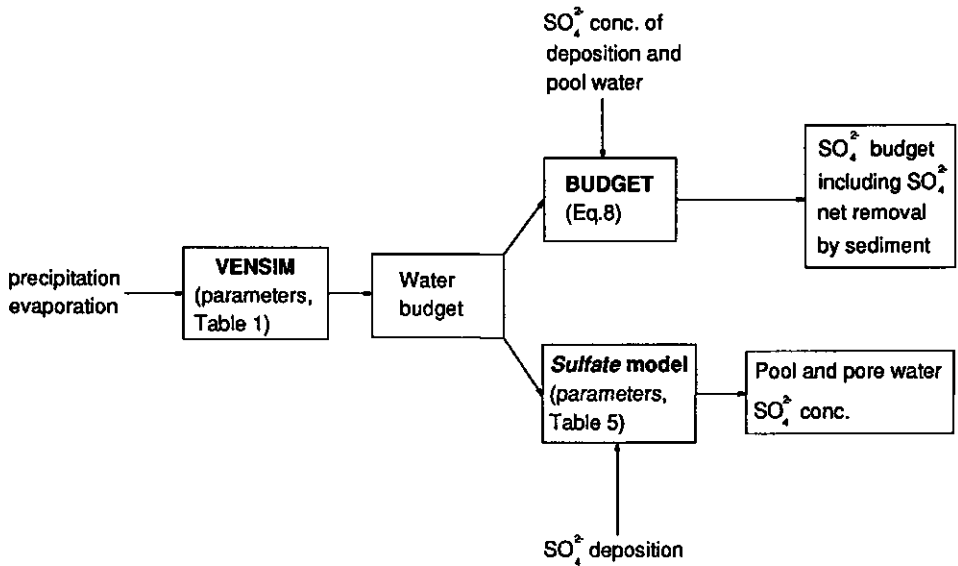
Fig.2. Schematic representation of the function and relationship between the models used.

Mass budgets of water

The model VENSIM (Van Dobben et al. 1992) was used to simulate the water budgets of the moorland pools for the years 1982-1990. VENSIM applies to well-mixed non-stratifying lakes. The water budget can be described as follows:

$$dV_i^{\cdot}/dt + \sum F_i = 0 \tag{1}$$

where

t   = time [y]
V_1 = water volume of the pool [m^3]
ΣF_i = sum of inflow and outflow fluxes [m^3 y^{-1}].

If Cl$^-$ is considered to be conservative and the pool water is well-mixed, the chloride budget equation can be written as

$$d(V_i * C_i)/dt + \sum (F_i * C_i) = 0 \tag{2}$$

where

C_l = Cl⁻ concentration in the pool [mmol m⁻³]

C_i = Cl⁻ concentration in F_i (inflow and outflow fluxes) [mmol m⁻³]

Figure 3 is a schematic representation of the pool system. The surface area of the pool depends on the water level. The hydraulic resistance of the pool bottom
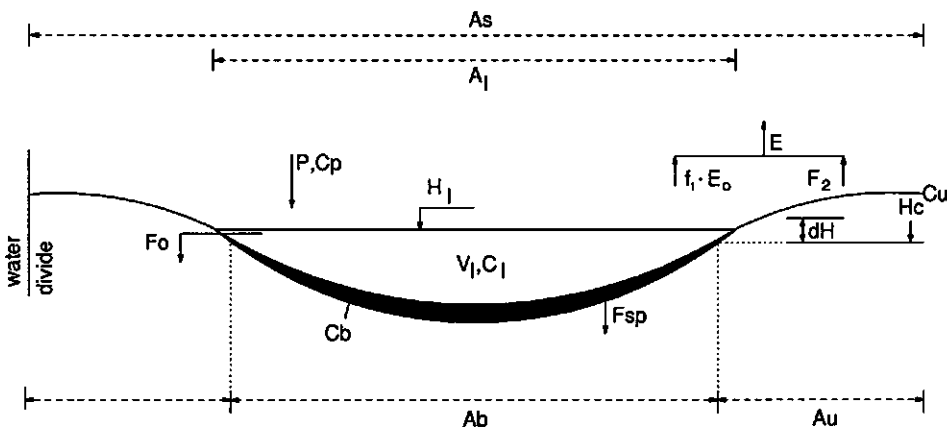
Fig.3. Schematic representation of the pool system (for explanation of the symbols see Table 1 and text).

decreases near the border. The parameters and variables of the model are listed in Table 1. Since both pools have a perched water table, inseepage does not occur. The concentration of Cl⁻ ions in the evaporation flux is neglected so F_e*C_e can be left out from Eq.(2) and the concentration of Cl⁻ in the outflow fluxes equals the pool water concentration. With these assumptions Eqs.(1) and (2) can be written as

$$F_p + F_e + F_{sp} + F_o + dV_l/dt = 0 \tag{3}$$

$$F_p * C_p + (F_{sp} + F_o) * C_l + d(V_l * C_l)/dt = 0 \tag{4}$$

Table 1. Variables and parameters of the VENSIM model.

	Symbol	Unit	
Input variables			
Precipitation per 10 days	P	mm	
Evaporation per 10 days	E_o	mm	
Cl⁻ concentration in precipitation	C_p	mmol m⁻³	
State variables			
Cl⁻ concentration in pool water	C_l	mmol m⁻³	
Pool water volume	V_l	m⁻³	
Parameters			
Catchment area	A_s	m²	*
Pool water area	Al	m²	
Surface area of the border strip with hydraulic bottom resistance c_u	A_u	m²	
Surface area of the central part of the pool with hydraulic bottom resistance c_b	A_b	m²	
Empirical evaporation coefficient in resp. around pool	f_1, f_2	-	*
Hydraulic resistance of pool bottom	c_b	d	*
Hydraulic resistance of pool bottom above $H_c + dH$	c_u	m + MSL	*
Highest level where hydraulic bottom resistance is c_b	H_c	d	*
Range over which c_b reduces to c_u	dH	m	*
Water pressure below pool bottom	H_r	m + MSL	

* Calibrated parameters

where the subscripts p, e, sp and o denote precipitation, evaporation, outseepage and overflow respectively. We use the convention that inflow and decrease of storage have a positive sign.

The components of Eq.(3) and (4) are calculated as follows:

$$F_p = P \cdot A_s \tag{5}$$

$$F_e = f_1 \cdot E_o \cdot A_l + F_2 \cdot (A_s - A_l) \tag{6}$$

where
$$F_2 = f_2 \cdot E_o \quad \text{if } P > f_2 \cdot E_o$$
$$F_2 = P \quad \text{if } P \leq f_2 \cdot E_o$$

$$F_{sp} = (H_l - H_r) \cdot (A_b/c_b + A_u/c_u) \tag{7}$$

VENSIM integrates Eqs.(3) and (4). The initial values of the state variables are

taken from observations. The pool water surface A_l, the pool water level H_l and the pool water volume V_l are related by morphometric data. The model was calibrated by minimizing the root mean square difference between observed and calculated pool water levels and chloride concentrations over the period 1982-1990. With the calibrated model components of the water budget are calculated with Eq.(3).

Mass budgets of SO_4^{2-}

The model BUDGET (Van Dobben et al. 1992) was applied to calculate budgets of SO_4^{2-} for the years 1982-1990 using Eq.(4), extended with the term LOSS:

$$F_p * C_p + (F_{sp} + F_o) * C_l + d(V_l * C_l)/dt + LOSS = 0 \qquad (8)$$

where C denotes the concentration of SO_4^{2-}. The LOSS term is used to balance the budget and refers to the amount of SO_4^{2-} that is removed or gained from the pool water by processes other than by mass transport with water, i.e. biogeochemical reactions. We will refer to the LOSS as the net removal of SO_4^{2-}. The water fluxes and pool water volume are taken from the VENSIM output (Fig.2). Pool water SO_4^{2-} concentrations are measured values.

Modelling of pool water SO_4^{2-} concentrations

To investigate how pool waters react on a change in S-deposition, we developed a simple model, the *Sulfate* model. Gerritsfles and Kliplo were represented as box-shaped lakes with a constant water level. The nine-year average water budgets were used as hydrological input (Fig.2). Overflow, outseepage and evaporation were expressed as fraction of precipitation, and the change of storage was set to zero (while in fact it amounted ~2% of the precipitation). Two dissolved sulfur species has been considered; SO_4^{2-} and any form of reduced dissolved sulfur. We estimated the uptake of SO_4^{2-} in the water column by *Sphagnum* (in Gerritsfles) and by algae (in Kliplo) from the concentration of organic S in the upper 2 cm of the sediment (non-publ.) and the sedimentation rate (for both pools about 1 mm y^{-1}, Van Dam 1987). Sulfate reduction rates in the sediment, sulfur oxidation rates in the water column and sulfur fixation rates in the sediment were modelled by first order reaction kinetics using the parameters Kred, Kox and Kfix respectively. Transport of sulfur species occurs via diffusion and mass flow (downward transport).

Because values for the parameters Kox, Kred and Kfix in Gerritsfles and Kliplo are not known, we made a combination of these parameters such that 1) a steady

state SO_4^{2-} pore water profile was reached which agreed with periodic measurements during 1990 of SO_4^{2-} concentrations in pore waters within a range of ±SD, 2) a steady state SO_4^{2-} pool water concentration was reached i.e. the mean SO_4^{2-} concentration over 1982-1990, 3) the modelled steady state SO_4^{2-} flux across the sediment water interface was of the same order of magnitude than calculated from field observations. We used mean pool water SO_4^{2-} concentrations instead of the individual values because it requires a much more simple model and it well serves the purpose, i.e. to investigate whether SO_4^{2-} pool water concentrations were reacting fast on a decrease of SO_4^{2-} input or whether there was a slow reaction yielding SO_4^{2-} pool water concentrations within the range of the measured fluctuations.

Deposition estimates

Model input consists of data collected at Gerritsfles and Kliplo during the period 1982-1990. The amount of precipitation and its chemical composition was not monitored continuously at both locations. Missing data were replaced by data from nearest monitoring stations (Table 2, Fig.1). Bulk deposition of Cl⁻ and precipitation at the Gerritsfles and Kliplo locations were measured by open funnel samplers. The total deposition of SO_x onto both pool surfaces was estimated by the sum of the wet S-deposition and the dry S-deposition.

Up to 1988, wet S-deposition in The Netherlands was measured using open funnel samplers (bulk samplers), which also included dry S-deposition onto the capture surface. Since 1988, wet-only collectors were used with the funnel open to the atmosphere during rain events only. Deposition of SO_4^{2-} calculated from precipitation data collected by bulk samplers was estimated to be about 25% higher than those collected with wet-only samplers (Erisman et al. 1989). The wet S-deposition estimates before 1988 are corrected accordingly. Yearly average wet deposition fluxes for each monitoring station in the Netherlands (20 in 1982 and 14 in 1987 and following years) were calculated by multiplying the SO_4^{2-} concentration and the amount of rain. The local fluxes at Gerritsfles and Kliplo were subsequently estimated by interpolation. The uncertainty in the annual average wet deposition flux is 25% (Erisman 1992).

Dry S-deposition at Gerritsfles and Kliplo was estimated using interpolated SO_2 and particulate SO_4^{2-} concentrations and meteorological parameters ($10 \times 10 \ km^2$ grid) based on measurements at stations of the National Air Quality Monitoring Network (NAQMN, Elskamp 1989, Fig.1). Roughness characteristics of the areas surrounding the stations differ from those of water surfaces. Therefore, before interpolation of SO_2 and SO_4^{2-} concentrations to the Gerritsfles and Kliplo site, the

Table 2. Monitoring stations and data that were used for calculating budgets in Gerritsfles and Kliplo.

	amount evap.	amount prec.	Cl prec.	water level	solutes in prec.	solutes in lake water
Gerritsfles site						
Gerritsfles[1,2]		+	+	+	+	+
Radio Kootwijk[3]	+	+				
Kootwijk[2]			+			
Deelen[3]					+	
Druten[3]					+	
Kliplo site						
Kliplo[1,2]		+	+	+	+	+
Witteveen[3]	+	+			+	
Eelde[3]	+					

evap. = evaporation, prec. = precipitation
[1]: Monitoring site of the DLO Institute for Forestry and Nature Research
[2]: Monitoring site of the Agricultural University.
[3]: Monitoring station of The Royal Meteorological Institute
   Monitoring at station Deelen was moved to Druten starting at 01-01-1986.

measured concentrations and meteorological data were extrapolated to a height (50m) where deposition and roughness characteristics hardly influence the concentration profile of SO_2 (Erisman 1993). Hourly average dry deposition was then inferred from interpolated concentrations and an estimated local dry deposition velocity. The dry deposition velocities were calculated with the resistance analogy (Hicks et al. 1987) using interpolated meteorological data and the roughness characteristics for water surfaces. The annual average dry deposition flux is calculated by summing two-hourly average values. This dry deposition flux is currently the best estimate available for the locations Gerritsfles and Kliplo. The uncertainty in the annual average dry deposition flux is 45% (Erisman 1992, 1993). For the year 1986 we do not have a reliable estimate of dry and wet S-deposition because the configuration of the monitoring network was changed. For budget calculations of 1986 we therefore used interpolated values between 1985 and 1987.

Analyses of Cl, SO_4^{2-} were carried out by different laboratories. Chloride was determined by potentiometrical titration with a silver nitrate solution (Waterleidingbedrijf Midden-Nederland, WMN and National Institute of Public Health and Environmental Protection, RIVM) or by ion chromatography (Dionex or HPLC, Agricultural University, LUW). Sulfate was analyzed through coloring

of excess barium with thorium after addition of a barium perchlorate solution (RIVM, WMN) or by ion chromatography (Dionex or HPLC, LUW). pH was determined potentiometrically using a combination electrode. Parallel samples of several pools were taken to compare the different methods. No appreciable differences between results of the methods were found for Cl^- and SO_4^{2-} (Van Dobben et al. 1992, two tailed T-Test, p>0.31).

Pore water analyses and fluxes

Fluxes across the sediment/water interface were determined to estimate within-year variation in SO_4^{2-} fluxes and to compare the fluxes with modelled net removal of SO_4^{2-} from the water column. To assess fluxes of SO_4^{2-} over the sediment water interface, pore water was collected during the year 1990 in Gerritsfles and Kliplo.

Pore water was sampled by *in situ* dialysis using a sampling device ("peeper", lxhxw=60x30x4 cm) that contained 10 membrane cells (modified after Oenema 1990) with slits parallel to the sediment-water interface, covered with a 0.2 µm biologically inert acrylic copolymer membrane filter (Versapor-200: Gelman Sciences). The upper 6 cells (width of slit 5 mm) of the peeper comprised about 40 ml, the lower 4 cells (width of slit 1 mm) about 80 m. Pore water samples were withdrawn through tubing that was connected with the cells and that reached to the water surface. Sulfate was measured by High Performance Liquid Chromatography (KH-phtalate, pH 4 as eluent). The peeper was installed permanently for one year. The water inside the membrane cells was allowed to equilibrate with the pore water for about a month.

Fluxes were calculated according to the equation (Lerman 1978)

$$J_{SO_4^{2-}} = -\phi \cdot D_s \cdot \frac{d[SO_4^{2-}]}{dx} \qquad (9)$$

where ϕ is porosity and D_s denotes the whole sediment diffusion coefficient. The D_s was determined in the lab on duplicate cores using tritiated water (Sweerts et al. 1991; Marnette et al. 1992a) and was corrected for temperature.

Pore water Al, SO_4^{2-} and K^+ were used to calculate equilibria with (K-)Al-SO_4^{2-} phases. Al was determined colorimetrically on acidified samples (pH ~ 2) using pyrocatechol violet. Pyrocatechol violet complexes essentially all dissolved Al except very strong organic-Al complexes as Al-citrate or Al-salicylate (J Mulder, pers. comm.). Potassium was determined by Atomic Absorption Spectrometry.

RESULTS

Mass budgets of water

To test the model assumption that the pool waters are well-mixed, Cl^- and SO_4^{2-} concentrations were determined at the surface, at ca. 30 cm and at ca. 80 cm depth (Table 3). The coefficient of variation (CV) of SO_4^{2-} and Cl- concentrations in Gerritsfles was less than 2% except for Cl^- and SO_4^{2-}- concentrations in July. The CV at Kliplo were somewhat higher than in Gerritsfles but still less than 4%, with exception of SO_4^{2-} in June, July and December and of Cl^- in December. Although these data only cover a limited period, they indicate that in most cases the pool waters approach a well-mixed state.

Table 3. Variation of pool water Cl^- and SO_4^{2-} concentrations in Gerritsfles and Kliplo. Values represent means (± SD) of three samples collected at one sampling date, each sample taken at a different depth (surface, 30 cm and 80 cm depth).

Gerritsfles			Kliplo		
Date	[Cl⁻]	[SO₄²⁻]	Date	[Cl⁻]	[SO₄²⁻]
			1 May 90	400 ± 1	75 ± 1
1 Jun 90	389*	136 ± 1.3	1 Jun 90	438 ±17	93 ±18
2 Jul 90	191 ± 9	116 ± 9.4	2 Jul 90	267 ± 4	92 ±12
31 Jul 90	332 ± 4	109 ± 0.4	3 Aug 90	448 ± 8	92 ± 1
4 Sep 90	318 ± 2	102 ± 1.1	4 Sep 90	395 ± 4	80 ± 2
1 Oct 90	317 ± 1	101 ± 0.2	1 Oct 90	391 ± 2	75 ± 1
1 Nov 90	315 ± 4	95 ± 0.5	1 Nov 90	389 ± 5	78 ± 1
3 Dec 90	318 ± 4	103 ± 0.6	3 Dec 90	399 ±30	82 ± 8

* [Cl⁻] at surface and at 30 cm depth

The water levels in Gerritsfles could be simulated rather precisely using VENSIM (Fig.4). The root mean square error (RMSE) between measured and simulated water levels was 2.83 cm (~4% of mean depth). Chloride concentrations could be simulated reasonably well (Fig.4), with a RMSE between measured and calculated values of 33.9 mmol m^{-3} (~14% of mean Cl^- concentration). Chloride concentrations were overestimated during 1987 and slightly underestimated during the following period. The trends of measured and simulated Cl^- concentrations, however, agreed well. Simulation of water levels in Kliplo (Fig.5) resulted in a RMSE of 4.12 cm (~5.5% of mean depth). Simulation of the Cl^- concentration was
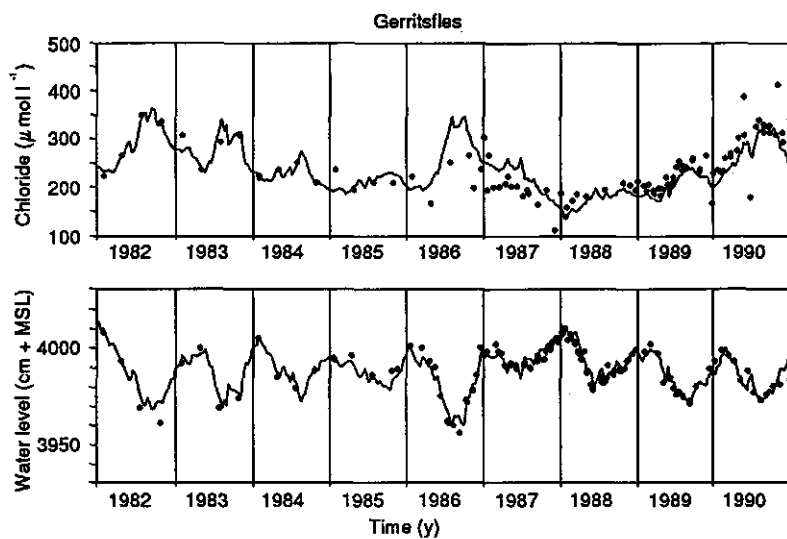
Fig.4. Measured and simulated Gerritsfles pool water Cl⁻ concentrations and pool water levels. Dots represent measurements, solid lines simulations.
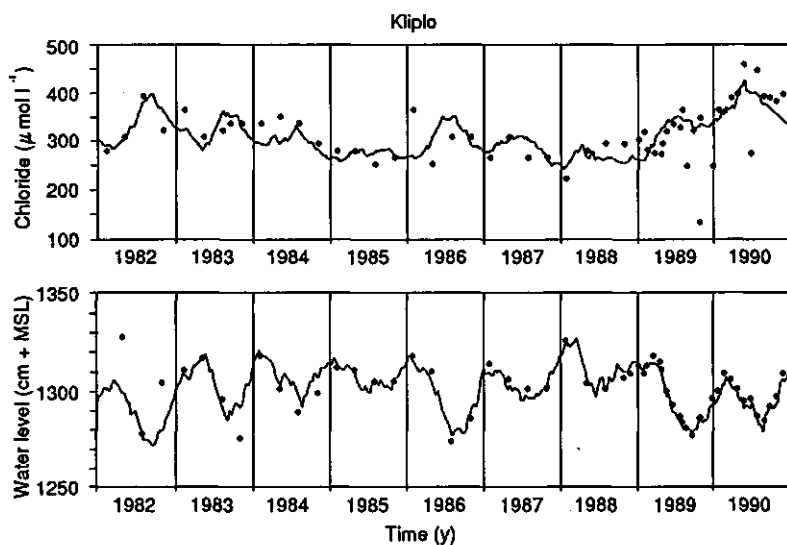
Fig.5. Measured and simulated Kliplo pool water Cl⁻ concentrations and pool water levels. Dots represent measurements, solid lines simulations.

slightly more accurate as in Gerritsfles (RMSE 32.4 mmol m^{-3}, ~10% of mean Cl$^-$ concentration). Also in Kliplo, Cl$^-$ concentrations were underestimated during the period 1988-1990.

The budgets of water and SO$_4^{2-}$ in Gerritsfles and Kliplo are depicted in Fig.6. The outseepage flux depends on bottom resistance, water level and the water pressure below the pool water, neither of which varied much over the whole period. Annual precipitation varies from 719 mm (1982) to 1013 mm (1983) in Gerritsfles and from 667 mm (1989) to 1042 mm (1988) in Kliplo. Generally the change of water storage in Gerritsfles and Kliplo is small compared to precipitation. The total change of storage over nine years comprises about 2% of the total precipitation.
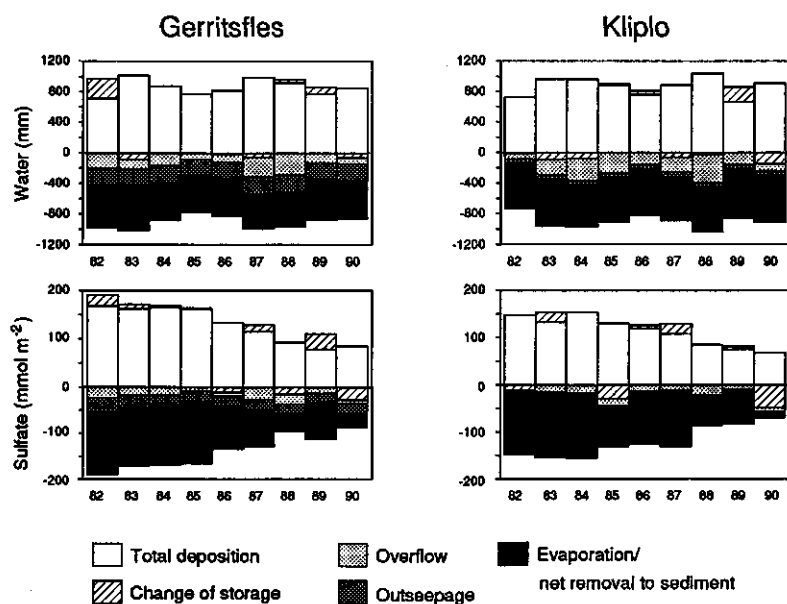
Fig.6. Water and SO$_4^{2-}$ budgets of Gerritsfles and Kliplo over the period 1982-1990.

Input and output budgets of SO$_4^{2-}$

The budgets of SO$_4^{2-}$ in Gerritsfles and Kliplo are shown in Fig.6. In Gerritsfles the annual net removal of SO$_4^{2-}$ to the sediment clearly decreased after 1986 (Fig.6). In Kliplo the net removal follows the same trend but the decrease was less pronounced than in Gerritsfles.

Estimates for the annual total S deposition and for the wet S deposition at Gerritsfles and Kliplo are shown in Fig.7a,b. Wet S-deposition fluxes were rather

constant over the years at both locations, whereas total deposition showed a clear decrease after 1986 as a result of a decrease in dry deposition.
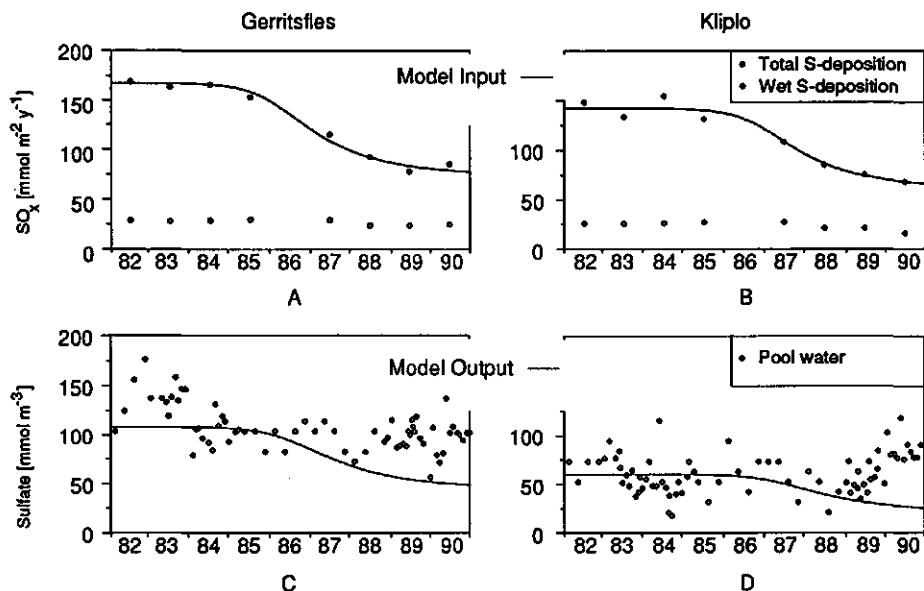
Fig.7. A, B) Annual total and wet deposition of SO_x and/or SO_4^{2-}. Total S deposition was fitted as a function of time and was used as input for the *Sulfate* model. C,D) pool water SO_4^{2-} concentrations as function of time, measured and modelled by the *Sulfate* model.

Pool waters

Temporal variation in SO_4^{2-} concentrations of Gerritsfles and Kliplo pool waters is considerable (Fig.7c,d). In Gerritsfles pool water SO_4^{2-} concentrations decreased significantly (t-test, p<0.0001) from about 140 µmol l^{-1} (over 1982 and 1983) to around 100 µmol l^{-1} (1984-1990). The decrease of SO_4^{2-} concentration in pool water did not coincide with that of total S deposition (Fig.7). A trend analysis (procedure Autoreg, SAS) over the years 1982-1990, using a linear model with corrections for periodicity, gave a significant (p<0.005) decrease of pool water SO_4^{2-} concentrations but a poor fit (R^2=0.34). Sulfate pool water concentrations in Kliplo did not follow a linear trend in time and neither did they show a significant decrease over 1982-1990.

Fluxes

The temporal variation of sulfate pool and pore water concentrations in Gerritsfles and Kliplo (Fig.8) and calculated fluxes across the sediment water interface (Table 4) was large. In both Gerritsfles and Kliplo fluxes from the sediment into the water column (negative sign) temporarily occurred, although at different times of the year.

Fig.8. Pore water concentrations of SO_4^{2-} in Gerritsfles and Kliplo sediment during 1990.

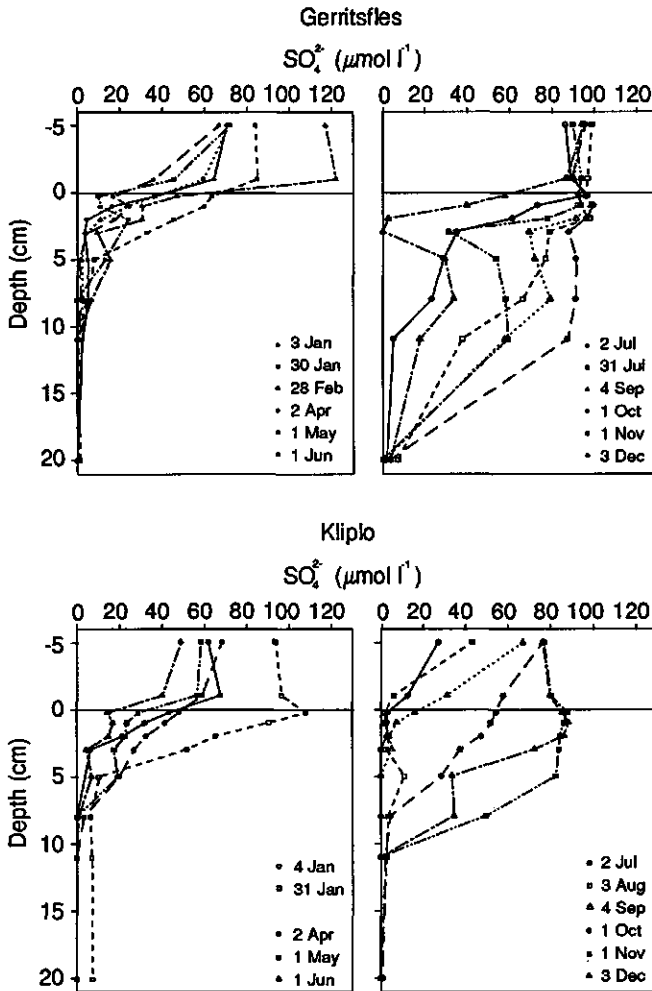**Table 4.** Diffusive flux of SO_4^{2-} over the sediment-water interface in Gerritsfles and Kliplo during the year 1990, calculated from pore water gradients. Positive fluxes are directed downwards.

	Gerritsfles		Kliplo	
Date	SO_4^{2-} flux mmol m^{-2} d^{-1}	Date	SO_4^{2-} flux mmol m^{-2} d^{-1}	
03-Jan-90	0.12	04-Jan-90	0.09	
30-Jan-90	0.08	31-Jan-90	-0.04	
28-Feb-90	0.11			
02-Apr-90	0.10	02-Apr-90	0.05	
01-May-90	0.21	01-May-90	0.15	
01-Jun-90	0.49	01-Jun-90	0.15	
02-Jul-90	-0.05	02-Jul-90	0.06	
31-Jul-90	0.01	03-Aug-90	0.03	
04-Sep-90	-0.03	04-Sep-90	0.10	
01-Oct-90	-0.04	01-Oct-90	0.02	
01-Nov-90	0.01	01-Nov-90	0.04	
03-Dec-90	0.13	03-Dec-90	-0.02	

Modelling of pool water SO_4^{2-} concentrations

The main purpose of the *Sulfate* model was to investigate whether SO_4^{2-} pool water concentrations were reacting fast on a decrease of SO_4^{2-} input or whether there was a slow reaction yielding SO_4^{2-} pool water concentrations within the range of the measured fluctuations (Fig.7c,d).

The most important model parameters and their (steady state) values are listed in Table 5. Before imposing the decrease of S-deposition on the model system (Figs 7a,b), the unknown reduction, oxidation and fixation rate constants (Kred, Kox and Kfix) were tuned to achieve a steady state pool water SO_4^{2-} concentration. Only Kred has been estimated earlier in Gerritsfles and varied considerably with time and depth (0.6-5 d^{-1}, Feijtel et al. 1989). As steady state concentrations were taken the mean values of pool water SO_4^{2-} concentrations over the whole period 1982-1990 (Table 5). The oxidation (in the water column) and fixation (in the sediment) rate constants have never been estimated in these sediments. Biological uptake of . sulfate in the water column calculated from organic-S contents in the upper 2 cm of the sediment (13.3 μmol cm^{-3} for Gerritsfles and 28.3 μmol cm^{-3} for Kliplo) and sedimentation rates (1 mm y^{-1}), was estimated as 6.7 mmol m^{-2} y^{-1} and 14.2 mmol m^{-2} y^{-1} for Gerritsfles and Kliplo respectively. These values can be considered as either under- or overestimates because organic S may be mineralized by (an)aerobic

Table 5. The most important parameters used for predicting the SO_4^{2-} pool water concentration using the *Sulfate* model.

			Gerritsfles	Kliplo	units
amount of precipitation			0.00236	0.00239	m d^{-1}
biol. uptake of SO_4^{2-} in water			6.7	14.2	mmol m^{-2} y^{-1}
overflow			0.17	0.23	frac. of prec.
seepage			0.23	0.08	frac. of prec.
evaporation			0.60	0.69	frac. of prec.
depth			0.68	0.82	m
area			56000	6500	m^2
number of sediment layers			10	10	-
thickness of sediment layer			0.01	0.01	m
mean pool water SO_4^{2-} concn. used					
for tuning Kred, Kox and Kfix			108	60	mmol m^{-3}
	model run #	Kred (d^{-1})	Kox (d^{-1})	Kfix (d^{-1})	SO_4^{2-} flux[*]
Gerritsfles	1	0.410	1.00e-3	0.9	127
	2	0.382	1.00e-4	0.9	123
	3	0.384	1.00e-4	0.5	124
	4	0.381	1.00e-4	1.5	123
	5	0.500	4.38e-3	0.9	137
Kliplo	1	2.345	1.00e-4	0.9	112
	2	2.283	1.00e-5	0.9	112
	3	2.285	1.00e-5	0.5	112
	4	2.281	1.00e-5	1.5	112
	5	3.000	9.36e-4	0.9	117

[*] SO_4^{2-} flux across sediment water interface (mmol m^{-2} y^{-1})

decomposition or diagenetically formed by reaction of sulfides with organic matter. The uptake of S from the water column in Gerritsfles however agrees rather well with the 5.5 mmol m^{-2} y^{-1} estimated from the annual production of *Sphagnum* and its S content (Feijtel et al. 1989).

We listed five different combinations of Kred, Kox and Kfix that yielded a steady state (Table 5). All these combinations of rate constant values for Gerritsfles yielded steady state interstitial SO_4^{2-} concentrations that just fall within the range of pore water measurements (Fig.9). For Kliplo the pore water steady state SO_4^{2-} concentrations were below the range of measured concentrations and could not be improved using the current model. The model could not reach steady state below a Kred value of 0.38 (Gerritsfles) and 2.28 d^{-1} (Kliplo), because the SO_4^{2-} concentration of the deposition was so much higher than that of the pool water.
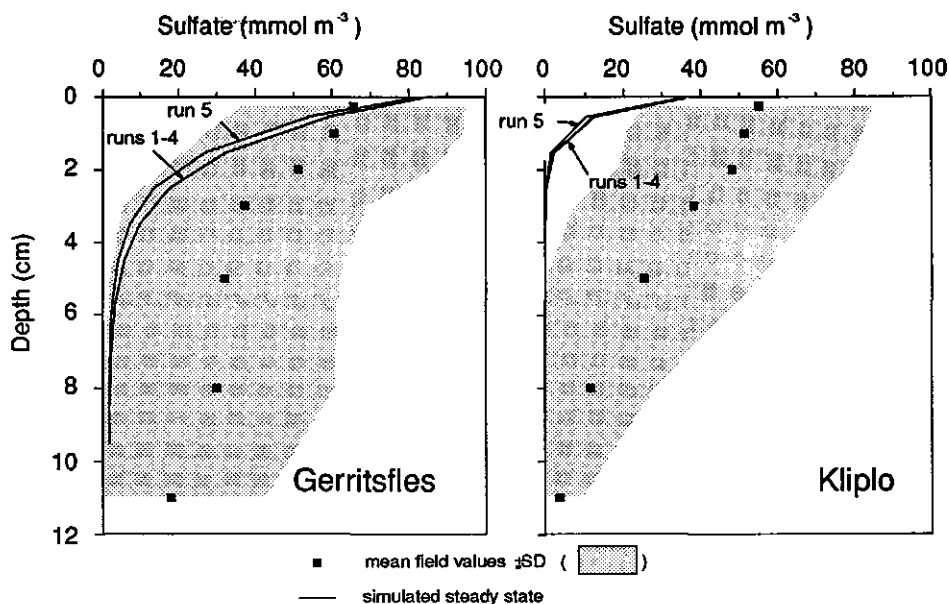
Fig.9. Mean pore water SO_4^{2-} concentrations ($\pm$ SD) during the year 1990 and steady state SO_4^{2-} profiles as calculated by different runs of the *Sulfate* model.

Only reduction rate constants above these values could bring the pool water SO_4^{2-} concentration at the preset steady state level (mean SO_4^{2-} pool water concentration over the whole period). The change in modelled pool water SO_4^{2-} concentrations is only dependent on the change in S deposition; different combinations of Kred, Kox and Kfix that lead to steady state situation resulted in the same rates of change of pool water SO_4^{2-} concentrations.

Over the period that the S deposition did not decrease and the model was at steady state (Fig.7) we calculated a SO_4^{2-} flux across the sediment/water interface of 123 mmol m^{-2} y^{-1}, which is in fair agreement with measured integrated annual SO_4^{2-} flux of 111 mmol m^{-2} y^{-1} in 1987 (Feijtel et al. 1989).

When steady state was reached, the model was run for 9 years which included a decrease in S-deposition according a sigmoid function (Fig.7a,b). The model runs with different combinations of rate constants (Table 5) yielded the same results; the model calculated a decrease of the pool water SO_4^{2-} concentration as a reaction on decreased S deposition that clearly did not match the measured SO_4^{2-} concentrations (Fig.7c,d).

DISCUSSION

Baker et al. (1986) and Kelly et al. (1987) developed a model that predicts the SO_4^{2-} removal and the resulting acid neutralization within acid-sensitive lakes requiring the water residence time, mean depth and the average mass transfer coefficient for SO_4^{2-}. The model only applies to lakes with oxic hypolimnia and might be used for Gerritsfles and Kliplo. At steady state the removal of SO_4^{2-} by in-lake processes is expressed by the removal coefficient R, which is the proportion of incoming mass which is removed from the water column, either to the sediments or to the atmosphere or to a new form within the water column (Kelly et al. 1987):

$$R = \frac{mass\ in\ -\ mass\ out}{mass\ in} \tag{10}$$

At steady state, mass in = mass out + mass lost within the lake. We may consider the amount of SO_4^{2-} in Gerritsfles and Kliplo is in a steady state over the period 1982-1990 because the change of storage is only 2.5% of the SO_4^{2-} input for Gerritsfles and 3% for Kliplo. The change of storage for the individual years however may be high and ranges from 0.7-41% for Gerritsfles and from 0.3-69% for Kliplo. So the model of Baker et al.(1986) and Kelly et al.(1987) is only applicable when using mean data values during 1982-1990. The removal coefficient of Gerritsfles and Kliplo can easily be calculated from the SO_4^{2-} budgets (Fig.6) with Eq.(10) where "mass in - mass out" equals the net SO_4^{2-} removal and "mass in" equals the total S deposition. Mass balance data were related with the SO_4^{2-} mass transfer coefficient S, the water residence time τ_w and the mean depth $\bar{z}$ (Kelly et al. 1987) according

$$R = \frac{S}{(\bar{z}/\tau_w)\ +\ S} \tag{11}$$

with the assumption that SO_4^{2-} reduction follows first order kinetics. The mass transfer coefficient S (in m y^{-1}) can be seen as the height of the water column from which SO_4^{2-} is removed each year. Estimates of the mass transfer coefficient were calculated as follows (Kelly et al.1987):

$$S = \frac{f}{[SO_4^{2-}]} \tag{12}$$

where $[SO_4^{2-}]$ is the mean pool water SO_4^{2-} concentration (mmol m^{-3}) and f the SO_4^{2-} reduction rate (mmol m^{-2} y^{-1}) estimated as the net removal of SO_4^{2-} from the water

column derived from the mass budgets.

To compare our budget calculations with the model developed by Baker et al. (1986) and Kelly et al. (198)7, the SO_4^{2-} removal coefficient (Table 6) was calculated from mass budgets of Gerritsfles and Kliplo using Eq.(10) and from the model formulations of Baker et al. (1986) and Kelly et al. (1987) using Eqs.(11) and (12). The removal coefficients derived directly from the mass budgets are

Table 6. Removal coefficients calculated from 1) mass transfer coefficients (S), mean depth ($\bar{z}$) and water residence time (τ_w), ($R^#$) and from 2) mass budgets (R). Data are means over the period 1982-1990.

	$\bar{z}$	τ_w	$[SO_4^{2-}]$	f	S	$R^#$ (Eq.11)	R (Eq.10)
	(m)	(y)	(mmol m^{-3})	(mmol m^{-2} y^{-1})*	(m y^{-1})	(-)	(-)
Gerritsfles	0.68	0.77	108	96	0.89	0.50	0.74
Kliplo	0.82	0.96	60	95	1.58	0.65	0.83

* f is the mean net SO_4^{2-} removal rate over 1982-1990 estimated from budgets
$^#$ calculated with the model developed by Baker et al. (1986) and Kelly et al. (1987)

much lower than those which were modelled (Baker et al. 1986), perhaps because the net removal as a first order function of the pool water SO_4^{2-} concentration (one of the model conditions) does not apply for both pools. This is supported by the fact that we observe a decrease in the net SO_4^{2-} removal while there is not a concomitant decrease of pool water SO_4^{2-} concentrations (Figs.6 and 7).

The removal coefficients of Gerritsfles and Kliplo as function of $\bar{z}/\tau_w$ (the height of the water column that is displaced by new water each year) fit rather well in the trend reported by Baker et al. (1986) and Kelly et al. (1987) for a number of lakes (Fig.10). The authors concluded that the contact time of the water with sediments is crucial in determining the fraction of SO_4^{2-} removed from the water as it passes through the lake which is evidenced by a decreasing SO_4^{2-} removal coefficient with increasing $\bar{z}/\tau_w$.

As an independent check of the SO_4^{2-} net removal calculated by the BUDGET model, we used annual fluxes across the sediment/water interface. The time-integrated flux of SO_4^{2-} over 1987 was estimated by Feijtel et al. (1989). In our study SO_4^{2-} fluxes were calculated over the year 1990 (Table 4). In some cases fluxes may have been underestimated because the spatial resolution at which pore water concentrations were measured (1 cm above the sediment and 0.25 cm below) may have been insufficient to reliably estimate the concentration gradients. In most
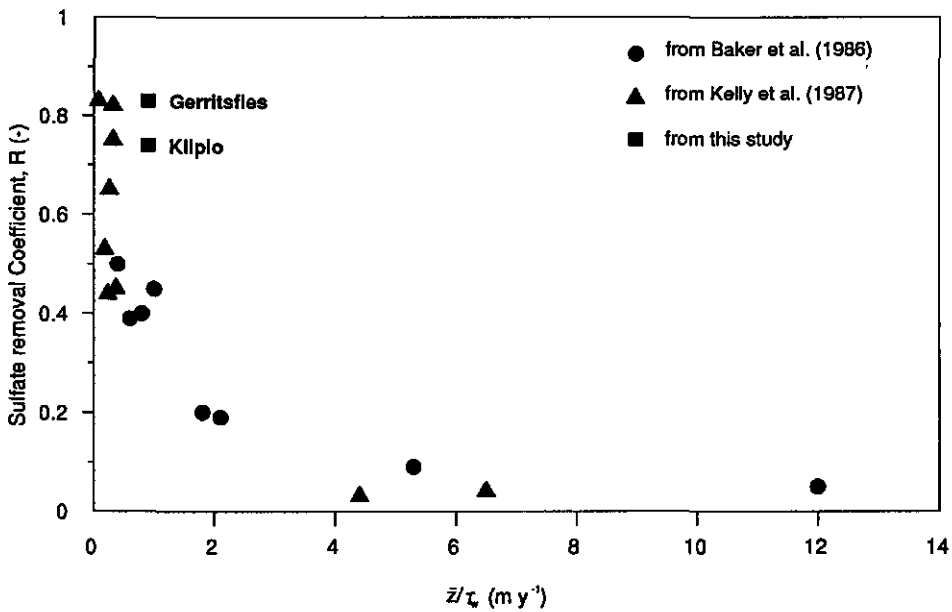
Fig.10. Removal coefficients of SO_4^{2-} as function of $\bar{z}/\tau_w$ for a number of lakes. The removal coefficients and $\bar{z}/\tau_w$ of Gerritsfles and Klipo are mean values over 1982-1990 derived from mass balances of SO_4^{2-} and water.

cases there is a gradual decrease of SO_4^{2-} with dep⊹ :F゚ ⠂ ⠊⠵ fluxes ⠊⊺⠕ considered to be well estimated.

In Table 7 the diffusive transport of SO_4^{2-} into the sediment is compared with the net removal of SO_4^{2-} by the sediment from the budget calculations. The annual

Table 7. Annual net removal of SO_4^{2-} from the water column in Gerritsfles and Kliplo from budget calculations and from diffusive fluxes of SO_4^{2-} across the sediment/water interface calculated from pore water gradients.

		Net removal to sediment (from mass budgets), mmol m^{-2}	Net removal into sediment (from diffusive fluxes), mmol m^{-2}
Gerritsfles	1987	83[*]	111[*]
	1990	32[#]	35[#]
Kliplo	1990	9[#]	22[#]

[*] from Feijtel et al. 1989
[#] from this study

fluxes and modelled net removal are in the same order of magnitude and, especially for Gerritsfles in 1990, agree very well. Also they both show a decrease from 1987 to 1990 for Gerritsfles. The calculation of the net diffusive SO_4^{2-} flux from pore water gradients is a completely different approach to estimate net removal of SO_4^{2-} from the water column than is the budget calculation using hydrochemical models. The good agreement between these approaches indicates that the net SO_4^{2-} removal has been fairly well estimated.

The total S-deposition in The Netherlands has decreased considerably after 1986. This temporal change in S deposition is mainly the result of a decrease in West European SO_2 emissions and thus SO_2 concentrations (Erisman, 1992). Also a decline in total S-deposition at our study sites, based on regional data, has been calculated (Fig.7a,b). There is a large discrepancy between measured lake water SO_4^{2-} concentrations in both pools and SO_4^{2-} concentrations modelled by the *Sulfate* model (Fig.7). Measured pool water concentrations remained about constant while model calculations indicated a fast decrease of lake water SO_4^{2-} concentrations to the lowering of the S-deposition. So most likely, a net source of SO_4^{2-} makes up for the lowered input of atmospheric S. From the model simulations a supply rate of 89 mmol m^{-2} y^{-1} SO_4^{2-} for Gerritsfles and 75 mmol m^{-2} y^{-1} for Kliplo at the end of 1990 was estimated in order to maintain constant pool water SO_4^{2-} concentrations. Uptake of SO_4^{2-} by primary production in the water column or on top of the sediment is accounted for in the model. Therefore, the most likely source of extra SO_4^{2-} is the sediment, because besides atmospheric S deposition there are no other quantitatively important sources of SO_4^{2-}. We suggest three processes that may result in more or less constant SO_4^{2-} concentrations in spite of declining SO_4^{2-} inputs: 1) equilibrium control by SO_4^{2-}- containing mineral phases, 2) desorption of SO_4^{2-} from positively charged surfaces and 3) input of SO_4^{2-} formed by oxidation of sedimentary reduced S through desiccation of a part of the pool bottom after dry summers. The first two processes represent a causal link between the supply of SO_4^{2-} and the decreased S-deposition, whereas the last process would be coincidental.

We investigated the possibility of equilibrium control of SO_4^{2-} containing minerals because this process may have a regulating effect on the SO_4^{2-} concentration. The only SO_4^{2-} containing minerals that may be considered under the current chemical pore water conditions of both study sites are aluminum (potassium) sulfate minerals because of their low solubility (Table 8). Data on pH, SO_4^{2-}-, total Al and K concentrations over a one year (1989) period (not published) have been used to check whether pore waters were in equilibrium with respect to (K-)Al-SO_4^{2-} mineral phases. Equilibria of Al^{3+} with hydroxide ligands and sulfate ligands were

Table 8. Thermodynamic constants at 298°K

Reaction	pK	ΔH_r°†	Ref.
<u>Hydroxide ligands</u>			
$Al^{3+} + H_2O \rightleftharpoons Al(OH)^{2+} + H^+$	4.98	8.33	1,2
$Al^{3+} + 2H_2O \rightleftharpoons + Al(OH)_2^+ + 2H^+$	10.13		1
$Al^{3+} + 4H_2O \rightleftharpoons + Al(OH)_4^- + 4H^+$	22.16	-38.99	1,3
<u>Sulfate ligands</u>			
$Al^{3+} + SO_4^{2-} \rightleftharpoons AlSO_4^+$	-3.21	9581	4,5
$Al^{3+} + 2SO_4^{2-} \rightleftharpoons Al(SO_4)_2^-$	-5.11	12845	4,5
<u>Natural gibbsite</u>			
$Al(OH)_3 + 3H^+ \rightleftharpoons Al^{3+} + 3H_2O$	-8.77		1
<u>Alunite</u>			
$KAl_3(SO_4)_2(OH)_6 \rightleftharpoons K^+ + 3Al^{3+} + 2SO_4^{2-} + 6OH^-$	85.4		6
<u>Basaluminite</u>			
$Al_4(SO_4)(OH)_{10} \rightleftharpoons 4Al^{3+} + SO_4^{2-} + 10OH^-$	117.7		6
<u>Jurbanite</u>			
$AlOHSO_4 \rightleftharpoons Al^{3+} + SO_4^{2-} + OH^-$	17.23		7

†Enthalpy values in J mol^{-1}
1: May et al. 1979; 2: Hem 1968; 3: Wagman et al. 1969;
4: Behr & Wendt 1962; 5: Izatt et al. 1969;
5: Adams & Rawajfih 1977; 6: Van Breemen 1973

calculated using equilibria constants and reaction enthalpies as reported by Von Freiesleben (1988, Table 8). No information was available about the fraction of Al^{3+} complexed with organic matter. Helmer et al. (1990) reported that in surface water samples from peatlands with low DOC ([DOC] $\approx$ 5mg l^{-1}, concentrations comparable with those found in Gerritsfles; 1-6.5 mg l^{-1}), 54-86% of total dissolved Al existed as Al^{3+} or other inorganic Al species. In surface waters with high DOC ([DOC] $\approx$ 50 mg l^{-1}, similar to those in Kliplo; 20-60 mg l^{-1}) about 10-20% of total dissolved Al existed as inorganic Al. In Fig.11 2pH+SO$_4$ values of pore waters collected at 0.25 cm and 1 cm depth over 1989 are plotted against pAl(OH)$_3$ values together with solubility curves (T=298°K) for natural gibbsite, Al(OH)$_3$; alunite, KAl$_3$(SO$_4$)$_2$(OH)$_6$; basaluminite, Al$_4$SO$_4$(OH)$_{10}$·5H$_2$O and jurbanite, AlOHSO$_4$·5H$_2$O (Table 8). The Al^{3+} activities were calculated without complexation with organic matter. If 50% and 90% of the total dissolved Al would be complexed by organic matter in Gerritsfles and Kliplo respectively, the pH$_2$SO$_4$-pAl(OH)$_3$ values plotted in Fig.11 would shift upwards along the y-axis by 0.3 units for Gerritsfles and by 1.0 unit for Kliplo. If pore waters are regulated by one of the minerals considered,
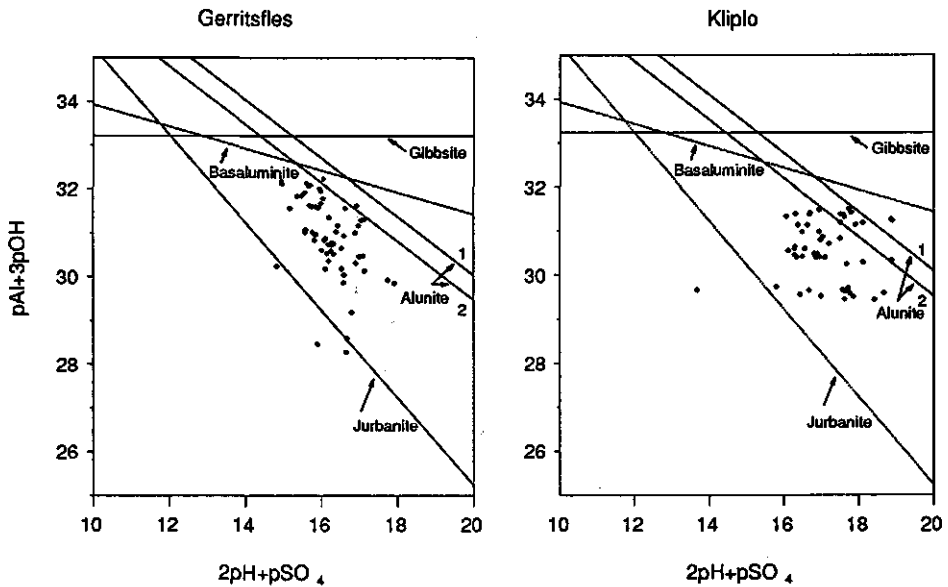
Fig.11. The pAl+3pOH and 2pH+pSO$_4$ values of pore waters of Gerritsfles and Kliplo at 0.25 and 1 cm sediment depth during collected during 1989. Solubility curves are plotted for natural gibbsite, alunite (minimum (1) and maximum (2) pK+pOH were calculated from pore waters and yielded 11.3 and 13.0 for Gerritsfles and 11.1 and 12.8 for Kliplo), basaluminite and jurbanite.

than the plotted values would follow the solubility curve of this mineral. Pore waters of Gerritsfles and Kliplo were undersaturated with respect to jurbanite and oversaturated with respect to basaluminite and alunite (except some of the samples of Kliplo) but none of the Al(K)-SO$_4$ minerals are in equilibrium with the pore water even if Al complexation to organic matter is taken into account. Summarizing we may conclude that SO$_4^{2-}$ concentrations in pore waters are most likely not regulated by equilibrium control of SO$_4^{2-}$ containing minerals.

Sulfate concentration may be regulated by adsorption or desorption at positively charged surfaces in the sediment. Ensminger (1954) carried out extractions with sodium acetate (pH 4.8) on Florida peat which was presaturated with SO$_4^{2-}$. The peat released 160 mg S per kg material. Taking a dry bulk density of peat of 0.35 g cm^{-3} for the Dutch study sites, the potential adsorption of SO$_4^{2-}$ can be estimated as about 175 mmol S per m^2·10 cm sediment depth. If Gerritsfles and Kliplo sediments would possess the same properties as the peat used for the extractions, the modelled release of SO$_4^{2-}$ from the sediment (about 75 - 89 mmol m^{-2} y^{-1}) could be explained by desorption of SO$_4^{2-}$ from peat. Recharging of the adsorption complex is necessary to provide a sustained supply of SO$_4^{2-}$ to the water column.

We have indications that periodical shifts of the redox boundary occur (Marnette et al. 1992, 1993a), so the adsorption complex can be recharged by SO_4^{2-} that has been supplied by reoxidation of reduced S compounds.

Van Dam (1988a) reported a concomitant increase of SO_4^{2-} concentrations and a decrease of alkalinity and pH in Gerritsfles and several other pools after the extremely dry summer of 1976. Because of exposure of a part of the pool bottom to the atmosphere and subsequent oxidation of large quantities of reduced S, SO_4^{2-} concentrations reached extremely high levels of about 450 µmol l^{-1} (Van Dam & Buskens, 1993). During the following years, SO_4^{2-} concentrations decreased again through dilution with rain and by SO_4^{2-} reduction. The dry summers of 1986, 1989 and 1990 may have lead to pulses of SO_4^{2-} that replenished the amount of pool water SO_4^{2-}. However, since there is no causal link between increased S-oxidation through desiccation and decrease of S-deposition, this replenishment of SO_4^{2-} only could have happened by chance, since the amount of SO_4^{2-} released through oxidation should have been in the same order of magnitude in order to complement decreasing depositional SO_4^{2-} input. Nevertheless this might be a possible mechanism to explain the more or less constant pool water SO_4^{2-} concentrations in Gerritsfles in spite of decreasing S-deposition. In Kliplo after the dry summer in 1976, the SO_4^{2-} concentration and pH remained relatively constant because the pool morphometry does not allow large parts of the bottom to desiccate.

In any case it is clear that the mechanism which is responsible for the net release of SO_4^{2-} to the water column will eventually lead to a strong decrease in sedimentary S.

CONCLUSIONS

The decrease of total S deposition onto two moorland pool systems, did not lead to decreased pool water SO_4^{2-} concentrations. The supply of SO_4^{2-} cannot be explained by the regulation of SO_4^{2-}-containing minerals but might be achieved by desorption processes in the sediment or by pulse-releases of SO_4^{2-} through desiccation of a part of the pool bottom after dry summers.

Future research will be necessary to establish the mechanisms which are responsible for the delivery of SO_4^{2-} from sediments to the water column.

Chapter 5

Estimation of mineralization rates of organic S in a moorland pool sediment

Emile C.L. Marnette

ABSTRACT. In an oligotrophic moorland pool mineralization rates of organically bound S was estimated by diagenetic modelling using porewater ammonia concentrations and sedimentary N:S ratios. Estimated maximum sulfur mineralization rates were 25 mmol m^{-2} y^{-1} and play a minor role in the overall S-cycling. High S mineralization rates relative to rates of input of organic S and the absence of a decrease of organic S with depth, point towards diagenetic formation of organic S compounds.

INTRODUCTION

Questions about the ecological effects of increased atmospheric S-deposition has stimulated research on the S-cycling in freshwater ecosystems. Sulfate reduction was not only found to be an important alkalinity generating process (Kelly et al., 1982; Kelly and Rudd, 1984; Cook et al., 1986), but also appeared to play a major role in the anaerobic mineralization of organic matter (Cappenberg et al., 1984) in sediments.

A great deal of work has been done on S mineralization in cultivated soils, forest soils and pastures with respect to soil fertility, forest productivity (e.g. Autry and Fitzgerald, 1990) and atmospheric deposition (Fitzgerald et al., 1988). In terrestrial soils, organic S generally comprises the major part of the total S pool with the small amounts of inorganic S mostly present as SO_4^{2-}. In (anaerobic) freshwater sediments organic S is often predominant too, but an appreciable part of the total S may also be inorganic. There are three possible pathways of organic S formation in sediments. First, the uptake of SO_4^{2-} by plants and subsequent reduction and assimilation into proteins, and second, esterification can contribute to the initial S pool of dead organic matter. A third possible way is the reaction of humic materials with H_2S produced by putrefaction of organic S or by SO_4^{2-} reduction. Experiments with labelled SO_4^{2-} evidenced that organic S may be the major initial product of dissimilatory SO_4^{2-} reduction (Nriagu and Soon, 1985, Brown, 1986, Marnette et al., 1992).

Investigation of the mineralization rates of organic S in sediments, coupled with solid phase data on sedimentary organic S fractions may provide information on the origin of organic S and on the importance of organic S in the fixation (and thus the internal alkalinity generation) of S in the sediment.

Mineralization of organic S is much more difficult to assess than its formation partly because it can be studied only by indirect methods. Usually, mineralization of S is estimated from the difference of S input by (non-mineralized) seston and

the S content of the top sediment which has been subject to mineralization for a period depending on the accumulation rate of the sediment (e.g. David and Mitchell, 1985). In this study the mineralization rate of organic sulfur of the top 10 cm of sediment in a shallow moorland pool was estimated by diagenetic modelling of porewater ammonia concentration profiles using sedimentary N/org-S ratios.

MATERIALS AND METHODS

Study site

Experiments were carried out in Gerritsfles (5°49'E, 52°10'N, 40 m above mean sea level), a shallow freshwater lake in the centre of The Netherlands. The pool has a simple hydrology, characterized by a small catchment area and a perched water table due to an impermeable iron pan (Schimmel and Ter Hoeve, 1952). The surface area of the pool is about 5 ha and the mean depth 0.65 m. The mean pH and SO_4^{2-} concentration of the lake water are 4.4 and 102 µM respectively. Gerritsfles is located in a heath-dominated ecosystem. The sediments are unconsolidated quartz sand covered with a detrital layer of variable thickness (0 - 50 cm), mainly originating from peat moss (*Sphagnum*).

Solid phase analyses

Sediment was sampled using a corer device as described by Ali (1984). Sediment cores were sliced in 2 cm horizontal sections. Four sediment cores were collected, two at a location with organic rich top sediment (mean C content over top 10 cm = 9.8% dry weight) and two at a sandy location (mean C content over top 10 cm = 1.4% dry weight). The sediment samples were analyzed for inorganic S and organic S fractions, total S and organic matter content. Of the organic S fractions, ester sulfate S, amino acid S and a non-reducible fraction C bonded S was determined. Ester S was estimated as hydriodic acid (HI)-reducible S (Kowalenko, 1985; Wieder et al., 1985) minus acid-volatile S (AVS). Amino acid S was determined by reduction with Raney nickel (Freney et al., 1970). The C-bonded organic S that could not be reduced by these reagents was calculated as the difference between total S and ester sulfate S, amino acid S and inorganic S (i.e. AVS + pyritic S). A wide variety of alkane sulfonates was not reduced by the HI and Raney-nickel reagents (Fitzgerald and Franklin, 1982). Carbon-bonded S that is not reduced by these agents is therefore provisionally considered to represent sulfonate S. Pyritic S makes up the major part of the inorganic S fraction (Marnette et al., 1993). Total S was determined through oxidation with a sodium

hypobromide solution to sulfate (Tabatabai and Bremner, 1970) and subsequent reduction of sulfate with HI reagent to H_2S. Total S and organic S forms were determined colorimetrically with bismuth nitrate (Dean, 1966) after conversion of the S compounds to H_2S in a digestion-distillation apparatus. The H_2S was trapped in a sodium hydroxyde solution. Pyrite content was assayed as Fe after HF extraction of non-pyritic Fe followed by oxidation of pyrite·with HNO_3 (Begheijn et al., 1978). Iron was determined colorimetrically with orthophenanthroline (Begheijn et al., 1978). The organic matter content was estimated by loss on ignition (LI) of oven dried samples (105°C) at 450°C, a common procedure for non-clayey material. Dry bulk densities were estimated from a relationship between LI and dry bulk density (Marnette and Stein, 1993). Total nitrogen and carbon were analyzed with a CHN Carlo Erba Elemental Analyzer. Of one core, depths 2-4 and 4-6 cm could not be analyzed for C and N, because no sample was left for analysis. At these depths C was estimated from the LI and the relationship between LI and total C content (Marnette and Stein, 1993). AVS was determined by sparging 1-3 g of wet sediment with high purity grade N_2 after addition of 8 ml of 12 M (concd) HCl (Wieder et al., 1985). The sample was heated to boiling and the liberated sulfide was trapped in 50 ml of 5% (w/v) zinc acetate. Sulfide was measured with a spectrophotometer as a methylene-blue complex (modified after Johnson and Nishita, 1952).

Porewater analyses

Porewater samples were collected using permanently installed *in situ* dialyses cells ("peepers") which could be sampled at the water surface (cf. Oenema, 1990). Porewater was sampled monthly throughout 1989. Ammonia was measured colorimetrically with a Technicon autoanalyzer as a complex of ammonia, sodium salicylate, sodium nitroprusside and sodium hypochloride (Harwood and Huyser, 1970).

Calculation of mineralization rates

From measured depth profiles of NH_4^+ concentrations, mineralization rates of organic N can be estimated by steady state diagenetic modelling (Berner, 1980). The following assumptions were made to calculate N mineralization rates: 1) material denoted by N is entirely converted to ammonia following first order kinetics:

$$\frac{\partial N}{\partial t} = -kN \tag{1}$$

with k is the mineralization rate constant (d^{-1}), 2) NH_4^+ is transported by molecular diffusion and there is a steady state sedimentation of organic matter and mineralization of organic matter 3) at the sediment pH (between 5 to 6), any ammonia is protonated and is rapidly and reversibly exchanged on negatively charged surfaces according to a simple linear isotherm, and 4) NH_4^+ is not involved in irreversible fixation or mineral formation. Under these conditions, the rates of N mineralization at each depth can be calculated using the steady state diagenetic equation:

$$\frac{R_{NH_4^+}}{(1+Q_n)} - R_{nit} = -\frac{D_n}{(1+Q_n)}\frac{\partial^2 C}{\partial x^2} + \omega\frac{\partial C}{\partial x} \tag{2}$$

where C is the concentration of NH_4^+ (nmol cm^{-3}), D_n the sediment diffusion constant of NH_4^+ (cm^2 d^{-1}), Q_n the linear adsorption constant for NH_4^+ (-) and R_{NH4+} is the rate of NH_4^+ formation through mineralization of organic N, whereas N_{nit} is the nitrification rate of NH_4^+. The values of $\partial^2 C/\partial x^2$ and $\partial C/\partial x$ were calculated by fitting NH_4^+ profiles using the function:

$$C_x = (C_\infty - C_0)\exp(ax) + C_\infty \tag{3}$$

with C_∞ is the NH_4^+ concentration at infinite depth and C_0 the concentration at the sediment water interface. The sediment diffusion coefficient of NH_4^+ was determined with tritiated water (Sweerts et al., 1991; Marnette et al., 1992) assuming a ratio of the molecular diffusion coefficients of NH_4^+ and ^3H_2O of 0.89 ($D_{o,NH4+}=9.8\cdot10^{-6}$ cm^2 sec^{-1}, $D_{o,3H2O}=11\cdot10^{-6}$ cm^2 sec^{-1} at T=0°C). Sediment diffusion coefficients were temperature corrected (Li and Gregory, 1974) and calculated as function of porosity (Marnette et al., 1992).

After calculation of the mineralization rate of N the mineralization rate of S was estimated from the org.N/org.S ratio and the assumption that the mineralization constant k for N is the same as for S, in other words, that the ratio of the amount of N and S mineralized is equal to the N/S ratio of the organic matter.

RESULTS

Solid phase analyses

The contents of the different S fractions are shown in Fig.1. AVS comprised only <5% of the total S content. Pyrite contents peaked in the subsurface sediment at 2-4 cm depth. In all four cores, both ester sulfate S and amino acid S decreased with depth, whereas ester sulfate S showed a small subsurface peak at 2-6 cm. Sulfonate S (non-reducible carbon-bonded S) varied irregularly with depth.

The contents of N and C decreased with depth and increased again downcore. Mean C:organic S, N:organic S ratios (Table 1) show the highest values at the surface sediment whereas also a slight increase was observed at greater depth.
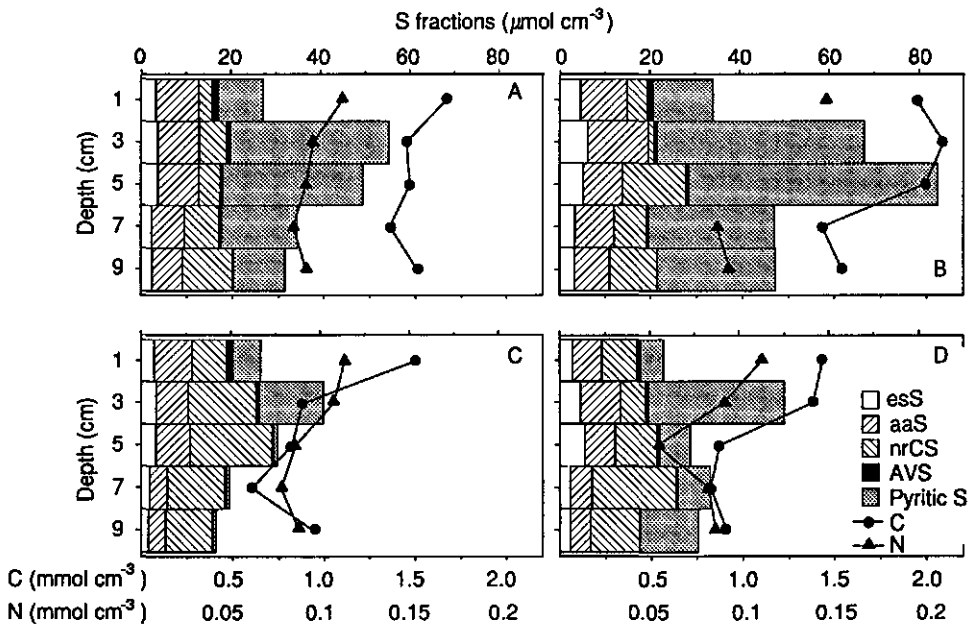
Fig.1 Sulfur fractions and total C and N contents in Gerritsfles sediment. Cores A and B are from a organic rich location, cores C and D from a sandy location. esS = ester sulfate S (HI reducible S minus AVS), aaS = amino acid-S (Raney-nickel reduced S), nrCS = non-reducible carbon-bonded S (rest fraction of organic S) also refered in the text as sulfonate S, AVS = acid volatile sulfur.

Porewater ammonia concentrations

Ammonia concentrations invariably increased with depth from a mean concentration of about 115 μmol l^{-1} at the sediment surface to about 300 μmol l^{-1} at 20 cm sediment depth. Although NH$_4^+$ concentrations in the three peepers

followed the same trend with depth, the variation between the three peepers was quite high. The mean porewater NH_4^+ concentration at the sediment surface in two peepers was about 20-30 μmol l^{-1} lower than in the third peeper and at 20 cm depth the NH_4^+ concentration in the third peeper was about 100 μmol l^{-1} lower than in the first.

Table 1. Mean N, C, total S, organic S (org.S) and N:org.S, C:org.S and C:N ratios (± SE).

Depth cm	N %	C %	total S %	org.S %	N:org.S (wt/wt)	C:org.S (wt/wt)	C:N (wt/wt)
0-2	0.65 (0.16)	7.71 (1.90)	0.36 (0.09)	0.23 (0.05)	2.72 (0.12)	32.2 (1.81)	11.8 (0.36)
2-4	0.30 (0.14)	6.21 (2.61)	0.59 (0.23)	0.21 (0.07)	1.93 (0.08)	25.5 (4.18)	11.2 (1.63)
4-6	0.24 (0.14)	5.62 (2.61)	0.59 (0.29)	0.22 (0.09)	1.48 (0.28)	20.3 (4.01)	12.2 (1.55)
6-8	0.27 (0.10)	3.55 (1.51)	0.29 (0.12)	0.14 (0.05)	1.76 (0.13)	19.8 (4.05)	10.9 (1.66)
8-10	0.28 (0.11)	3.73 (1.60)	0.28 (0.13)	0.14 (0.06)	2.05 (0.10)	23.6 (1.66)	11.8 (1.27)

number of samples, n=4 except for N, N:org.S and C:N where n=3.
N:org.S, C:org.S and C:N are means of ratios, not ratios of means

Mineralization rates
Mineralization rates of S at the top 10 cm of the sediment were calculated by diagenetic modelling of monthly collected NH_4^+ porewater profiles (Eqns.2,3) and N:org.S ratios. An accumulation rate of 1 mm y^{-1} was used (Van Dam et al., 1988b). The linear adsorption constant K was estimated to be 1.7±0.16 (±SE, n=3) from NH_4^+ extractions by shaking sediment with 0.5M K_2SO_4 (Van der Linde, pers. comm.). While the nitrification was not investigated in this study, preliminary results of experiments carried out by Van der Linde (pers. comm.) revealed that in 10 cm sediment columns, about 85% of the NH_4^+ in the water phase was consumed by nitrification in the upper 2 cm of the sediment. Therefore Rnit was set equal to $0.85*R_{NH4+}/1+K$ (Eqn.2) for the upper 2 cm and below to zero.

The mean org.N/org.S ratios (Table 1) were used to calculate the organic S mineralization from the N mineralization. The estimated S mineralization rate over 1989 is shown in Fig.2. Mineralization followed a seasonal trend with moderately high rates in spring, high rates in summer and low rates in winter. The mean

annual integrated mineralization rate over 1989 of N amounts 133 mmol m^{-2} y^{-1} and that of S amounts 25 mmol m^{-2} y^{-1}.

DISCUSSION

The inorganic S content in the top sediment (0-2 cm) of Gerritsfles is low relative to the subsurface sediment (Fig.1). An explanation for this may be that in the top sediment, overlain by a oxygenated water layer, the oxidation of inorganic S is
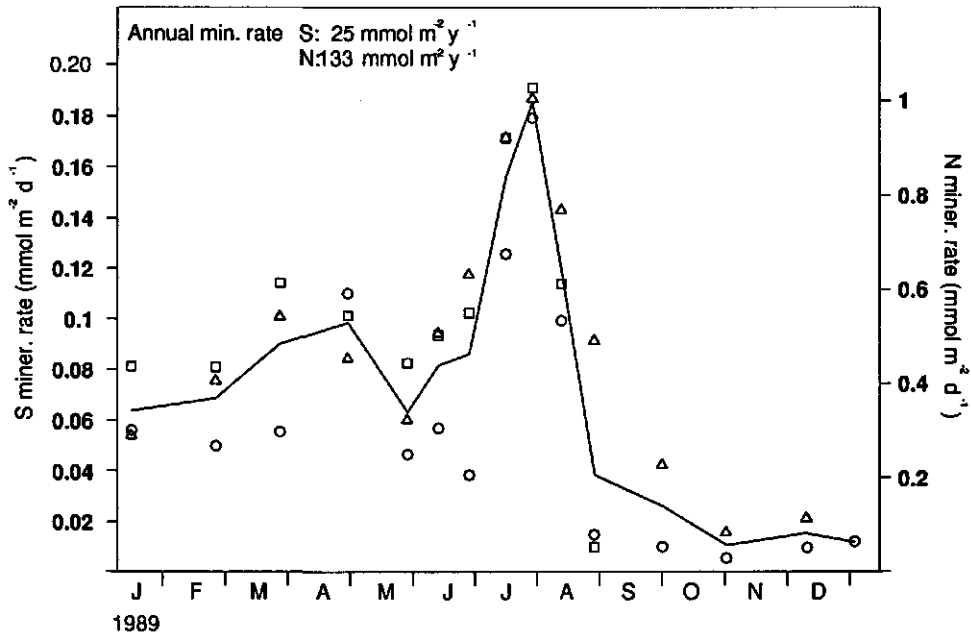
Fig.2 Mineralization rates of N and S during 1989. Different symbols represent mineralization rates calculated by using the different peepers for the collection of porewater ammonia. The solid line connects mean values.

faster than at greater depth. In the more organic sediment profiles (A,B, Fig.1), the inorganic S content (mainly consisting of pyrite) is higher than in the sandy profiles (C,D), which is in agreement with the hypothesis that pyrite, associated with organic matter is better protected against oxidation (Marnette et al., 1993b).

The organic S contents as shown in Fig.1 are the result of formation and decay of organic S compounds. The small subsurface (2-6 cm) peaks of ester sulfates may be explained by a net formation of ester sulfates where SO_4^{2-} concentrations are still relatively high whereas in the more oxic top sediment there is a net

mineralization of ester sulfates. Going down the profile, ester sulfate contents decrease presumably because of decreasing interstitial SO_4^{2-} concentrations. Breakdown of ester sulfates is mediated by extracellulair enzymes which show enhanced microbial production at low availability of SO_4^{2-} (Fitzgerald, 1976). Thus the (anaerobic) decomposition of ester sulfates will likely be faster at greater depth where SO_4^{2-} concentrations are lower. The carbon-bonded S makes up the largest part of the organic S pool, which is common in peaty sediments (Wieder and Lang, 1988, Wieder et al., 1985). Carbon-bonded S may form through uptake by plants of SO_4^{2-} and subsequent assimilation mainly into proteins (e.g. thioether, $-C-S-CH_3$ in methionine or disulfides, $-C-S-S-C-$ in cysteine) and sulfolipids (Stanko-Golden and Fitzgerald, 1990, 1991). Sulfolipids are constituents of photosynthetic tissues and contain sulfonate ($-C-SO_3H$) linkages (Harwood, 1980). Additional S may be fixed in a similar way by microbial assimilation in the sediment. In Gerritsfles, the contribution of microbial biomass to organic S is probably small compared to the organic matter derived from the *Sphagnum*. Both proteins and sulfolipids are readily metabolizible constituens and therefore accumulation of their sulfur-containing components seems unlikely. This is supported by the decrease of the protein (Raney-nickel reducible) S with depth (Fig.1). In terrestrial studies, the difference between protein S and the total organic S contents is usually assigned to sulfonate S (Stanko-Golden and Fitzgerald, 1990, 1991). In Gerritsfles however this "rest fraction" (here denoted by nrCS, non-reducible carbon bonded S), does not decrease with depth and probably also comprises of organic S compounds other than sulfonates. Together with the fact that the C:org.S ratio decreases with depth it seems plausible that addition of sulfur takes places to organic substances. This phenomena has earlier been recognized by many workers (e.g. Nriagu and Soon, 1985, Brown, 1986; Rudd et al., 1986a). Considering the reactivity of inorganic sulfur and its presence in Gerritsfles sediments, a chemical reaction seems the most likely mechanism. Organic matter may react with H_2S or HS^- produced by SO_4^{2-} reducing microorganisms through nucleophilic substitution or addition yielding thiols ($-C-SH$). Also polysulfides, which are intermediate oxidation products of H_2S or which may form from the reaction between elemental S with sulfide, may react with organic matter and form organic polysulfides (Francois, 1987, Losher and Kelts, 1989).

The S mineralization rate over the year 1989 was estimated to be 25 mmol m^{-2} y^{-1} (Fig.2). This value probably overestimates real net S mineralization rates and must therefore be considered as a maximum value. The overestimation may be due to the fact that the rate of net S mineralization was calculated with the assumption that the ratio of the net mineralization rate of N and S was equal to the organic

matter N:S ratio. However lower N:S ratios at greater depth (Table 1) imply higher net mineralization rates of N than of S. Differences between N:S ratios (wt/wt) in seston (3.8) and profundal sediment (2.0) in Wintergreen Lake (King and Klug, 1982) also pointed to a greater net release of N than of S. While the annual integrated SO_4^{2-} reduction rates over 1989 in Gerritsfles sediment are unknown, SO_4^{2-} reduction rates were estimated using different techniques in November 1990 (0.44 mmol m^{-2} d^{-1}) and July 1990 (10.9 mmol m^{-2} d^{-1}, Marnette et al., 1992). Net S mineralization rates calculated in November 1989 (0.01 mmol m^{-2} d^{-1}) and in July 1989 (0.15 mmol m^{-2} d^{-1}) amounted ~1-2% of the SO_4^{2-} reduction rates. Similarly, Cook and Schindler (1983) reported that microbial breakdown of S-containing organic matter accounted for no more than 5% of the reduced SO_4^{2-} in the hypolimnion of the acidified Lake 223, northwestern Ontario. The same value could be calculated from net mineralization rates of total S input and SO_4^{2-} reduction rates in the hypereutrophic Wintergreen Lake (King and Klug, 1982). From those findings it appeared that in these freshwater systems, the net mineralization of S plays a minor role in the overall S cycling.

Because the estimated net S mineralization rate (~ 25 mmol m^{-2} y^{-1}) is almost 5 times greater than the organic S input (~5.5 mmol S m^{-2} y^{-1}, Feijtel et al., 1989) it is evident that diagenetic formation of organic S must be an important process in Gerritsfles sediments. Although we must realize that the net S mineralization rate is overestimated, the large difference between the net S mineralization rate and the rate of organic S input, diagenetic formation of organic S is probably of the same order of magnitude than the net S mineralization rate. For a more accurate estimation of organic S mineralization, the method to estimate net S mineralization rates from diagenetic modelling of NH_4^+ profiles needs to be refined with respect to the stoichiometry of S and N mineralization.

Summarizing can be concluded that the net mineralization of S (<25 mmol m^{-2} y^{-1}) plays a minor role in the overall S cycle in Gerritsfles.

Chapter 6

Spatial variability of chemical compounds related to S-cycling in two moorland pools

Emile C.L. Marnette & Alfred Stein

ABSTRACT. Underwater sediments of two Dutch moorland pools, Gerritsfles and Kliplo, have been compared statistically with respect to total S and S-related sediment contents. Horizontal and vertical distribution of S in the two pools are significantly different from each other. Statistical analyses indicate that in Gerritsfles there is no spatial interrelation between S, C and Fe and that spatial variation of S in Kliplo is due to variations in organically bound S.

As evidenced by this study, a choice for a measurement unit like mass fraction (g g^{-1}) or volumetric mass (mg cm^{-3}) is crucial for the interpretation of spatial variability. In spatial studies of sediment constituents, it is essential to express contents of these constituents in volumetric mass fractions, since spatial sediment patterns are often obscured by spatial variations in bulk density. Taking spatial variability into account may highly affect the quantification of S-budgets of pools or lakes.

INTRODUCTION

Recently, increased atmospheric deposition of sulfur compounds has stimulated research into S-cycling of freshwater systems. Increased input of anthropogenically derived sulfate not always resulted in increasing sulfate concentrations in limnetic waters (Van Dam 1988a), presumably due to increased dissimilatory sulfate reduction (Kelly & Rudd 1984) and subsequent sulfur accumulation. Sulfur accumulation may occur through particle sedimentation and accumulation, as well through sulfate reduction and precipitation of sulfides with iron or other metals (Holdren et al. 1984; Carignan & Tessier 1985, 1988).

In many whole-lake studies on sulfate reduction and sulfur accumulation, chemical observations at a few sites are supposed to be representative for a whole lake area (e.g. Rudd et al. 1986a). Little attention has been given to horizontal variability of chemical characteristics related to sulfur accumulation. Horizontal spatial variability is known to be of great importance for areal calculations of quantitative soil and sediment variables (Stein et al. 1988a,b).

In this study we established the relationship between diagenetic processes involved in sulfur accumulation and spatial variability of data collected through intensive sampling of the sediment. To do so, attention is given to carbon (C), total sulfur (S) and iron (Fe). In order to model the diagenetic processes the most important depth is close to the water-sediment interface. We therefore measured intensively at 0-2 cm depth and at 4-6 cm depth. Geostatistical methods were used to assess the spatial distribution of C, S and Fe. The semivariogram was used for interpolation purposes and for obtaining a sampling strategy for future studies. A

simple sulfur budget calculation model was used to illustrate the effects of taking horizontal spatial variability into account.

In numerous reported studies on element distribution and accumulation in marine and freshwater systems, contents are expressed either as mass fraction (e.g. Berner & Raiswell 1983; Giblin et al. 1990; Swider & Mackin 1989) or as volumetric mass (Howarth & Jørgensen 1984; Rudd et al. 1986a). In this paper we will discuss the importance of choosing the right unit to express measured contents.

MATERIAL AND METHODS

Study sites

Two Dutch moorland pools, different in size, morphometry and vegetation, were selected to study sulfur budgets in underwater sediments (Fig.1). Both pools are located in an unconsolidated quartz sand area. They have a simple hydrology, characterized by small catchment areas and a perched water table due to an impermeable iron pan (Schimmel & Ter Hoeve 1952). The first pool, Gerritsfles (5°49'E, 52°10'N, 40 m above mean sea level), is located in a heath-dominated ecosystem. The sediments are mainly covered with a peat-moss (*Sphagnum*) detritus layer of variable thickness (0-16 cm). The surface area of the pool is approximately 7 ha and the mean depth 0.64 m (at time of sampling). The second pool, Kliplo (52°50'N, 6°26'E, 13 m above mean sea level), has a surface area of approximately 0.5 ha and a mean water depth of 0.58 m. The western side has a strip of bog vegetation (5-10 m) that separates the pool from a heathland. At the southeastern side the pool has a sandy beach, all the other sides are enclosed by forest.

Sediment sampling

The bottom sediment of the pools was sampled according to a grid pattern. Poles were lined up at 10m intervals in two parallel rows. The distance between both rows was 70m at Gerritsfles and 60m at Kliplo. Thin fishing lines, labelled every 5m, were stretched between the poles. At 10 m intervals along these lines sediment cores were collected with a coring device (Ali 1984) using plexiglas tubes ($\emptyset = 7$ cm, length 30 cm). To assess variability at distances smaller than 5m, additional observations, separated by 1m, were carried out in six clusters of four samples. The clusters were evenly spread over the pool area. The sampling locations in Kliplo covered the entire pool area. Gerritsfles was sampled only partly, covering an area
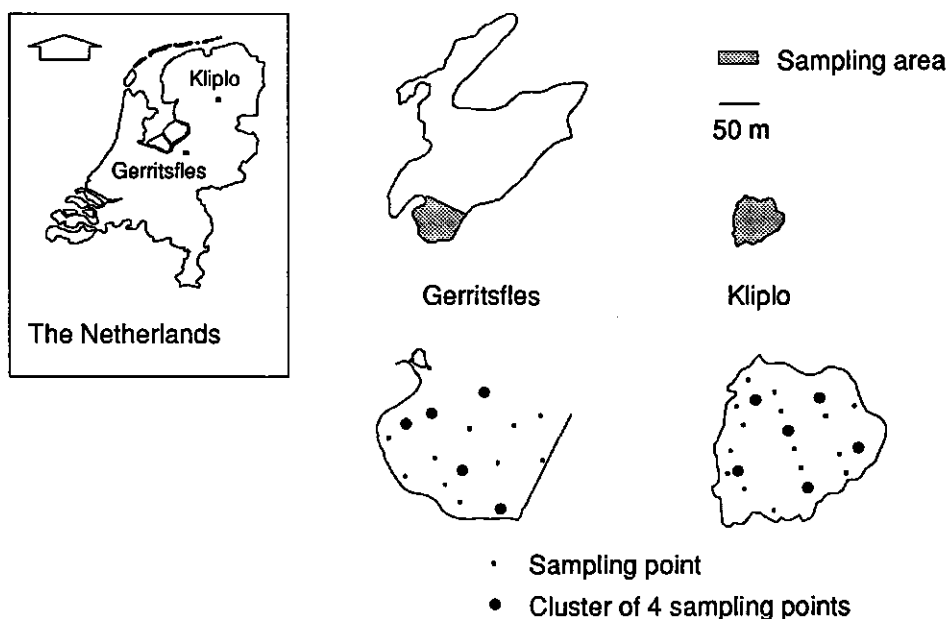
Fig.1. Location of the moorland pools with the sampling points in The Netherlands. Thicker dots indicate sample clusters.

of approximately the same size as the whole Kliplo pool. In the field, sediment cores were immediately sliced into 2 cm sections and the sections were stored at 5°C. After return to the lab, samples were frozen to -20°C and within 24 hours centrifuged in 100 ml centrifuge bottles at 3000 rpm. The residue was dried at 70°C prior to analysis.

Because previous studies indicated that sulfate reduction mainly occurs above 10 cm depth in both Gerritsfles and Kliplo (Gerritsfles: Marnette et al. 1992, Kliplo: not published) solid phase analyses were carried out on sections sampled at 0-2cm and at 4-6 cm depth. Further, analyses were performed in a selected subset of the observation locations (about 30 for Gerritsfles and 40 for Kliplo), evenly spread over the pool area including 5 clusters in Gerritsfles and 6 in Kliplo. Measurements included contents of total iron, organic matter, total carbon and total sulfur. Total S was analyzed using indirect photometric chromatography after half fusion with a $KNO_3/NaCO_3$ mixture (Hordijk et al. 1989). Total carbon was measured on a CHN Carlo Erba Elemental Analyzer. Organic matter content (OM) was estimated from the weight loss upon ashing at 430°C, being a common procedure for sandy sediments. Concentrations of total iron were determined by X-ray fluorescence spectrometry on samples fused with $Li_2B_4O_7$.

All measurements were originally expressed as mass fractions (%). Since budget calculations should be carried out with volumetric mass contents, the solid phase analyses were converted from mass fraction (MF) into volumetric mass (VM), expressed in mg cm^{-3}, by means of dry bulk densities. The dry bulk density of water saturated samples is calculated from the weight of the dry sediment, the organic matter, the inorganic sediment and the weight of H$_2$O. Density of the individual components water, inorganic sediment and organic matter can be taken as 1, 2.6 and 1.2 g cm^{-3} respectively (Håkanson & Janson 1983; Hillel 1980; Sweerts et al. 1991). Because organic matter content was the only variable measured in all observation points, an exponential regression equation between dry bulk density and organic matter was estimated from samples of four cores which were collected for this purpose. The dry bulk density-organic matter relation has been used to calculate dry bulk density values.

Statistical analyses

We used summary statistics (means, standard deviations and ranges) and autocorrelations to describe the order of magnitude of S, C and Fe contents in the sediment and to investigate whether significant relations exist between these elements. Such statistics however mask the spatial character of the variability. To define spatial variability of the elements, we used geostatistical methods (Journel & Huijbregts 1978). The variables are treated as regionalized variables, i.e. they are considered as a spatially varying (stochastic) function of the location x of sampling. We will give a short explanation of the geostatistical methods used.

First, we define the regionalized variables C(x), Fe(x) and S(x), being the carbon content, the iron content and the total sulfur content as a function of the location x. The spatial variability will be described by means of the semivariograms $\gamma_C(h)$, $\gamma_{Fe}(h)$ and $\gamma_S(h)$, defined as half the variance of the differences of observations on C, Fe and S, respectively, at distance h (Journel & Huijbregts 1978). To estimate the semivariograms, one uses the differences between the values in n locations of variables C(x), Fe(x) and S(x). The estimated semivariograms $g_z(h)$, where z = C, Fe and S, for the distance h between observations is half the average of the squared differences of all pairs of points which are separated by approximately a distance h:

$$g_z(h) = \frac{1}{2N_z(h)} \sum_{i=1}^{N_z(h)} (y_i - y_{i+h})^2 \tag{1}$$

Here y_i and y_{i+h} denotes the ith pair of observations on z=C, Fe or S, separated by distance h. $N_z(h)$ is the total numbers of such pairs.

Commonly, for n observations, semivariogram values calculated for each of the ½n(n-1) pairs of observation points are grouped into lags (distance classes). For each lag the distances between the points are approximately the same for all pairs in this class. Each lag should contain at least 30 pairs of observation points (Journel & Huijbregts 1978).

An exponential model was fitted through the semivariogram values in the lags. The exponential model was defined as

$$\hat{g}_z(h) = \alpha_z * (1 - \delta(h)) + \beta_z * (1 - e^{-\frac{h}{\gamma_z}}) \tag{2}$$

where $\delta(h) = 1$ if $h = 0$ and $\delta(h) = 0$ elsewhere. The parameters α_z represent the nugget effect, $\alpha_z + \beta_z$ the sill value, which is reached at the range, defined in this study to be equal to 2.3 $*\gamma_z$ (where 90% of the sill value is reached) for z = C, Fe and S. The values of the parameters were determined by means of a weighted fit of the models, weights being proportional to the number of pairs of observation points in each lag (Cressie 1985).

Semivariograms were determined for all variables measured at the two depths in the two pools, modelling the spatial variability for interpretative purposes. Important properties of a semivariogram include (1) the sill, i.e. the maximum of the semivariance that is reached at such a distance that spatial dependence between pairs of observation points ceases to exist, (2) the range, i.e. the distance between observations where the sill is reached, and (3) the nugget effect, i.e. the value of the semivariogram as h tends to 0. Such a nugget effect may be due to non-spatial variation (observation errors, measurement errors) or by spatial variability at very short distances (in this study: distances shorter than 1m, the minimum distance between observations). The nugget/sill ratio and the range will mainly be used to evaluate the spatial variability of a variable, in combination with the shape of the corresponding variogram. A low nugget/sill ratio implies that the variability due to measurement errors or variability at very short distance is low as compared to the spatial variability at larger distances.

Semivariograms were also used to map these variables by means of kriging, which is the optimal procedure for contouring spatially dependent data (Webster 1985; Stein 1991). The form, shape and values of a semivariogram influence the kriging equations. For example, when observations have a strong spatial correlation, the closest observations are assigned a larger weight than the observations at a

larger distance, but when observations are uncorrelated, all observations are weighed equally.

In order to determine the grid spacing necessary for obtaining predictions at unvisited locations with a prescribed precision, different grid spacings with the resulting standard deviation of the prediction error have been compared.

RESULTS

Summary statistics and correlations

To convert from mass fraction (MF) into volumetric mass (VM), all measurements must be multiplied by the bulk density. The regression equation between the calculated bulk density by means of Eqn.(1) and the organic matter content yielded a R^2 value equal to 0.91 for Gerritsfles and 0.74 for Kliplo (Fig.2). This relationship gives a good estimation of bulk density, and justifies its use for the conversion. Predicted BD values were obtained with a standard deviation equal to 0.32, being an absolute measure of the uncertainty in the individual predictions. Higher OM contents imply lower bulk densities of the sediment.
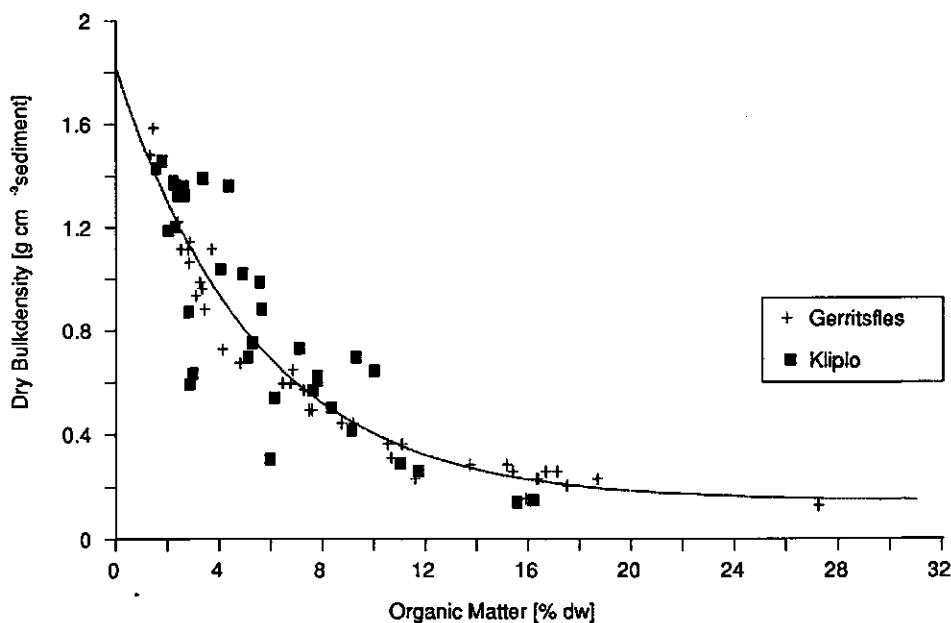

Fig.2. Relation between dry bulk density and organic matter content for Gerritsfles and Kliplo.

Summary statistics for all elements both in MF and in VM for the two pools at the different depths are given in Table 1a,b. As concerns MF, in both pools mean values of all elements were higher at 0-2 cm depth than at 4-6 cm depth, except for S in Gerritsfles. Mean values of all elements are lower in Gerritsfles than in Kliplo except for S at 4-6 cm depth.

As concerns VM, differences between element contents at two depths and between the two pools were much smaller; the conversion from MF into VM resulted in less scattered data. We notice that in both pools mean Fe contents are higher at 0-2 cm than at 4-6 cm depth when expressed as MF (Table 1a) while they are lower at 0-2 cm than at 4-6 cm when expressed as VM (Table 1b).

The MF-correlations (Table 2) between the contents of the different elements are high and nearly always significantly different from 0 (P = 0.999), whereas the VM-correlations are much lower. It appears that the high MF-correlation are obscured by the bulk density as a common factor. In Gerritsfles at 4-6 cm depth, S, Fe and C were significantly correlated. This was also the case in Kliplo at 0-2 cm depth for S with C and for Fe with C, but not for S and Fe.

Spatial variability

Semivariograms of VM fractions of C, Fe and S at 0-2 cm and 4-6 cm in Gerritsfles and Kliplo are shown in Fig.3a,b and c. Semivariograms were calculated using 6 lags, while the width of the lags was set to 9 m for Gerritsfles and 8 m for Kliplo. So the maximum distance between observations in Gerritsfles was 54 m and in Kliplo 48 m. One may notice that some of the lags contain less than 30 pairs of points (indicated with brackets). Semivariogram values for these lags are likely to be too high and should be neglected. Estimated parameters of the semivariograms are given in Table 3. Below we will discuss the interpretation of the semivariograms.

To test the significance of the differences in total S-content, a χ^2-test was used for spatially dependent observations (Stein et al. 1988a). In Gerritsfles mean total S at 0-2 cm sediment depth was lower than at 4-6 cm depth. Despite the large differences in mean values, the differences were not significant (Table 4) probably because there were a number of sampling points south-east in Gerritsfles where the total S content was higher at 0-2 cm than at 4-6 cm depth. In Kliplo differences between total S at 0-2 and 4-6 cm depth were significant (Table 4).

Table 1a. Summary statistics of the element contents expressed as mass fractions ovendried sediment at different depths in Gerritsfles and Kliplo.

Depth	Var.		Mean	SD	Min	Max	N
GERRITSFLES							
0-2	C	(%)	4.65	3.74	0.56	15.66	33
	Fe	(%)	0.42	0.22	0.20	1.06	33
	S	(%)	0.25	0.30	0.01	1.27	33
4-6	C	(%)	1.90	1.99	0.13	6.95	35
	Fe	(%)	0.33	0.20	0.19	1.06	34
	S	(%)	0.71	0.55	0.01	1.94	35
KLIPLO							
0-2	C	(%)	13.81	9.32	0.44	35.08	42
	Fe	(%)	0.72	0.35	0.13	1.69	43
	S	(%)	0.92	0.65	0.00	2.60	41
4-6	C	(%)	6.29	4.94	0.18	19.84	47
	Fe	(%)	0.42	0.24	0.11	1.28	46
	S	(%)	0.29	0.29	0.01	1.41	45

Table 1b. Summary statistics of the element contents expressed as volumetric mass fractions wet sediment at different depths in Gerritsfles and Kliplo.

Depth	Var.		Mean	SD	Min	Max	N
GERRITSFLES							
0-2	C	(mg cm^{-3})	19.51	4.60	6.12	26.82	33
	Fe	(mg cm^{-3})	2.23	0.79	0.88	3.60	33
	S	(mg cm^{-3})	1.10	1.26	0.19	7.45	33
4-6	C	(mg cm^{-3})	12.79	7.27	1.85	23.89	33
	Fe	(mg cm^{-3})	3.07	0.78	1.50	5.25	33
	S	(mg cm^{-3})	7.97	7.29	0.08	21.68	32
KLIPLO							
0-2	C	(mg cm^{-3})	24.44	10.10	5.60	51.67	41
	Fe	(mg cm^{-3})	1.57	0.45	0.89	2.60	43
	S	(mg cm^{-3})	1.69	0.97	0.00	3.94	41
4-6	C	(mg cm^{-3})	21.76	9.42	3.11	66.58	44
	Fe	(mg cm^{-3})	1.80	0.58	0.50	3.09	46
	S	(mg cm^{-3})	0.90	0.43	0.06	2.11	45

Table 2. Correlation coefficients in Gerritsfles and Kliplo. MF data are above the diagonal, VM data are below the diagonal. One-tailed significance: * = .01 ** = .001.

Depth		C	Fe	S	OM
GERRITSFLES					
0-2	C	1.00	0.80**	0.64**	0.97**
	Fe	-0.38	1.00	0.82**	0.79**
	S	-0.16	0.28	1.00	0.61**
	OM	---	---	---	1.00
4-6	C	1.00	0.82**	0.23	0.93**
	Fe	-0.45*	1.00	0.42*	0.82**
	S	-0.63**	0.52*	1.00	0.19
	OM	---	---	---	1.00
KLIPLO					
0-2	C	1.00	0.89**	0.74**	0.98**
	Fe	-0.43*	1.00	0.83**	0.89**
	S	0.47*	-0.24	1.00	0.74**
	OM	---	---	---	1.00
4-6	C	1.00	0.76**	0.87**	0.97**
	Fe	-0.32	1.00	0.85**	0.81**
	S	0.31	-0.12	1.00	0.90**
	OM	---	---	---	1.00

DISCUSSION

Mass fraction vs. volumetric mass.

MF data for the different elements are all highly correlated with organic matter in Gerritsfles (Table 2) except for S. The correlation with BD explains this relationship, since low BD implies high MF contents. Sediments in Gerritsfles and Kliplo show large horizontal and vertical variation in porosity and organic matter content (and hence in bulk density). Therefore, interpretation of spatial patterns in MF contents in these sediments may be obscured by spatial variation in bulk densities. In the following discussion of spatial variability and the comparisons between different locations, we will therefore only consider VM-contents.

Table 3. Estimated parameters of exponential semivariogram models for all elements expressed as volumetric mass at different depth in Gerritsfles and Kliplo.

Depth (cm)	Var.	nugget	sill	range[†] (m)	nugget/sill (%)
GERRITSFLES					
0-2	C	17.1	-	>54	-
	Fe	0	0.61	10.3	0
	S	0	1.53	7.0	0
	C	0	73.7	43.6	0
4-6	Fe	0.51	0.58	0.19	87.4
	S	2.0	-	>54	-
KLIPLO					
0-2	C	16.5	107	39.8	15.5
	Fe	0	0.19	8.0	0
	S	0.34	1.69	>48	-
	C	34.0	-	>48	-
4-6	Fe	0.2	-	>48	-
	S	0	0.17	1.78	0

[†] Range = distance where 90% of the sill is reached, though reworking h from Eqn.(2) and $\hat{g}(h)=0.9*(\alpha_z+\beta_z)$; $(\alpha+\beta)=$sill, $z=$C,Fe and S.

Table 4. Significance of differences between S-contents. MF data are above the diagonal, VM data are below the diagonal. Two-tailed significance: * = .01 ** = .001.

		Gerritsfles		Kliplo	
		0-2	4-6	0-2	4-6
Gerritsfles	0-2	---	3.326	8.848*	
	4-6	0.081	---		2.489
Kliplo	0-2	1.332		---	7.861*
	4-6		0.115	21.624*	

Spatial variability of C, Fe and S

The semivariograms in Fig.3 can be used to evaluate spatial dependence of C, Fe and S in both pools. We would like to focus on a few features that are important in this.

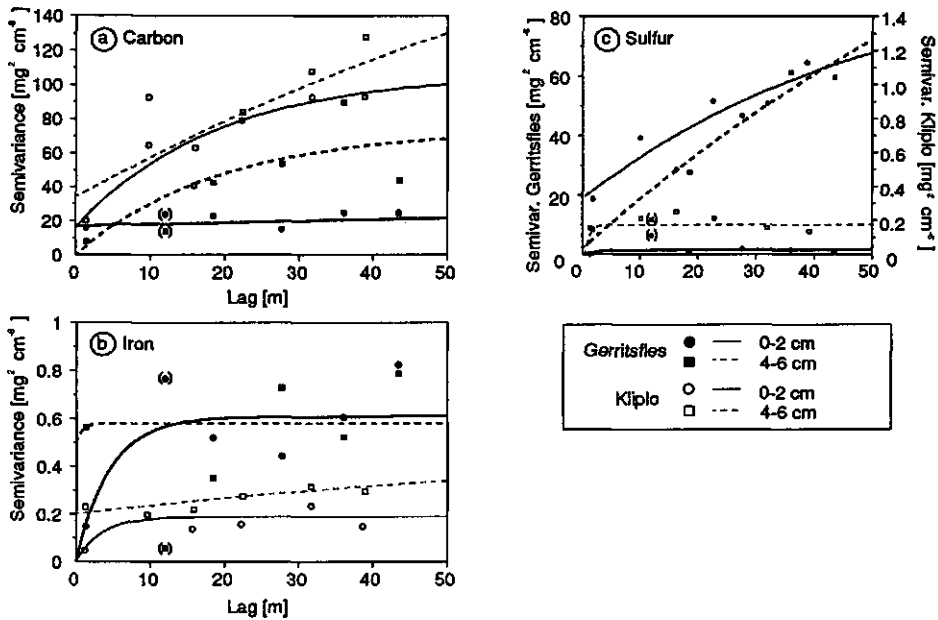Some semivariograms show a linear shape (Fig.3), yielding a range that

Fig.3. Semivariograms of total C (a), Fe (b) and S (c). Symbols in parentheses indicate that the number of pairs of observations, on which the estimate of the semivariogram was based is lower than 30.

exceeds the size of the pool (Table 3). In case of C at Gerritsfles (0-2 cm) and of Fe at Kliplo (4-6 cm) the semivariogram is flat and shows a nugget-type behaviour (Figs.3a,b). We also observe a strong nugget effect when the range is very small, which is the case for Fe at Gerritsfles (4-6 cm) and for S at Kliplo (4-6 cm, Figs.3b,c). All elements with a strong nugget effect show spatial independence at that particular depth. On the contour maps in Figs.4e and 5f the pure nugget effect can be recognized by relatively large differences in C or Fe content very near the sampling points, while at larger distances the contents are about equal.

The linear shape of a semivariogram may be an indication of a trend, but the number of observations was too small to study this in detail. A stationary analysis well serves the purpose of this study especially because we did not need to extrapolate the data (Journel 1992). The contour maps of C and S in Kliplo at 0-2 cm and of C at 4-6 cm depth show a clear trend for both elements (Figs.5a,c,d). The trend in C contents at the top sediment layer in Kliplo corresponds to a sandy area at the southeast side of the pool whereas the top sediment gets more organically rich ending up as a small bog at the northwest side. The trend in C contents at Kliplo at 0-2 cm depth coincides with the trend observed in S contents (Fig.5c), suggesting that differences in total S content may be determined by

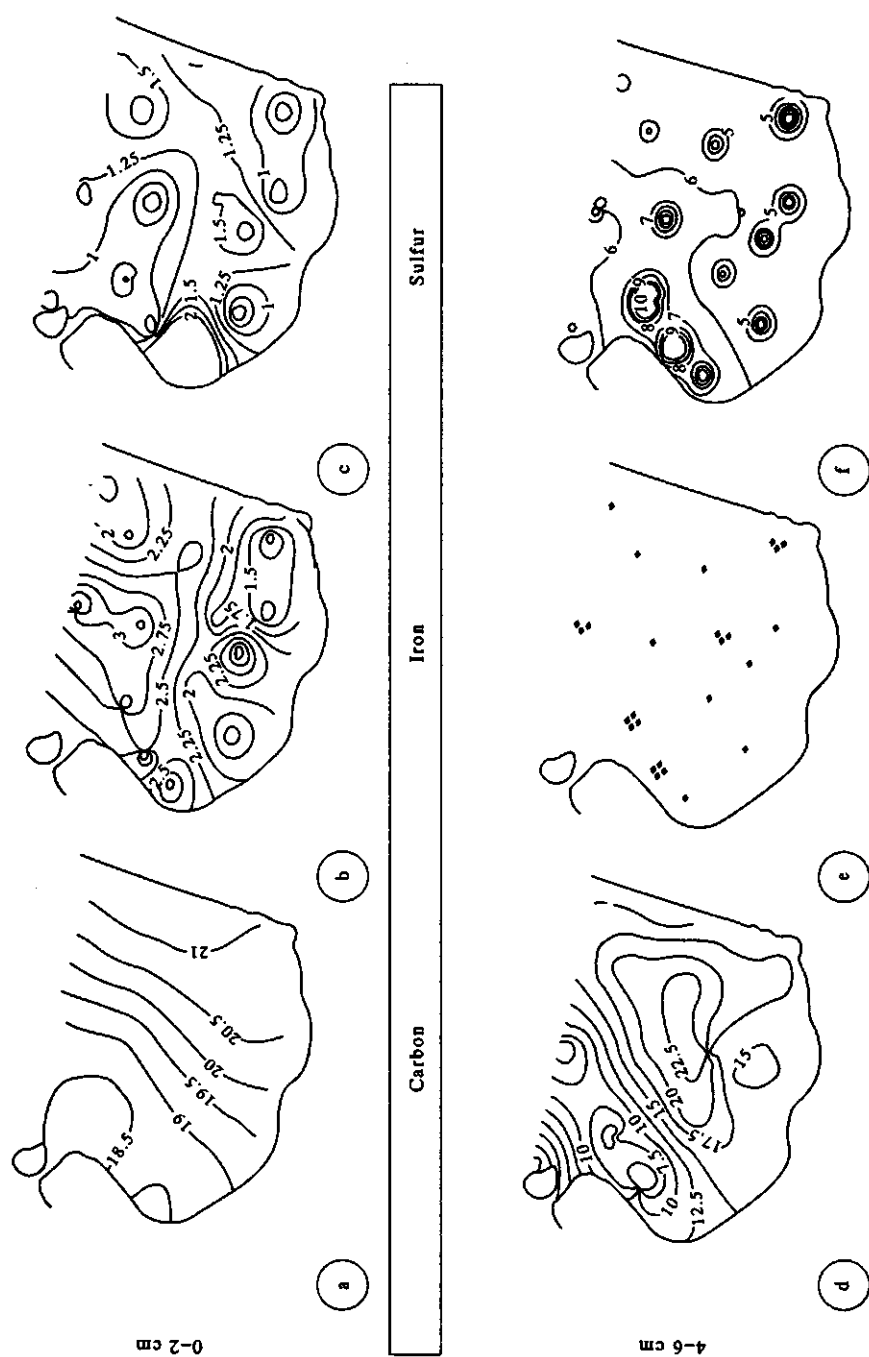**Fig.4.** Interpolated contour maps of C, Fe and S volumetric mass fractions [mg cm^{-3}] in Gerritsfles sediment at 0-2 cm and 4-6 cm depth.

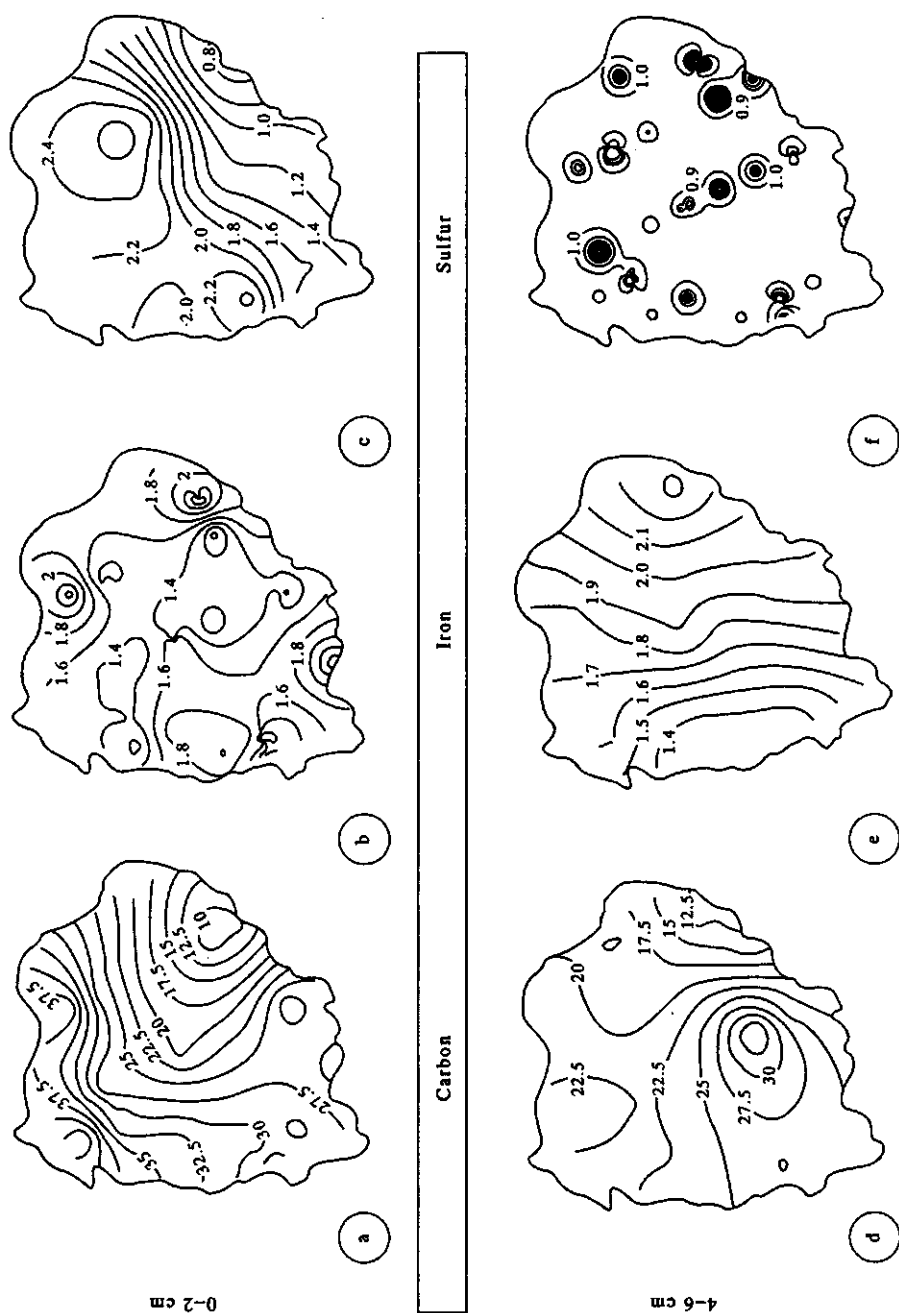**Fig.5.** Interpolated contour maps of C, Fe and S volumetric mass fractions [mg cm^{-3}] in Kliplo sediment at 0-2 cm and 4-6 cm depth.

differences in organically bound S at the upper sediment layer.

Data suggest that S cycling in both pools is different; in Gerritsfles more S has accumulated at 4-6 cm depth than at 0-2 cm depth while in Kliplo an opposite pattern is observed (Table 1b). One may notice that at these depths also the strongest relations exist between S, C and Fe, while such relationships are weaker or even absent at depths where S-accumulation is lower (Table 2). Sulfur can accumulate in both organic and inorganic form. Iron sulfides are the main form of inorganic S. In marine sediments iron-sulfides constitute the major pool of sulfur in sediments
(Jørgensen 1983). In freshwater sediment, however, this may not necessarily be true (e.g. Nriagu & Soon 1985). Organic S may consist of organic C sulfidized by the reaction of H_2S with organic matter (Nissenbaum & Kaplan 1972; Mango 1983) and of organic S deposited as seston. In Gerritsfles the inversed significant relationship between C and Fe and C and S, and the relationship between Fe and S at 4-6 cm depth indicate that variation in S is due to variations in the inorganic S content. This is supported by detailed solid phase analyses of cores taken in highly organic and low organic sediment in Gerritsfles (not published). In these cores differences in total S could be attributed to differences in iron sulfides. However, the fact that S (4-6) seems to be spatially dependent (low nugget/sill, Table 3, Fig.3c) while Fe is not (pure nugget effect, Fig.3b), suggests that S and Fe are not spatially interrelated.

In Kliplo at 0-2 cm depth, C and Fe are also negatively correlated, but C and S show a positive correlation while no significant correlation exists between Fe and S. This supports our earlier suggestion that spatial variation in total S is determined by spatial variation in organically bound S.

There may be several reasons for preferential S accumulation at certain regions. One may think of spatial differences in sulfate reduction rates, sedimentation rates, in the ability of the sediment to trap sulfides or in local reoxidation. For logistic reasons it would be almost impossible to assess processes as reduction and reoxidation rates on areal basis. We do have indications, that (net) reduction rates in Gerritsfles, measured at two extreme sites (highly organic and sandy sediments) do not differ systematically (Marnette *et al.* 1992). Spatial differences in sedimentation rates may also be responsible for the uneven horizontal distribution of total S in the sediment. The question is if sedimentation rates are positively correlated with S contents. Most of the accumulating material is of organic origin, since sediment accumulation in the pools is mainly determined by growth of *Sphagnum* (Gerritsfles), sedimentation of seston (Kliplo), input of organic material from surrounding vegetation and input of particulate material from the atmosphere.

The lack of a C-S correlation in Gerritsfles at 0-2 cm and an inverse relationship at 4-6 cm depth between C and S, indicate that spatial variation in sedimentation rate does not directly influences the spatial S-distribution. In Kliplo however, there is a significant correlation between S and C at 0-2 cm depth, so here sedimentation rates may directly determine S-distribution.

Spatial variability and calculation of sulfur budgets

To illustrate how the horizontal variation in S is reflected in sulfur budget calculations, a simple sulfur budget for Gerritsfles is examined. One can assume that both the atmospheric deposition (Erisman et al. 1989) and the sedimentation rate have been constant over the area during the last two decades.

The mean S pool in the upper 2 cm of the sediment amounts to 688 mmol m^{-2} (1.10 mg S cm^{-3}, Table 1b, times $2 \cdot 10^4/32$ gives 688 mmol S m^{-2} in the upper 2 cm sediment layer). At a sedimentation rate of 1 mm yr^{-1} (Van Dam 1988b), and an atmospheric input of 80 mmol m^{-2} yr^{-1} SO$_4^{2-}$ (Feijtel et al. 1989), this amounts to 43% of the atmospheric input. Assuming that SO$_4^{2-}$ concentrations in pool water have been practically constant over the last decades (Van Dam 1987), and that internal cycling of S does not affect the overall S retention in the upper 2 cm, 57% of the atmospheric S input must be removed to the groundwater or reenter into the atmosphere. However, taking into account the spatial variability of total S, the S retention (as fraction of atmospheric input) ranges from 4 - 390%, yielding a pattern which is similar to the total S map (Fig.4). The value 390% is based on a very high S measurement (7.45 mg cm^{-3}, Table 1b). Taking the next highest value, S retention amounts 78%, which illustrates that spatial variability needs to be taken into account when calculating S-budgets.

Sampling strategy for future studies

Finally one may question whether the analysis of spatial variability may be helpful when carrying out a future investigation in a similar ecosystem. For this purpose, we determined the necessary grid spacing to achieve a prescribed precision on an interpolated map (Fig.6). For Gerritsfles we notice that to obtain interpolated maps of total S content at a higher precision than 1%, the grid spacing should be equal to 4m at 0-2cm depth, and equal about 14m at 4-6cm depth. For Kliplo a very small grid mesh (< 1m) is needed to obtain interpolated maps at a higher precision than 1%. For such cases, using contour maps for the characterization of the S-content with increased precision, will put an (extremely)

high burden on the sampling effort as compared to a few measurements needed to estimate the mean value of S.

Precision obtained
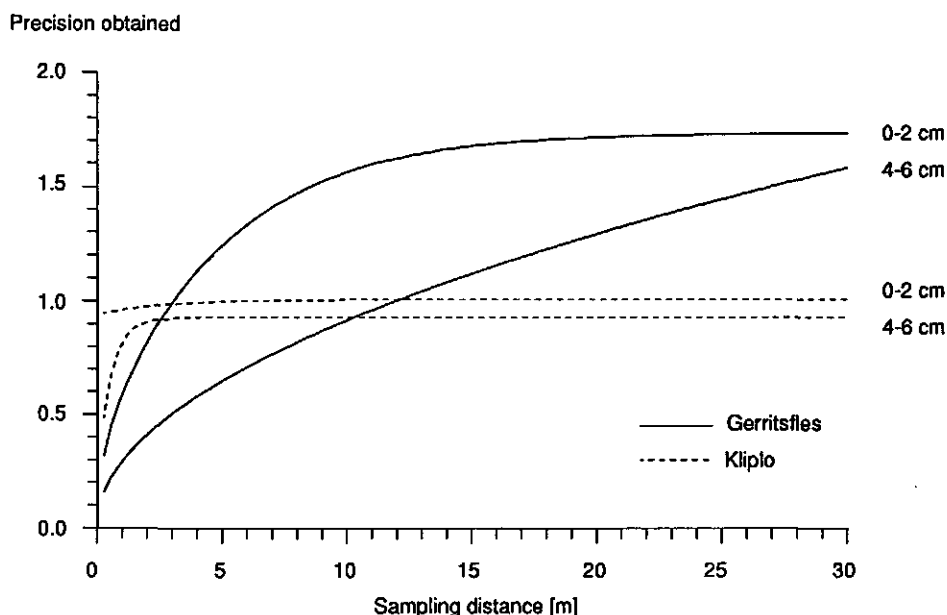
Fig.6. The required grid mesh to measure total S as a function of the required precision for Gerritsfles and Kliplo.

CONCLUSIONS

1. In spatial variability studies of elemental sediment constituents, it is essential to express the elemental contents in volumetric mass fractions, since spatial sediment patterns are often obscured by spatial variations in bulk density.
2. Spatial variation of S in Kliplo is due to organically bound S. For Gerritsfles spatial interrelation between C, S or Fe could not be recognized.
3. To obtain interpolated maps of total S content at a higher precision than 1%, a very small (< 1m) grid spacing is needed for Kliplo. For Gerritsfles the grid spacing should be 4m at 0-2cm depth and 14m at 4-6cm depth for a precision higher than 1%.

Chapter 7

Epilogue

EPILOGUE

The previous chapters of this thesis presented some aspects of the sulfur cycling in poorly buffered freshwater systems in The Netherlands. This chapter is reserved for the main conclusions that can be drawn from this study and for some afterthoughts concerning aspects that remained underexposed and future research necessary to answer yet unresolved problems.

MAIN CONCLUSIONS

- A tracer $^{35}S^{2-}$ study indicated that a part of reduced S introduced into the sediment was transferred from the sediment into the overlying water. Only a small fraction of labelled S in the water column could be recovered as either SO_4^{2-} (3%) or S^{2-} (0.3%), indicating rapid transport of this mobile reduced S to an unknown form of S e.g. organic-S or S of intermediate oxidation state.
- Results of whole core injections of $^{35}SO_4^{2-}$ and measurements about removal of SO_4^{2-} in overlying water in July 1990 demonstrated that there must be a flux of reduced S from the sediment into the water column of which possibly >90% was reoxidized to SO_4^{2-}.
- Sulfate reduction rates in sediments with higher volumetric mass fraction of organic matter did not differ significantly from those in sediments with a lower mass fraction of organic matter.
- $^{35}SO_4^{2-}$ core injections indicated that organically bound S is a major (75-88%) initial product of sulfate reduction in Gerritsfles sediments.
- The decrease of total atmospheric S deposition onto two moorland pool systems, did not lead to decreased pool water SO_4^{2-} concentrations. The supply of SO_4^{2-} cannot be explained by the regulation of SO_4^{2-}-containing minerals but might be achieved by desorption processes in the sediment or by pulse-releases of SO_4^{2-} through desiccation of a part of the pool bottom after dry summers.
- This research demonstrated that the moorland pools can effectively cope with inputs of S by reducing SO_4^{2-} and by subsequently storing the reduced S in either organic or inorganic form. In Gerritsfles and Kliplo respectively about 70% and 80% of the incoming S is lost to the sediment, i.e. reduced and buried. Hence, the reduction of SO_4^{2-} is an important mechanism to buffer the incoming acidic S compounds.
- Pore water chemistry in both pool sediments is extremely dynamic. Pore water data indicate rapid formation and reduction of Fe-oxides. In Gerritsfles and Kliplo, pyrite was the most important iron sulfide phase. The clear

distinction between sedimentary molar FeS_2/AVS ratios in stratified lakes (<1) and in both Dutch study sites with a continuously oxic water column (>30) indicate that the redox status may be a main factor in determining whether pyrite or AVS is formed.

The slow formation of framboidal pyrite through sulfurization of iron sulfide precursors is thought to be an important pathway of pyrite formation in the freshwater sediments of Gerritsfles and Kliplo. The presence of single-crystal morphology of pyrite indicates that pyrite in both sediments may also form rapidly. The close association of pyrite framboids and organic matter, and the undersaturation of bulk pore waters with respect to amorphous FeS suggest that the framboidal pyrite is formed at microsites within organic matter.

The net mineralization of S plays a minor role in the overall S cycle in Gerritsfles and was estimated to be maximally 25 mmol m^{-2} y^{-1}.

In spatial variability studies of elemental sediment constituents, it is essential to express the elemental contents in volumetric mass fractions, since spatial sediment patterns are often obscured by spatial variations in bulk density.

Spatial variation of S in Kliplo is due to organically bound S. For Gerritsfles spatial interrelation between C, S or Fe could not be recognized.

To obtain interpolated maps of total S content at a higher precision than 1%, a sampling scheme with a very small (< 1m) grid spacing is needed for Kliplo, which implies an extremely high sampling effort. For Gerritsfles the grid spacing should be 4m at 0-2cm depth and 14m at 4-6cm depth for a precision higher than 1%.

FINAL CONSIDERATIONS AND FUTURE RESEARCH

Methods to estimate SO_4^{2-} reduction.

Sulfate reduction rates were estimated using different methods. The net removal of SO_4^{2-} in the overlying water column is the result of several processes other than SO_4^{2-} reduction (Chapter 2). Sulfate profiles are the net result of SO_4^{2-} reduction and reoxidation of reduced S compounds to SO_4^{2-}. Hence diagenetic modelling of these profiles on basis of SO_4^{2-} reduction only, underestimates the real SO_4^{2-} reduction rate. In case incorporation of reduced S into organic substances takes place and adsorption of SO_4^{2-} to the sediment matrix is negligible, depletion of $^{35}SO_4^{2-}$ added to the sediment is the only reliable method available to estimate the real SO_4^{2-} reduction rate. In the present study there seems to be quite a discrepancy between reduction rates estimated by diagenetic modelling and from depletion of $^{35}SO_4^{2-}$ (Chapter 2). It was suggested that adsorption of $^{35}SO_4^{2-}$ to e.g. Fe(hydr)oxides could

not contribute to the depletion of $^{35}SO_4^{2-}$, because separate experiments revealed that after inhibition of SO_4^{2-} reduction with Na_2MoO_4, recovery of $^{35}SO_4^{2-}$ was almost complete. However, MoO_4^{2-} not only has the same charge, but it is stereochemically similar to SO_4^{2-} and therefore competes with $^{35}SO_4^{2-}$ for adsorption at positively charged surfaces. Although addition of zinc acetate solution before measuring the rest activity of $^{35}SO_4^{2-}$ may have released some of the $^{35}SO_4^{2-}$ eventually adsorbed to the sediment matrix, the aspect of possible adsorption of SO_4^{2-} in the sediment needs further investigation.

Sulfate reduction rates in Gerritsfles sediment estimated in sediment slurries spiked with $^{35}SO_4^{2-}$ (Feijtel et al. 1989) and with whole core $^{35}SO_4^{2-}$ injection (this study) agreed very well. The use of batches is much cleaner, easier and faster than the use of whole sediment cores. Therefore, if adsorption of SO_4^{2-} seems to play a minor role, the measurement of $^{35}SO_4^{2-}$ depletion in batches is considered to be an excellent way to estimate real SO_4^{2-} reduction rates in these types of sediment.

The flux of non-SO_4^{2-} across the sediment/water interface
Two findings in the study described in Chapter 2 point to the existence of a flux of yet unidentified S species from the sediment into the water column: 1) the increase of the SO_4^{2-} concentration in the overlying water column during enclosure experiments, combined with a SO_4^{2-} concentration gradient resulting in downward diffusive transport of SO_4^{2-} across the sediment/water interface 2) the small fraction of labelled SO_4^{2-} of the total activity recovered in the water column after injection of labelled Na_2S in sediment cores. Above observations were explained by a diffusive flux of one or more reduced S species from the sediment into the water column with subsequent oxidation to SO_4^{2-}. During the core incubation experiment, labelled reduced S recovered in the water column appeared to be persistent against chemical oxidation. The same phenomenon has been observed by Hordijk et al. (submitted) in Lake Vechten, a meso-eutrophic freshwater. The authors reported that under oxic conditions over 60% of the sulfur was released as non-SO_4^{2-} species. If this non-SO_4^{2-} pool in the lake water of moorland freshwater systems is quantitatively important, as is the case in Lake Vechten, then S-budgets, which are based on SO_4^{2-} data, must be re-estimated. Identification and quantification of this non-SO_4^{2-} sulfur in the lake water should be one of the subjects in future research.

Estimation of dry deposition
Dry deposition estimates are still an uncertain factor in the S budgets of both moorland pools. Interpolated values based on measurements at stations of the National Air Quality Monitoring Network are the best estimates so far (Chapter 4).

Based on the uncertainty of interpolated deposition values at the moorland pool location for wet deposition (25%) and dry deposition (45%), the uncertainty for total deposition estimates is about 40%. The budget terms outseepage and overflow are directly related to measured SO_4^{2-} pool water concentrations and do not show a trend over the period considered (1982-1990). Therefore changes in total S deposition are proportional to the remaining "rest term" indicated as the net SO_4^{2-} removal, resulting in lower net removal rates when the S deposition decreases (Chapter 4). The mean (1982-1990) SO_4^{2-} removal coefficient, which is the proportion of incoming SO_4^{2-} removed from the water column by biochemical processes was calculated as 74% for Gerritsfles and 83% for Kliplo. Using the uncertainty in total S deposition of 40%, the SO_4^{2-} removal coefficients range from 55-81% for Gerritsfles and from 72-88% for Kliplo. These ranges are quite high although for Kliplo the conclusion holds that the SO_4^{2-} removal coefficient is relatively high compared with other oxic seepage lakes (Kelly et al. 1986; Baker et al. 1987). A study should be carried out to get more accurate estimates of dry S deposition on both pool water surfaces.

The extra SO_4^{2-} source to the lake water of Gerritsfles and Kliplo
The study described in Chapter 4 is an example of the fact that research inevitably raises new questions. In this thesis these questions have not been answered adequately, but some suggestions were brought about.

The decrease of atmospheric S deposition starting around 1986 was not reflected in a decrease of pool water SO_4^{2-} concentrations. Consequently there must be a, yet unidentified, source of SO_4^{2-}, which has not been included as such in the S budgets. Two theoretically possible SO_4^{2-} sources were proposed: 1) desorption of SO_4^{2-} from the sediment matrix, and 2) desiccation of sediment at low water levels during dry summers, oxidation of reduced S to SO_4^{2-} and entering of the SO_4^{2-} in the pool water after rise of the water level. The second mechanism has been observed earlier in Gerritsfles during the dry summer of 1976 (Van Dam 1987). Future studies should show whether indeed sediments may act as a buffer for changes in pool water SO_4^{2-} concentrations, by desorption/adsorption reactions or by oxidation/reduction processes.

Chapter 8

References

REFERENCES

Adams F. & Rawajfih Z. (1977) Basaluminite and alunite: A possible cause of sulfate retention by acid soils. Soil Sci. Soc. Am. J. **41**: 686-692.

Ali A. (1984) A simple and efficient sediment corer for shallow lakes. J. Environ. Qual. **13**: 63-66.

Aller R. and Rude P.D. (1988) Complete oxidation of solid phase by manganese and bacteria in anoxic marine sediments. Geochim. Cosmochim. Acta **52**: 751-765.

Andrews D. & Bennet A. (1981) Measurements of diffusivity near the sediment-water interface with a fine-scale resistivity probe. Geochim. Cosmochim. Acta. **45**: 2169-2175.

Archie G.E. (1942) The electrical resistivity log as an aid in determining some reservoir characteristics. Trans.Am.Inst.Min. Metall.Pet.Eng. **146**: 54-62.

Arnston R.H., Dickson F.W. and Tunnel G. (1960) Systems S Na_2O-H_2O and SH_2O:application to the mode of origin of natural alkaline polysulfide and thiosulfate solutions. Amer. J. Sci. **258**: 574-582.

Autry A.R. and Fitzgerald J.W. (1990) Application of the heterotrophic activity method to organosulfur formation on forest soils. Soil Biol. Biochem. **22**: 743-748.

Bak F. and Pfennig N. (1987) Chemolithotrophic growth of *Desulfovibrio sulfodismutans* sp. nov. by disproportionation of inorganic sulfur compounds. Arch. Microbiol. **147**: 184-189.

Bak F. (1988) Sulfatreduzierende Bakterien und ihre Aktivitat im Littoralsediment der unteren Gull (Uberlinger See). Ph.D dissertation Univ. of Konstanz, Germany.

Bak F. and Cypionka H. (1987) A novel type of energy metabolism involving fermentation of inorganic sulphur compounds. Nature **326**: 891-892.

Bak F., Scheff G. & Jansen K.H. (1991) A rapid and sensitive ion chromatographic technique for the determination of sulfate and sulfate reduction rates in freshwater lake sediments. FEMS Microbiology Ecology **85**: 23-30.

Baker L.A., Brezonik P.L. & Pollman C.D. (1986) Model of internal alkalinity generation: sulfate retention component. Water, Air, and Soil Pollution **31**: 89-94.

Baker L.A., Pollman C.D. and Eilers J.M. (1988) Alkalinity generation in softwater Florida lakes. Water Resources Research **24**: 1069-1082.

Baker L.A., Urban N.R., Brezonik P.L. & Sherman L.A. (1989) Sulfur cycling in an experimentally acidified seepage lake. In: Saltzman ES & Cooper WJ (Ed) Biogenic Sulfur in the Environment (pp 79-100). Am. Chem. Soc., Washington, DC

Begheijn L.Th., Van Breemen N. and Velthorst E.J. (1978) Analysis of sulfur compounds in acid sulfate soils and other recent marine soils. Commun. in soil science and plant analysis **9**: 873-882.

Behr B. & Wendt H. (1962) Fast ion reactions in solution (I) Formation of the aluminum sulfate complexes. Z. Elektrochem. **66**: 223-228.

Berner R.A. (1964) An idealized model of dissolved sulfate distribution in recent sediments. Geochim. Cosmochim. Acta. **28**: 1497-1503.

Berner R.A. (1967) Thermodynamic stability of sedimentary iron sulfides. Am. Jour. Sci. **265**: 773-785.

Berner R.A. (1970) Sedimentary pyrite formation. Amer. J. Sci. **268**: 1-23.

Berner RA (1980) Early diagenesis: A theoretical approach. Princeton.

Berner R.A. and Raiswell R. (1983) Burial of organic carbon and pyrite sulfur in sediments of Phanerozoic times: a new theory. Geochim. Cosmochim. Acta **47**: 855-867.

Berner R.A. (1984) Sedimentary pyrite formation: an update. Geochim. et Cosmochim. Acta **48**: 605-615.

Bettany J.R. and Stewart J.W.B. (1980) Comparison of the amounts anf forms of sulfur in soil organic matter fractions after 65 years of cultivation. Soil Sci. Soc. Am. J. **44**: 70-75.

Boulegue J. (1978) Solubility of elemental sulfur in water at 298K. Phosphorus and Sulfur **5**: 127-128.

Brown K.A. (1986) Formation of organic sulphur in anaerobic peat. Soil Biol. Biochem. **18**: 131-140.

Canfield D.E., Raiswell R., Westrich J.T., Reaves C.M., & Berner R.A. (1986) The use of chromium in the analysis of reduced inorganic sulfur in sediments and shales. Chemical Geology **54**: 149-155.

Cappenberg Th.E., C.A. Hordijk and C.P.M.M. Hagenaars (1984) A comparison of bacterial sulfate reduction and methanogenesis in the anaerobic sediments of a stratified lake-ecosystem. Arch. Hydrobiol. Beih. Ergebn. Limnol. **19**: 191-199.

Carignan R. and Tessier A. (1985) Zinc deposition in acid lakes: The role of diffusion. Science **228**: 1524-1526.

Carignan R. and Nriagu J.O. (1985) Trace metal deposition and mobility in the sediments of two lakes near Sudbury, Ontario. Geochim. Cosmochim. Acta

49: 1753-1764.

Carignan R. (1988) Seasonal dynamics of sulfate and hydrogen sulfide near the sediment-water interface of an oligotrophic acid lake. Verh. Internat. Verein. Limnol. **23**: 106-115.

Carignan R. and Tessier A. (1988) The co-diagenesis of sulfur and iron in acid lake sediments of southwestern Quebec. Geochim. Cosmochim. Acta **52**: 1179-1188.

Chen K.Y., J.C. Morris (1972) Kinetics of Oxidations of Aqueous Sulfide by O2. Environ. Science & Technology **6**: 529-537.

Cook R.B., C.A. Kelly, D.W. Schindler and M.A. Turner (1986) Mechanisms of hydrogen ion neutralization in an experimentally acidified lake. Limnol. Oceanogr. **3**: 134-148.

Cook R.B. and D.W. Schindler (1983) The biogeochemistry of sulfur in an experimentally acidified lake. Environmental Biogeochemistry Ecol. Bull. **35**: 115-127.

Cressie N.A.C. (1985) Fitting variogram models with weighted least squares. Journal of the International Association for Mathematical Geology **17**: 563-586.

David M.B. and Mitchell M.J. (1985) Sulfur constituents and cycling in waters, seston, and sediments of an oligotrophic lake. Limnol. and Oceanogr. **39**: 1196-1207.

Davison W. (1988) Interactions of iron, carbon and sulphur in marine and lacustrine sediments. In Lacustrine Petroleum Source Rocks (ed. A.J. Fleet et al.), No.40, pp. 131-137, Geol. Soc. Spec. Publ.

Davison W., Lishman J.P. and Hilton J. (1985) Formation of pyrite in freshwater sediments: Implications for C/S ratios. Geochim. Cosmochim. Acta **49**: 1615-1620.

Dean G.A. (1966) A simple colorimetric finish for the Johnson-Nishita micro-distillation of sulphur. Analyst **91**: 530-532.

Duursma E.K. & Bosch C.J. (1970) Theoretical, experimental and field studies concerning diffusion of radioisotopes in sediments and suspended particles of the sea. Netherlands J. Sea Res. **4**: 395-469.

Elskamp H.J. (1989) National Air Quality Monitoring Network, Technical description. Report no. 228702017, National Institute of Public Health and Environmental Protection, Bilthoven, The Netherlands.

Ensminger E.L. (1954) Some factors affecting the adsorption of sulfate by Alabama soils. Soil Sci. Soc. Proc. **18**: 259-264.

Erisman J.W., De Leeuw F.A.A.M. and Van Aalst R.M. (1989) Deposition of the

most acidifying components in The Netherlands during the period 1980-1986. Atmospheric Environment **23**: 1051-1062.

Erisman J.W. (1992) Atmospheric deposition of acidifying compounds in The Netherlands. Ph.D diss. University of Utrecht, The Netherlands.

Erisman J.W. (1993) Acid deposition onto nature areas in the Netherlands; Part I. Methods and results. Submitted to Water, Air and Soil Pollution.

Feijtel T.C., Salingar Y., Hordijk C.A., Sweerts J.P.R.A., Van Breemen N. and Cappenberg Th.E.(1989) Sulfur cycling in a Dutch moorland pool under elevated atmospheric S-deposition. Water, Air, Soil Pollution **44**: 215-234.

Feijtel T.C. (1986) Ph.D. diss. Louisiana State University, Baton Rouge.

Ferdelman T.G., Church T.M. & Luther III G.W. (1991) Sulfur enrichment of humic substances in a Delaware salt marsh sediment core. Geochim. Cosmochim. Acta **55**: 979-988.

Fitzgerald J.W. (1976) Sulfate ester formation and hydrolysis: a potentially important yet often ignored aspect of the sulfur cycle of aerobic soils. Bacteriological Reviews **40**: 698-721.

Fitzgerald J.W. and Franklin B.L. (1982) The primary alkylsulfatase of *Pseudomonas aeruginosa*: inducer specificity and induction kinetics. Canadian Journal of Microbiology **28**: 1296-1299.

Fitzpatrick F.A. (1970) A technique for the preparation of large thin sections of soils and consolidated material. In Micromorphological techniques and applications. Techn. monogr. 2, Soil Survey of England and Wales, Rothhamsted Exp. Sta., Harpenden (D.A. Osmond and P. Bullock) pp 3-13.

Fossing H. & Jørgensen B.B. (1989) Measurement of bacterial sulfate reduction in sediments: Evaluation of a single-step chromium reduction method. Biogeochemistry **8**: 205-222.

Fossing H. and Jørgensen B.B. (1990) Oxidation and reduction of radiolabeled inorganic sulfur compounds in an estuarine sediment, Kysing Fjord, Denmark. Geochim. Cosmochim. Acta **54**: 2731-2742.

Francois R. (1987) A study of sulphur enrichment in the humic fraction of marine sediments during early diagenesis. Geochim. Cosmochim. Acta **51**: 17-27.

Freney J.R., Melville G.E. and Williams C.H. (1970) The determination of carbon bonded sulfur in soil. Soil Science **109**: 310-318.

Giblin A.E. and Howarth R.W. (1984) Porewater evidence for a dynamic sedimentary iron cycle in salt marshes. Limnol. Oceanogr. **29**: 47-63.

Giblin A.E., Likens G.E., White D. and Howarth R.W. (1990) Sulfur storage and alkalinity generation in New England lake sediments. Limnol. Oceanogr. **35**: 852-869.

Goldhaber M.B. (1983) Experimental study of metastable sulfur oxyanion formation during pyrite oxidation at pH 6-9 and 30°C. American Journal of Science **283**: 193-217.

Håkanson L. and Jansson M. (1983) Principles of lake sedimentology. Springer, Berlin, 316p.

Harwood J.E. and Huyser D.J. (1970) Automated analyses of ammonia in water. Water Research **4**: 695-704.

Harwood J.E. (1980) Sulfolipids. In: The biochemistry of plants (P.K. Stumpf and E.E. Conn, Eds), vol. 4, pp. 301-320. Academic Press, New York.

Helmer E.H., Urban N.R. & Eisenreich S.J. (1990) Aluminum chemistry in peatland waters. Biogeochem. **9**: 247-276.

Hem J.D. (1968) Graphical methods for studies of aqueous aluminum hydroxide, fluoride and sulfate complexes. Geol. Surv. Water Supply Pap. **1827**: 1-33.

Herlihy A.T. & Mills A.L. (1989) Factors controlling the removal of sulfate and acidity from the waters of an acidified lake. Water, Air and Soil Pollution **45**: 135-155.

Hicks B.B., Baldocchi D.D., Meyers T.P., Hosker Jr. R.P. & Matt D.R. (1987) A preliminary multiple resistance routine for deriving dry deposition velocities from measured quantities. Water, Air, and Soil Pollution **36**: 311-330.

Hillel D. (1980). Fundamentals of soil physics. Academic Press Inc., Orlando, 413p.

Holdren G.R., Brunelle T.M., Matisoff G. and Whalen M. (1984) Timing the increase in atmospheric sulfur deposition in the Adirondack Mountains. Nature **311**: 245-247.

Hordijk C.A., Hagenaars C.P.M.M. & Cappenberg Th.E. (1984) Analysis of sulfate at the mud-water interface of freshwater lake sediments using indirect photometric chromatography. J. Micr. Methods **2**: 49-56.

Hordijk C.A., Hagenaars C.P.M.M. & Cappenberg Th.E. (1985) Kinetic Studies of Bacterial Sulfate Reduction in Freshwater Sediments by High-Pressure Liquid Chromatography and Microdistillations. Appl. Environ. Microbiol. **49**: 434-440.

Hordijk C.A, Van Engelen J.J.M., Jonker F.A. and Cappenberg Th.E. (1989) Determination of total sulfur in freshwater sediments by ion chromatography. Wat. Res. **23**: 853-859.

Hordijk C.A., Marnette E.C.L. & Cappenberg Th.E. (1993) Factors affecting the sulfur cycle in a stratifying freshwater lake: Indications for substantial cycling of unknown sulfur species. Submitted

Howarth R.W. (1979) Pyrite: Its rapid Formation in a Salt Marsh and Its

Importance in Ecosystem Metabolism. Science **203**: 49-50.

Howarth R.W. (1984) The ecological significance of sulfur in the energy dynamics of salt marsh and coastal marine sediments. Biogeochemistry **1**: 5-27.

Howarth R.W. and Jørgensen B.B. (1984) Formation of ^{35}S-labelled elemental sulfur and pyrite in coastal marine sediments (Limfjorden and Kysing Fjord, Denmark) during short-term $^{35}SO_4^{2-}$ reduction measurements. Geochim. Cosmochim. Acta **48**: 1807-1818.

Howarth R.W. and Merkel S. (1984) Pyrite formation and the measurement of sulfate reduction in salt marsh sediments. Limnol. Oceanogr. **29**: 598-608.

Ingvorsen K., Zeikus J.G., & Brock T.D. (1981) Dynamics of bacterial sulfate reduction in a eutrophic lake. Appl. Environ. Microbiol. **42**: 1029-1036.

Izatt R.M., Eatough D., Christensen J.J. & Bartholomew C.H. (1969) Calorimetrically determined log K, Ho and So values for the interaction of sulphate ion with several bi and ter-valent metal ions. J. Chem. Soc. (A): 47-53.

Johnson C.M. and Nishita H. (1952) Microestimation of sulfur. Analytical Chemistry **24**: 736-742.

Jørgensen B.B. & Fenchel T. (1974) The sulfur cycle of a marine model system. Marine Biology **24**: 189-201.

Jørgensen B.B. (1977a) The sulfur cycle of a coastal marine sediment (Limfjorden, Denmark). Limnol. Oceanogr. **22**: 814-832.

Jørgensen B.B. (1977b) Bacterial sulfate reduction within reduced microniches of oxidized marine sediments. Marine Biology **41**: 7-17.

Jørgensen B.B. (1978) A comparison of methods for the quantification of bacterial sulfate reduction in coastal marine sediments I.Measurement with radiotracer techniques. Geomicrobiology Journal **1**: 11-27.

Jørgensen B.B. (1982) Mineralization of organic matter in the sea bed - The role of sulfate reduction. Nature **296**: 643-645.

Jørgensen B.B. (1983) The microbial sulfur cycle, p. 91-124. In W.E.Krumbein (ed.), Microbial Geochemistry. Blackwell Scientific Publ., Oxford.

Jørgensen B.B. and Revsbech N.P. (1985) Diffusive boundary layers and the oxygen uptake of sediments and detritus. Limnol. Oceanogr. **30**: 11-21.

Jørgensen B.B. and Sørensen J. (1985) Seasonal cycles of O_2, NO_3^- and SO_4^{2-} reduction in estuarine sediments: the significance of an NO_3^- reduction maximum in spring. Mar. Ecol. Prog. Ser. **24**: 65-74.

Jørgensen B.B. (1990) The sulfur cycle of freshwater sediments: Role of thiosulfate. Limnol. Oceanogr. **35**: 1329-1342.

Jørgensen B.B. and Bak F. (1991) Pathways and microbiology of thiosulfate

transformations and sulfate reduction in a marine sediment (Kattegat, Denmark). Appl. Environ. Microbiol. **57**: 847-856.

Journel A.G. and Huijbregts C.R. (1978) Mining Geostatistics. Academic Press, New York, 600p.

Journel A.G. In press. Geostatistics - Roadblocks and challenges. Contribution to the 4th International Conference of Geostatistics, Troia, Portugal.

Kelly C.A., Rudd J.W.M., Cook R.B. and Schindler D.W. (1982) The potential importance of bacterial processes in regulating rate of lake acidification. Limnol. Oceanogr. **27**: 868-882.

Kelly C.A. and Rudd J.W.M. (1984) Epilimnetic sulfate reduction and its relationship to lake acidification. Biogeochemistry **1**: 63-77.

Kelly C.A., Rudd J.W.M., Hesslein R.H., Schindler D.W., Dillon P.J., Driscoll C.T., Gherini S.A. & Hecky R.E. (1987) Prediction of biological acid neutralization in acid-sensitive lakes. Biogeochemistry **3**: 129-140.

King G.M. and Klug M.J. (1982) Comparative aspects of sulfur mineralization in sediments of a eutrophic lake basin. Appl. Environ. Microbiol. **43**: 1406-1412.

KNMI/RIVM (1985) Chemical composition of precipitation over the Netherlands. Annual report 1983. KNMI-report 156-6/RIVM-report 217810009, De Bilt/Bilthoven, The Netherlands.

KNMI/RIVM (1990) Netherlands Precipitation Chemistry Network. Monitoring Results 1988.

KNMI (1983,1984,1985,1986,1987,1988,1989,1990,1991) Precipitation 1982, Precipitation 1983,...Precipitation 1990 KNMI-reports 117, De Bilt, The Netherlands.

KNMI/RIV (1983) Chemical composition of precipitation over the Netherlands. Annual report 1982. KNMI-report 156-5/RIV-report 217810006, De Bilt/Bilthoven, The Netherlands.

KNMI/RIVM (1986,1987,1988,1988) Chemische samenstelling van de neerslag over Nederland (Chemical composition of precipitation over the Netherlands) Jaarrapport (in Dutch) 1984,1985,1986,1987. KNMI-report 156-7/RIVM-report 218203003 (1984), KNMI-report 156-8/RIVM-report 228703001 (1985), KNMI-report 156-9/RIVM-report 228703004 (1986), KNMI-report 156-10/RIVM-report 228703005 (1987), De Bilt/Bilthoven, The Netherlands.

KNMI-report 156-11/RIVM-report 228703012, De Bilt/Bilthoven, The Netherlands.

Kohnen M.E.L., Sinninghe Damste J.S., Ten Haven H.L. and De Leeuw J.W. (1989) Early incorporation of polysulphides in sedimentary organic matter. Nature **341**: 640-641.

Kowalenko C.G. (1985) A modified apparatus for quick and versatile sulphate sulphur analysis using hydriodic acid reduction. Comm. in Soil and Plant analyses **16**: 289-300.

Kuivila K.M., Murray J.W., Devol A.H. & Novelli P.C. (1989) Methane production, sulfate reduction and competition for substrates in the sediments of Lake Washington. Geochim. Cosmochim. Acta **53**: 409-416.

Lerman A. (1978) Chemical exchange across sediment-water interface. Ann. Rev. Earth Planet. Sci. **6**: 281-303.

Li Y-H. & Gregory S. (1974) Diffusion of ions in sea water and in deep-see sediments. Geochim. et Cosmochim. Acta **38**: 703-714.

Likens G.E., Bormann F.H., Pierce R.S., Eaton J.S. and Johnson N.M. (1977) Biogeochemistry of a forested ecosystem. Springer.

Lindsay W.L. (1979) Chemical equilibriua in soils. 449 p. Wiley, NY.

Lord C.J. and Church T.M. (1983) The geochemistry of salt marshes: Sedimentary ion diffusion, sulfate reduction, and pyritization. Geochim. et Cosmochim Acta **47**: 1381-1391.

Losher A.J. and K.R. Kelts (1989) Organic sulphur fixation in freshwater lake sediments and the implications for C/S ratios. Terra Nova **1**: 253-261.

Luther G.W. III, Giblin A., Howarth R.W. and Ryans R.A. (1982) Pyrite and oxidized iron mineral phases formed from pyrite oxidation in salt marsh and estuarine sediments. Geochim. Cosmochim. Acta **46**: 2665-2669.

Luther III G.W., Church T.M., Scudlark J.R. and Cosman M. (1986) Inorganic and organic sulfur cycling in salt-marsh pore waters. Science **232**: 746-749.

Luther III G.W. (1987) Pyrite oxidation and reduction: Molecular orbital theory considerations. Geochim. et Cosmochim. Acta **51**: 3193-3199.

Luther III G.W. (1991) Pyrite synthesis via polysulfide compounds. Geochim. Cosmochim. Acta **55**: 2839-2849.

Luther G.W. III, Ferdelman T.G., Kostka J.E., Tsamakis E.J. and Church T.M. (1991) Temporal and spatial variability of reduced sulfur species ($FeS_2, S_2O_3^{2-}$) and porewater parameters in salt marsh sediments. Biogeochemistry **14**: 57-88.

Mango F.D. (1983) The diagenesis of carbohydrates by hydrogen sulfide. Geochim. Cosmochim. Acta **47**: 1433-1441.

Marnette E.C.L., Hordijk C.A., Van Breemen N. and Cappenberg Th.E. (1992) Sulfate reduction and S-oxidation in a moorland pool sediment. Biogeochemistry **17**: 123-143.

Marnette E.C.L. and Stein A. (1993a) Spatial variability of chemical compounds related to S-cycling in two moorland pools. Water Research **27**: 1003-1012.

Marnette E.C.L. Van Breemen N. Hordijk C.A. Cappenberg Th.E. (1993b) Pyrite formation in two freshwater systems in The Netherlands. Geochim. Cosmochim Acta in press.

Matisoff G., Fisher J.B. and Matis S. (1985) Effects of benthic macroinvertebrates on the exchange of solutes between sediments and freshwaters. Hydrobiologia **122**: 19-23.

May H.M., Helmke P.A. & Jackson M.L. (1979) Gibbsite solubility and thermodynamic properties of hydroxy-aluminum ions in aqueous solution at 25°C. Geochim. Cosmochim. Acta **43**: 861-868.

Millero F.J. (1986) The thermodynamics and kinetics of the hydrogensulfide in natural waters. Marine chemistry **18**: 121-147.

Mitchell M.J., Landers D.H., Brodowski D.F., Lawrence G.B., and David M.B. (1984) Organic and inorganic sulfur constituents of the sediments in three New York lakes: effect of site, sediment depth and season. Water, Air, and Soil Pollution **21**: 231-245.

Moses C.O. and Herman J.S. (1991) Pyrite oxidation at circumneutral pH Geochim. Cosmochim. Acta **55**: 471-482.

Mulder J. (1988) Impact of acid atmospheric deposition on soils: field monitoring and aluminum chemistry. Ph.D. diss. Agricultural University Wageningen, The Netherlands.

Nissenbaum A. and Kaplan I.R. (1972) Chemical and isotopic evidence for the in situ origin of marine humic substances. Limnol. Oceanogr. **17**: 570-582.

Nordstrom D.K. (1982) The effect of sulfate on aluminum concentrations in natural waters; Some stability relations in the system Al_2O_3-SO_3-H_2O at 298 K. Geochim. Cosmochim. Acta **46**: 681-692.

Nriagu J.O. and Y.K. Soon (1985) Distribution and isotopic composition of sulfur in lake sediments of nothern Ontario. Geochim. Cosmochim. Acta **49**: 823-834.

Oenema O. (1990) Pyrite accumulation in salt marshes in the Eastern Scheldt, southwest Netherlands. Biogeochemistry **9**: 75-98.

Pachmayr F. (1960) Vorkommen und bestimmung von Schwefelverbindungen in mineralwasser. Ph.D dissertation, University of München, Germany.

Psenner R. (1983) Die Entstehung von Pyrit in rezenten Sedimenten des Piburger Sees. Schweiz. Z Hydrol. **45**: 219-232.

Raiswell R. (1982) Pyrite texture, isotopic composition and the availability of iron. Amer. J. Sci. **282**: 1244-1263.

Raiswell R. and Berner R.A. (1985) Pyrite formation in euxenic and semi-euxenic sediments. Am. Jour. Sci. **285**: 710-724.

Rickard D.T. (1975) Kinetics and mechanism of pyrite formation at low temperatures. Amer. J. Sci. **275**: 636-652.

Robie R.A., Hemingway B.S. and Fisher J.R. (1978) Thermodynamic Properties of Minerals and Related Substances at 298.15 K and 1 Bar (10^5 Pascals) Pressure and at Higher Temperatures. Geological Survey Bulletin 1452. 456p. United States Government Printing Office, Washington.

Rudd J.W.M., Kelly C.A. and Furutani A. (1986a) The role of sulfate reduction in long term accumulation of organic and inorganic sulfur in lake sediments. Limnol. Oceanogr. **31**: 1281-1291.

Rudd J.W.M., Kelly C.A., Louis V.S., Hesslein R.H., Furutani A. and Holoka M.H. (1986b) Microbial consumption of nitric and sulfuric acids in acidified North temperate lakes. Limnol. Oceanogr. **31**: 1267-1280.

Schiff S.L. & Anderson R.F. (1987) Limnocorral studies of chemical and biological acid neutralization in two freshwater lakes. Can. J. Fish. Aquat. Sci. **44**: 173-187.

Schimmel H.J.W. and Ter Hoeve J. (1952) Bodemgesteldheid en waterhuishouding van de 'Gerritsflesch' bij Kootwijk. Tijdschrift van het Koninklijk Nederlandsch Aardrijkskundig Genootschap deel LXIX, 1, 1-28.

Schindler D.W., Wageman R., Cook R.B., Ruszcynski T. and Prokopowich J. (1980) Experimental background of Lake 223, Experimental Lakes Area: Background data and the first three years of acidification. Can. J. Fish. Aquat. Sci. **37**: 342-354.

Schindler D.W., Turner M.A., Stainton M.P. & Linsey G.A. (1986) Natural sources of acid neutralizing capacity in low alkalinity lakes of the Precambrian shield. Science **232**: 844-847.

Schoonen M.A.A. and Barnes H.L. (1991a) Reactions forming pyrite and marcasite from solution: I. Nucleation of FeS2 below 100°C. Geochim. et Cosmochim. Acta **55**: 1495-1504.

Schoonen M.A.A. and Barnes H.L. (1991b) Reactions forming pyrite and marcasite from solution II. Via FeS precursors below 100°C. Geochim. et Cosmochim. Acta **55**: 1505-1514.

Schuurkes J.A.A.R., Elbers M.A. & Gudden J.J.F. & Roelofs J.G.M. (1987) Effects of simulated ammonium sulphate and sulphuric acid on acidification, water quality and flora of small-scale soft water systems. Aquat. Bot. **28**: 199-226.

Sinke A.J.C., Cornelese A.A., Keizer P., Van Tongeren O.F.R. & Cappenberg Th.E. (1990) Mineralization, pore water chemistry and phosphorous release from peaty sediments in the eutrophic Loosdrecht lakes, The Netherlands. Freshw. Biol. **23**: 587-599.

Spratt Jr. H.G., Morgan M.D. and Good R.E. (1987) Sulfate reduction in peat from New Jersey pinelands cedar swamp. Appl. Environm. Microbiol. **53**: 1406-1411.

Stanko-Golden K.M. and Fitzgerald J.W. (1990) Sulfur transformations in forest soils collected along an elevational gradient. Soil Biol. Biochem. **22**: 213-216.

Stanko-Golden K.M. and Fitzgerald J.W. (1991) Sulfur transformations and pool sizes in tropical forest soils. Soil Biol. Biochem. **23**: 1053-1058.

Stanko-Golden K.M., Fitzgerald J.W. and Swank W.T. (1992) Sulfur processing in soil from high and low elevation forests in the southern Appalachians of the United States. Soil Biol. Biochem. **24**: 693-702.

Stein A., Bouma J., Van Dooremolen W. and Bregt A.K. (1988b) Cokriging point data on moisture deficits. Soil Sci. Soc. Am. J. **52**: 1418-1423.

Stein A., Hoogerwerf M. and Bouma J. (1988a) Use of soil map delineations to improve (co-)kriging of point data on moisture deficits. Geoderma **43**: 163-177.

Stein A. (1991) Spatial interpolation. Ph.D. thesis, Wageningen Agricultural University, Wageningen, 236p.

Sweeney R.E. and Kaplan I.R. (1973) Pyrite framboid formation: Laboratory synthesis and marine sediments.. Econ. Geol. **68**: 618-634.

Sweerts J.-P.R.A., Louis V.St. & Cappenberg Th.E. (1989) Oxygen concentration profiles and exchange in sediment cores with circulated overlying water. Freshw. Biol. **21**: 401-409.

Sweerts J.-P.R.A., Kelly C.A., Rudd J.W.M. & Cappenberg Th.E. (1991) Similarity of whole-sediment molecular diffusion coefficients in freshwater sediments of low and high porosity. Limnol. Oceanogr. **36**: 335-342.

Swider K.T. and Mackin J.E. (1989) Transformations of sulfur compounds in marsh-flat sediments. Geochim. Cosmochim. Acta **53**: 2311-2323.

Tabatabai M.A. and Bremner J.W. (1970) An alkaline oxidation method for determination of total sulfur in soils. Soil Sci. Soc. Am. J. **34**: 62-65.

Van Breemen N. (1973) Dissolved aluminum in acid sulfate soils and in acid mine waters. Soil Sci. Soc. Am. Proc. **37**: 694-697.

Van Dam H. and Kooyman-van Blokland H. (1978) Man-made changes in some Dutch moorland pools, as reflectedd by historical and recent data about diatoms and macrophytes. Int. Revue ges. Hydrobiol. **63**: 587-607.

Van Dam H. (1987) Acidification of moorland pools: a process in time. Ph.D. dissertation. Agricultural University Wageningen, The Netherlands, 175p.

Van Dam H. (1988a) Acidification of three pools in The Netherlands by acid

precipitation and extreme drought periods over seven decades. Freshwater Biology **20**: 157-176.

Van Dam H., Van Geel B., Van der Wijk A., Geelen J.F.M., Van der Heijden R. and Dickman M.D. (1988b) Paleolimnological and documented evidence for alkalization and acidification of two moorland pools (The Netherlands). Paleobotany and Palynology **55**: 273-316.

Van Dam H. & Buskens R.F.M. (1993) Ecology and management of moorland pools: Balancing acidification and eutrophication. Hydrobiologia, in press.

Van Dobben H.F., Mulder J., Van Dam H. & Houweling H. (1992) The impact of acid atmospheric deposition of the biogeochemistry of moorland pools and surrounding terrestrial environment. Agric. Res. Rep. 931, 231 pp., Pudoc Wageningen, The Netherlands.

Verschuren R.H. (1978) A microscope-mounted drill to isolate microgram quantities of mineral material from polished thin sections. Mineral. Mag. **42**: 449-503.

Von Freiesleben N.E. (1988) Sulfate mobility in an acid Danish forest soil. J. Environ. Qual. **17**: 278-284.

Wagman D.D., Evans W.H., Parker V.B., Hallow I., Baily S.M. & Schumm R.H. (1968) Selected values of chemical thermodynamic properties. Natl. Bur. Stand. Tech. Rep. 270-273,264. NBS, Washington, DC.

Webster R. (1985) Quantitative spatial analysis of soil in the field. In: B.A. Stewart (ed.), Advances in soil science 3. Springer Verlag, New York, 1-70.

White J.R., Gubala C.P., Fry B., Owen J. and Mitchell M.J. (1989) Sediment biogeochemistry of iron and sulfur in an acidic lake. Geochim. Cosmochim. Acta **53**: 2547-2559.

Wieder, R.K., Lang, G.E. and Granus, V.A (1985) An evaluation of chemical methods for quantifying sulfur fractions in freshwater wetland peat. Limnol. Oceanogr. **30**: 1109-1115.

Wieder R.K. and G.E. Lang (1988) Cycling of inorganic and organic sulfur in peat from Big Run Bog, West Virginia. Biogeochemistry **5**: 221-242.

SAMENVATTING

Als het gevolg van atmosferische zure depositie is een groot aantal heidevennen in Nederland verzuurd. Vele vennen hebben hierdoor hun oorspronkelijke karakter, dat gekenmerkt werd door een typische flora en fauna, verloren. Heidevennen zijn in het algemeen gevoelig voor verzuring omdat de onderliggende en omringende bodems een laag chemisch bufferend vermogen bezitten. Daarom zijn juist de interne biologische processen als denitrificatie en sulfaat reductie van essientieel belang voor het neutraliseren van inkomende verzurende stikstof en zwavel componenten. Deze studie had als doel een beter inzicht te verkrijgen in de zwavel cyclus van oligo-mesotrofe heidevennen.

De karakterisering en kwantificering van de zwavel reservoirs in het sediment en bovenliggende water. Bepaling van de ruimtelijke variabiliteit van chemische componenten die zijn gerelateerd aan de S cyclus.

In sedimenten met een hoog organische stof gehalte (gemiddelde C gehalte in de bovenste 10 cm = 9.8% droog gewicht) vormt organisch S ongeveer 46% van het totale S gehalte, terwijl in meer zandige sedimenten (gemiddeld C = 1.4% droog gewicht) het aandeel van organisch S in het totale S gehalte ongeveer 75% bedraagt. Totaal S, C en Fe gehaltes in waterbodems van twee Nederlandse heidevennen, Gerritsfles en Kliplo, zijn met elkaar vergeleken (Hfdst.6). De horizontale en verticale verspreiding van S in beide vennen was significant verschillend. Statistische analyse wees uit dat de ruimtelijke variabiliteit van S in Kliplo bepaald wordt door variaties in organisch S gehalte. In Gerritsfles was er geen ruimtelijke relatie te herkennen tussen S, C en Fe. Deze studie heeft aangetoond dat het gebruik van de juiste eenheden (g g^{-1} of g cm^{-3}) belangrijk is met betrekking tot de interpretatie van ruimtelijk variabiliteit, omdat ruimtelijke patronen van de concentratie van een bepaald element direct in verband staan met de ruimtelijke variabiliteit van de bulkdichtheid van de sedimenten. Voor het kwantificeren van S budgetten zal, indien mogelijk, rekening moeten worden gehouden met de ruimtelijke variabiliteit van S.

Bepaling van SO_4^{2-} reductiesnelheden en transformatiesnelheden van SO_4^{2-} naar organische en anorganische S fracties. Schatting van S oxidatiesnelheden in sediment en bovenliggend water.

De S-cyclus aan het sediment-water grensvlak was onderzocht aan de hand van 1)

SO_4^{2-} reductiesnelheden in het sediment, 2) afname van SO_4^{2-} in de bovenstaande waterkolom en 3) de afgifte van ^{35}S van het sediment naar de waterkolom (Hfdst.2). Twee locaties in Gerritsfles met een verschillend type sediment (organisch rijk en zandig) werden vergeleken wat betreft SO_4^{2-} reductie snelheden en afname van SO_4^{2-} in de waterkolom.

Sulfaat reductiesnelheden, geschat met behulp van een diagenetisch model en met injectie van $^{35}SO_4^{2-}$ in intacte sediment cores, bedroegen 0.27 tot 11.2 mmol m^{-2} d^{-1}. *Sulfaat consumptiesnelheden in het bovenstaande water werden bepaald door middel van in situ* geïnstalleerde klokken en varieerden van -0.51 tot 1.81 mmol m^{-2} d^{-1}. De maximale oxidatiesnelheid die werd geschat in juli 1990 aan de hand van SO_4^{2-} reductie snelheid en *in situ* opname van SO_4^{2-} in de klokken bedroeg 10.3 op de locatie met het organisch rijke sediment en 10.5 mmol m^{-2} d^{-1} op de zandige locatie.

Tracerexperimenten wezen op een snelle vorming van organisch gebonden S afkomstig van gereduceerd SO_4^{2-} en op het transport van gereduceerd S vanuit het sediment in de bovenstaande waterkolom. Deze gereduceerde S verbindingen bleken uitermate persistent te zijn tegen oxidatie naar SO_4^{2-}.

Sulfaatreductiesnelheden in organisch rijke sediment verschilden niet significant van die in de zandige sedimenten.

De rol van anorganisch S in de S cyclus van Gerritsfles en Kliplo.

In de sedimenten van beide vennen is pyriet (FeS$_2$) de meest voorkomende vorm van Fe sulfide (Hfdst.3). De redox potentiaal in het sediment bepaalt in belangrijke mate welke Fe sulfiden worden gevormd. In sedimenten van Gerritsfles en Kliplo, waarboven zich altijd een zuurstofrijke waterkolom bevindt, wordt relatief meer pyriet gevormd dan andere, meer reactieve FeS verbindingen, hier aangeduid met AVS ("acid-volatile sulfur"). De ratio FeS$_2$/AVS bedraagt voor Gerritsfles en Kliplo sedimenten 32 en 55 respectievelijk, terwijl in meren waarin zich jaarlijks een anoxisch hypolimnion ontwikkelt, hoofdzakelijk AVS wordt gevormd (FeS$_2$/AVS <1).

Microscopisch onderzoek van Gerritsfles en Kliplo sediment heeft aangetoond dat pyriet zowel als grote framboïden als in de vorm van kleine enkel-kristallen kan voorkomen. De aanwezigheid van framboïden duidt op een langzame vorming van pyriet door de sulfurizatie van FeS precursors. De associatie van de framboïden met organische stof en de onderverzadiging van het poriewater ten opzichte van amorf FeS, doet vermoeden dat de grote pyrietkristallen in anaerobe microniches ontstaan. Afwisselend gereduceerde en meer geoxideerde omstandigheden zorgen dan voor

de aanvoer van Fe^{2+} en elementair S dat noodzakelijk is voor de vorming van pyriet. Een verklaring voor de preferentiele aanwezigheid van pyriet in afgestorven plantencellen kunnen zijn dat pyriet, dat niet door organische stof wordt beschermd, bij voorkeur wordt geoxideerd.

S budgetten van Gerritsfles en Kliplo

De chemische samenstelling van het oppervlaktewater van beide vennen en van de neerslag werd bepaald gedurende de periode 1982-1990. Sulfaat- en water budgetten werden berekend met behulp van een model dat is ontwikkeld voor goed gemengde niet-stratificerende zoetwatersystemen (Hfdst.4). In Gerritsfles en Kliplo, respectievelijk 70 en 80% van de S input wordt vastgelegd in het sediment, voornamelijk door SO_4^{2-} reductie en Fe precipitatie. Hieruit blijkt dat SO_4^{2-} reductie een grote rol speelt in de buffering van zure S depositie.

De atmosferische S depositie is sinds 1986 afgenomen op beide locaties. Een model dat het zwavelbudget beschrijft aan de hand van input/output en . reductie/oxidatie processen in het sediment, voorspelde een snelle afname van de SO_4^{2-} concentratie in het venwater na de afname van de S depositie. Gemeten SO_4^{2-} concentraties in het venwater bleken echter nauwelijks of niet af te nemen, hetgeen wijst op een extra bron van SO_4^{2-}. Twee processen kunnen mogelijk verantwoordelijk zijn voor de extra bron van SO_4^{2-}: desorptie van SO_4^{2-} uit het sediment en het vrijkomen van SO_4^{2-} door oxidatie van gereduceerde S verbindingen na het droogvallen van sediment gedurende droge zomers. Het relative belang van beide processen zou in de toekomst nader onderzocht moeten worden.

Mineralisatie van organisch S

De mineralisatie van organisch S was onderzocht om een indruk te krijgen van het aandeel daarvan in de algehele S-cyclus (Hdst.5). De mineralisatie van organisch S is indirect geschat met behulp van modellering van NH_4^+ poriewater profielen en de ratio van het organisch N en S gehalte in het sediment. Omdat de mineralisatiesnelheid van N en S niet volgens dezelfde stoichiometrie verloopt als de N en S gehaltes in het sediment, was het alleen mogelijk een maximale snelheid te berekenen. De maximale mineralisatiesnelheid van organisch S is geschat op 25 mmol m^{-2} j^{-1}, en slechts 1-2% van de hoeveelheid SO_4^{2-} die jaarlijks wordt gereduceerd. De mineralisatie van organisch S speelt daarom een kleine rol in de algehele S-cyclus.

CURRICULUM VITAE

Emile Marnette werd geboren op 26 april 1962 te Eindhoven. In 1980 behaalde hij het Atheneum diploma aan het Pius X college te Almelo. In datzelfde jaar begon hij aan de studie Bodemkunde die hij in mei 1988 afrondde. De doctoraalvakken waren Bodemscheikunde in combinatie met Theoretische Productie Ecologie (toen nog "Theoretische Teeltkunde" geheten), Regionale bodemkunde en Microbiologie (chemisch-microbiologisch).

Per 1 september 1988 trad hij in dienst als toegevoegd onderzoeker bij de Landbouwuniversiteit te Wageningen bij de vakgroep Bodemkunde en Geologie, met de onderzoeksopdracht het kwantificeren van processen met betrekking tot de zwavelhuishouding in chemisch slecht gebufferede zoetwatersystemen. De resultaten van dit onderzoek worden gepresenteerd in dit proefschrift.